DISSERTATIONES
NEUROSCIENTIAE
UNIVERSITATIS
TARTUENSIS
35

KADRI SEPPA

The neuroprotective effect of GLP-1 receptor agonist liraglutide in a rat model of Wolfram syndrome

DISSERTATIONES NEUROSCIENTIAE UNIVERSITATIS TARTUENSIS
35

DISSERTATIONES NEUROSCIENTIAE UNIVERSITATIS TARTUENSIS
35

KADRI SEPPA

The neuroprotective effect of GLP-1 receptor agonist liraglutide in a rat model of Wolfram syndrome

UNIVERSITY OF TARTU
Press

Institute of Biomedicine and Translational Medicine, University of Tartu, Tartu, Estonia.

The dissertation was accepted for the commencement of the degree of Doctor of Philosophy in Neurosciences on the 4th of June 2021 by the council for the Curriculum of Neurosciences.

Supervisors: Mario Plaas, PhD, Head of Centre, Associate Professor, Laboratory Animal Centre, Institute of Biomedicine and Translational Medicine, University of Tartu, Tartu, Estonia

Anton Terasmaa, PhD, Senior Research Fellow, National Institute of Chemical Physics and Biophysics, Tallinn, Estonia

Eero Vasar, MD, PhD, Professor, Department of Physiology, Institute of Biomedicine and Translational Medicine, University of Tartu, Tartu, Estonia

Reviewers: Tambet Tõnissoo, PhD, Associate Professor, Institute of Molecular and Cell Biology, University of Tartu, Tartu, Estonia

Kalle Kilk, MD, PhD, Associate Professor, Department of Biochemistry, Institute of Biomedicine and Translational Medicine, University of Tartu, Tartu, Estonia

Opponent: Tamara Hershey, PhD, Professor, Psychiatry and Radiology; Lab Chief, Neuroimaging Labs, Washington University School of Medicine, St. Louis, MO, USA

Commencement: 24th of August 2021

ISSN 1736-2792
ISBN 978-9949-03-650-9 (print)
ISBN 978-9949-03-651-6 (pdf)

University of Tartu Press
www.tyk.ee

CONTENTS

LIST OF ORIGINAL PUBLICATIONS

I Plaas, M.*, Seppa, K*., Reimets, R*., Jagomäe, T*., Toots, M*., Koppel, T., Vallisoo, T., Nigul, M., Heinla, I., Meier, R., Kaasik, A., Piirsoo, A., Hickey, M.A., Terasmaa, A., Vasar, E., 2017. Wfs1 – deficient rats develop primary symptoms of Wolfram syndrome: insulin-dependent diabetes, optic nerve atrophy and medullary degeneration. Sci. Rep. 7, 10220. https://doi.org/10.1038/s41598-017-09392-x

II Toots, M.*, Seppa, K*., Jagomäe, T., Koppel, T., Pallase, M., Heinla, I., Terasmaa, A., Plaas, M., Vasar, E., 2018. Preventive treatment with liraglutide protects against development of glucose intolerance in a rat model of Wolfram syndrome. Sci. Rep. 8, 10183. https://doi.org/10.1038/s41598-018-28314-z

III Seppa, K., Toots, M., Reimets, R., Jagomäe, T., Koppel, T., Pallase, M., Hasselholt, S., Krogsbæk Mikkelsen, M., Randel Nyengaard, J., Vasar, E., Terasmaa, A., Plaas, M., 2019. GLP-1 receptor agonist liraglutide has a neuroprotective effect on an aged rat model of Wolfram syndrome. Sci. Rep. 9, 15742. https://doi.org/10.1038/s41598-019-52295-2

IV Seppa, K., Jagomäe, T., Kukker, K.G., Reimets, R., Pastak, M., Vasar, E., Terasmaa, A., Plaas, M., 2021. Liraglutide, 7,8-DHF and their co-treatment prevents loss of vision and cognitive decline in a Wolfram syndrome rat model. Sci. Rep. 11, 2275. https://doi.org/10.1038/s41598-021-81768-6

Contribution of the author:

I The author performed the MRI, histological and gene expression analysis of the brainstem and participated in writing the manuscript.

II The author participated in performing daily liraglutide injections, performing intraperitoneal glucose tolerance tests and blood serum preparation, performing histological analyses of Langerhans islets, and measuring Langerhans islet mass from histological slices.

III The author participated in designing the study, performing daily liraglutide injections, and performing intraperitoneal glucose tolerance tests. The author performed inferior olive immunostaining and subsequent stereology analysis, conducted MRI experiments, performed the analysis of MRI data, wrote the manuscript, and handled the correspondence.

IV The author participated in designing the study and performing animal experiments. The author performed gene expression analysis, conducted MRI experiments, performed the analysis of MRI data, wrote the manuscript, and handled the correspondence.

* These authors contributed equally to this work.

ABBREVIATIONS

7,8-DHF	7,8-dihydroxyflavone
ANOVA	Analysis of variance
ATF4	Activating transcription factor 4
ATF6	Activating transcription factor 6
Aβ	Amyloid beta
BDNF	Brain-derived neurotrophic factor
BSA	Bovine serum albumin
cAMP	Cyclic adenosine monophosphate
CD11b	Integrin alpha M
cDNA	Complementary DNA
CHOP	C/EBP homologous protein
CX3CR1	CX3C chemokine receptor 1
DAPI	4′,6-diamidino-2-phenylindol
DHF	7,8-dihydroxyflavone
DMSO	Dimethyl sulfoxide
dNTP	Nucleoside triphosphate
ELISA	Enzyme-linked immunosorbent assay
EMA	European Medicines agency
EPS	Extraparenchymal space
ER	Endoplasmic reticulum
F4/80	EGF-like module-containing mucin-like hormone receptor-like 1
Fisher's LSD	Fisher's least significant difference
FOXP2	Forkhead box protein P2
GABA	Gamma-aminobutyric acid
GFAP	Glial fibrillary acidic protein
GLP-1	Glucagon-like peptide-1
GRP78	Glucose-regulated protein 78, also known as BIP
HMOX1	Heme Oxygenase 1
HPRT1	Hypoxanthine-guanine phosphoribosyltransferase
i.p.	Intraperitoneal injection
IBA1	Ionized calcium-binding adapter molecule 1
iNOS	Nitric oxide synthases inducible isoform
IO	Inferior olive
IP10	Interferon gamma-induced protein 10
IPGTT	Intraperitoneal glucose tolerance tests
IRE1	Inositol-requiring enzyme 1
KI67	Antigen KI-67
KO Dhf	Wfs1 KO rats who were treated with 7,8-dihydroxyflavone
KO Lira	Wfs1 KO rats who were treated with liraglutide
KO Lira+Dhf	Wfs1 KO rats who were treated with the combination of liraglutide and 7,8-dihydroxyflavone

KO Sal	Wfs1 KO rats who were treated with saline
KO	Knock-out
LIRA	Liraglutide
MRI	Magnetic resonance imaging
NRF2	Nuclear factor erythroid 2-related factor 2
NTRK2	Neurotrophic Receptor Tyrosine Kinase 2
PBS	Phosphate buffered saline
PEG	Polyethylene glycol
PERK	Eukaryotic translation initiation factor 2α (eIF2α) kinase 3
PFA	Paraformaldehyde
PI3K	Phosphoinositide 3-kinase
PKA	Protein kinase A
PPARγ	Peroxisome proliferator-activated receptor-gamma
qRT-PCR	Real time quantitative polymerase chain reaction
RNA	Ribonucleic acid
ROI	Region of interest
RYR1	Ryanodine receptor 1
RYR2	Ryanodine receptor 1
s.c.	Subcutaneous injection
SEM	Standard error of the mean
Spliced XBP-1	Spliced X-box binding protein 1
SUR1	Sulfonylurea receptor
TLR2	Toll-like receptor 2
TLR4	Toll-like receptor 4
TNF-α	Tumor necrosis factor alpha
TRKB	Tropomycin receptor kinase B
Tukey's HSD	Tukey's honestly significant difference
UPR	Unfolded protein response
Wfs1 KO	Wolfram syndrome 1 gene knock-out rat
WFS1	Wolfram syndrome 1 gene in humans
Wfs1	Wolfram syndrome 1 gene in rats and mice
WFS1	Wolframin protein
WT Dhf	Wild-type rats who were treated with 7,8-dihydroxyflavone
WT Lira	Wild-type rats who were treated with liraglutide
WT Lira+Dhf	Wild-type rats who were treated with the combination of liraglutide and 7,8-dihydroxyflavone
WT Sal	Wild-type rats who were treated with saline solution
WT	Wild-type
XBP1	X-box binding protein 1

1 INTRODUCTION

Wolfram syndrome (OMIM #222300) is a rare hereditary neurodegenerative disorder that is caused by biallelic mutations in the *WFS1* gene, from which WFS1 (Wolframin) protein is encoded (Inoue et al., 1998; Strom, 1998). Wolfram syndrome prevalence varies worldwide, the highest prevalence has been reported in Lebanon (1 in 68 000 people) and the lowest in the United Kingdom (1 in 770 000 people) (Kumar, 2010). The first symptom of Wolfram syndrome is diabetes mellitus, followed by optic nerve atrophy, diabetes insipidus, deafness and progressive brainstem atrophy (Barrett et al., 1995). The inferior olive and other medullary nuclei induce most of the Wolfram syndrome patients' clinical neurological features (Hilson et al., 2009).

Currently, there is no cure for Wolfram syndrome, and only supportive treatment is used to relieve the symptoms (Urano, 2016). New treatment strategies for Wolfram syndrome should be directed toward finding prevention and treatment options for both Wolfram syndrome symptoms: diabetes mellitus and neurodegeneration. Diabetes mellitus can effectively be controlled with insulin replacement therapy; therefore, for Wolfram syndrome patients, it is most important to find a neuroprotective therapy that can prevent or delay brainstem neurodegeneration and thereby significantly improve quality of life. As no effective therapy is available, drug repurposing could be the best therapeutic option because the drugs are already approved and thus reach patients faster (Pallotta et al., 2019).

GLP-1 receptor agonists are used for the treatment of diabetes mellitus and have neuroprotective properties in addition to glucose-lowering effects. Hence, they could also have a potential therapeutic effect for the main symptoms of Wolfram syndrome. In addition to GLP-1 receptor agonists, the neurotrophic factor, such as brain-derived neurotrophic factor (BDNF) mimetic 7,8-dihydroxyflavone (7,8-DHF), has not been studied in connection with Wolfram syndrome. *In vivo* investigations for drug repurposing would not be possible without well-characterized animal models. Therefore, our research group has created Wfs1 KO rats with an exon 5 disruption. The aim of this dissertation is (i) to evaluate the symptoms of Wolfram syndrome in Wfs1 KO rats and (ii) to use it to test novel treatment strategies for Wolfram syndrome with an emphasis on neurodegeneration.

The current thesis demonstrates that Wfs1 KO rats developed the main symptoms of Wolfram syndrome: diabetes mellitus and neurodegeneration. This indicates that the Wfs1 KO rat is indeed a Wolfram syndrome animal model, and it can be used to test treatment strategies for Wolfram syndrome. The antidiabetic drug liraglutide protected Wfs1 KO rats against development of glucose intolerance. Moreover, liraglutide treatment had a neuroprotective effect in the olive nucleus, as measured by decreased neuroinflammation, ER stress and neuronal swelling. Additionally, BDNF mimetic 7,8-DHF had an anti-inflammatory effect on the hippocampus and maintained cognitive function in Wfs1 KO

animals. However, an anti-diabetic effect of 7,8-DHF was not detected. Therefore, liraglutide treatment alone or co-treatment with liraglutide and 7,8-DHF could be promising treatment strategies for Wolfram syndrome patients. Inspired by preclinical studies, a liraglutide clinical trial has been initiated, and further investigations will clarify the effect of liraglutide in Wolfram syndrome patients.

2 REVIEW OF LITERATURE

2.1 Clinical manifestation of Wolfram syndrome

Wolfram syndrome is diagnosed by (i) juvenile onset diabetes mellitus and by (ii) juvenile onset optic atrophy, and the diagnosis is confirmed by genetic testing to identify autosomal recessive mutations in the *WFS1* gene (Urano, 2016).

The schematic representation of Wolfram syndrome clinical symptoms is seen in Figure 1. The first symptom of Wolfram syndrome is non-autoimmune, insulin-dependent diabetes mellitus that is diagnosed around the age of six years (Rigoli et al., 2018). Compared to type 1 diabetes, Wolfram syndrome patients have lower insulin requirements and glycated hemoglobin levels (Cano et al., 2007). Additionally, Wolfram syndrome patients' insulinopenia is caused due to the degeneration of pancreatic beta cells, in which WFS1 is widely expressed, and not from autoimmune destruction of pancreatic beta cells (Cano et al., 2007).

The second symptom required for the diagnosis of Wolfram syndrome is optic nerve atrophy, which appears around the age of 11 years (Kumar, 2010). Optic nerve atrophy is characterized by a progressive decrease in visual acuity due to the development of cataracts, abnormal papillary light reflexes, nystagmus, glaucoma, and pigmentary maculopathy (Pallotta et al., 2019). Diabetes insipidus caused by vasopressin deficiency appears around the age of 14 years and the average age of hearing loss diagnosis is 16 years (Kumar, 2010).

Mental impairment with psychomotor delay and learning difficulties are mainly found in Wolfram syndrome patients who developed neurological symptoms before the age of 15 years (Chaussenot et al., 2011). Bischoff et al. compared genetically confirmed Wolfram syndrome patients to age- and gender-equivalent groups of individuals with type 1 diabetes and with healthy controls and found, by contrast, that cognitive performance and psychological health were relatively preserved in Wolfram syndrome patients. They concluded that cognitive and psychiatric issues might become more prominent later in life (Bischoff et al., 2015). Reduced cognitive function is strongly correlated with hippocampal shrinkage (Apostolova et al., 2012), although hippocampal atrophy is not detected in Wolfram syndrome patients (Hershey et al., 2012; Hilson et al., 2009; Lugar et al., 2016). Additionally, cognitive decline correlates with ventricular volume increase (Carmichael et al., 2007), which has been reported in connection with aging (Hamezah et al., 2017) and neurodegeneration (Carmichael et al., 2007). Mildly dilated lateral ventricles also have been described in one Wolfram syndrome patient's post-mortem study (Shannon et al., 1999), and additionally, mild third ventricle enlargement was also reported in Wolfram syndrome patients during an MRI study (La Morgia et al., 2020).

Progressive brainstem neurodegeneration is considered to be a common feature of Wolfram syndrome, and the most frequently described symptoms caused by it are gait and balance abnormalities, dysphagia, decreased ability to taste and

detect odours, and central apnea (Pallotta et al., 2019). Before quantitative neuroimaging, brainstem atrophy was detected by visual examination of MRI images or from post-mortem macroscopic examination. Thus, the data was obtained from individuals in the relatively late stage of the disease or from case studies without quantification or comparison with a control group. Modern *in vivo* brain quantitative neuroimaging is a powerful, non-invasive method to investigate histopathological abnormalities without the need for post-mortem tissue. Quantitative neuroimaging allows repetitive measurements and longitudinal studies in which changes of volume are monitored over time (Samara et al., 2019). Quantitative neuroimaging studies from genetically confirmed groups of Wolfram syndrome patients have revealed decreased brainstem volumes in almost all Wolfram syndrome patients regardless of age or duration of diabetes or other features of the disease (Hershey et al., 2012; Lugar et al., 2016). Additionally, Wolfram syndrome patients' brainstem volume decreased with age, whereas the volume usually increases in healthy controls (Lugar et al., 2019). Altogether, the prognosis of Wolfram syndrome is currently poor, and without treatment, patients die prematurely due to brainstem atrophy induced respiratory failure in their 30s (Urano, 2016).

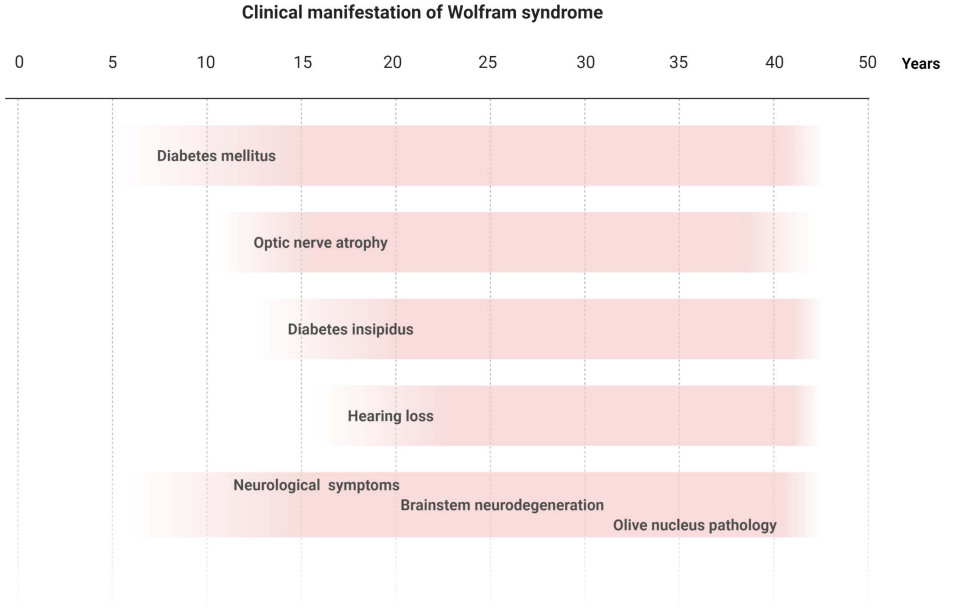

Figure 1. Temporal manifestation of Wolfram syndrome clinical symptoms. The first symptom of Wolfram syndrome is diabetes mellitus, followed by optic nerve atrophy, diabetes insipidus, hearing loss and progressive brainstem neurodegeneration. Figure is prepared according to (Kumar, 2010).

2.2 Olive nucleus pathology in Wolfram syndrome

Wolfram syndrome includes phenotypical manifestations of olivopontocerebellar atrophy (Leiva-Santana et al., 1993). Hence, it is suggested that the pathology of the inferior olive and other medullary nuclei produce most of the Wolfram syndrome patients' clinical neurological features (Hilson et al., 2009). The olive nucleus consists of three sub-nuclei: the medial nucleus, dorsal nucleus and principal nucleus, and is mostly associated with integrating motor and sensory information (Paul and M Das, 2019). Additionally, the inferior olive has a role in the central sympathetic functions and may also be involved in functional interactions between the motor and thermoregulatory systems, such as an increase in body temperature, convulsions and shivering (Uno and Shibata, 2001).

Olive nucleus pathology has been described in several Wolfram syndrome patients through post-mortem macroscopic examinations. Genís et al. reported post-mortem findings on a Wolfram syndrome patient who died at the age of 37 years because of food aspiration. They described the patient's mild olivopontocerebellar atrophy, moderate loss of neurons in the inferior olive and mild loss of motor neurons in the spinal cord accompanied by mild gliosis, as revealed in sections that were immunostained for Glial fibrillary acidic protein (GFAP). Additionally, a few of the remaining Purkinje cells showed axonal ballooning (Genís et al., 1997).

In a post-mortem macroscopic study of a 38-year-old female Wolfram syndrome patient, Shannon et al. noted atrophy of the medulla and axonal swelling in the pontocerebellar tracts and in the inferior olive. Additionally, chromatolytic neurons were noted in the pons, where neuronal cell loss was undetectable (Shannon et al., 1999). This suggests that neuronal swelling and chromatolysis might proceed to neuronal loss.

Moreover, one Wolfram syndrome patient who succumbed to complications of adult respiratory distress syndrome at the age of 24 years had lost about 60% of the inferior olive neurons in a diffuse pattern (Hilson et al., 2009).

Taken together, these results indicate that olive nucleus neurodegeneration plays an important role in Wolfram syndrome, although more detailed study is needed.

2.3 WFS1 and ER stress in Wolfram syndrome

The Wolfram syndrome causing gene – *WFS1* gene was identified by two independent research groups in 1998 (Inoue et al., 1998; Strom et al., 1998). From *WFS1* gene, WFS1 protein is encoded (Wolframin) which consists of 890 amino acids and has a molecular mass of 100 kDa (Inoue et al., 1998). WFS1 protein is highly expressed throughout the brain and in the heart, and pancreas (Hofmann, 2003). Subcellularly, WFS1 protein localizes primary in the endoplasmic reticulum (ER) membrane (Takeda, 2001), where it modulates Ca2+ concentration and thereby has an important role in the ER homeostasis (Takei et al., 2006).

Mutations in the WFS1 gene result in decreased or deficient WFS1 protein function, leading to the impairment of cellular calcium regulation and, thereby, to accumulation of unfolded proteins in the ER, a condition known as ER stress, which in turn activates the unfolded protein response (UPR) (Urano, 2016). A schematic representation of UPR pathways is seen in Figure 2. The aim of UPR pathways is to restore ER homeostasis through reducing the protein load in the ER and decreasing protein translation. Three transmembrane proteins mediate the UPR signal across the ER membrane: inositol-requiring enzyme 1 (IRE1), eukaryotic translation initiation factor 2α (eIF2α) kinase 3 (PERK) and activating transcription factor 6 (ATF6). In the physiological state, ATF6, IRE1 and PERK activity is suppressed because they are associated with glucose-regulated protein 78 (GRP78, also known as BIP). Under ER stress, unfolded proteins accumulate in the ER lumen, causing GRP78 to dissociate from ATF6, IRE1 and PERK, which causes their homodimerization, autophosphorylation and activation of cytoprotective downstream pathways (Lee, 2005). However, when cell survival is not anymore possible, excessive stress leads to the activation of C/EBP homologous protein (CHOP) apoptosis pathway (Figure 2) (Zinszner et al., 1998).

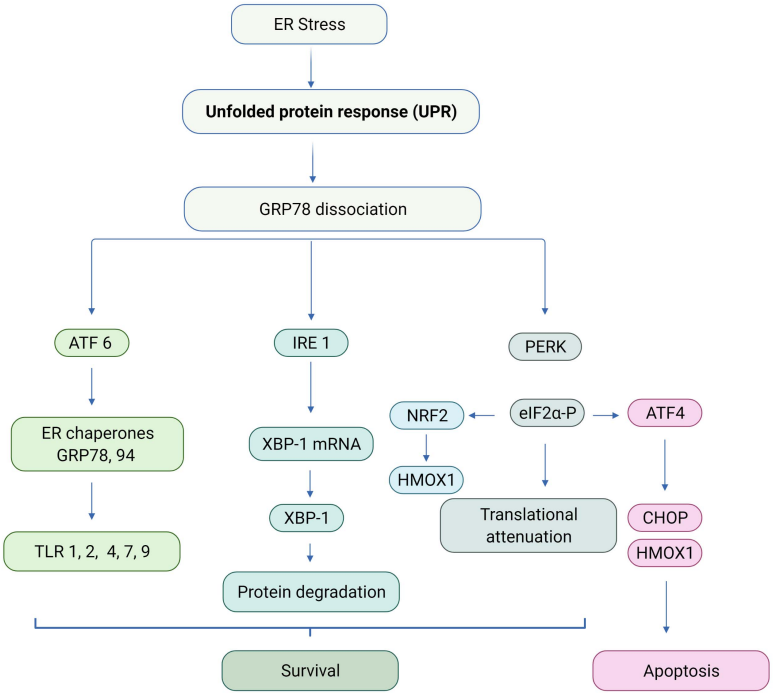

Figure 2. The UPR pathway. The UPR pathway's aim is to restore ER homeostasis. Three transmembrane proteins mediate the UPR signal across the ER membrane: ATF6, IRE1 and PERK. Figure is prepared according to (Jakobsen et al., 2008; Timberlake and Dwivedi, 2019; Wang et al., 2009).

WFS1 plays a key role in ER stress in beta-cells. WFS1 is a component of IRE1 and PERK signaling (Fonseca et al., 2005) and it negatively regulates ATF6. WFS1 dysfunction leads to chronic hyperactivation of ATF6 signalling, which is involved in apoptosis through apoptotic effectors of the UPR, such as CHOP (Fonseca et al., 2010).

ER stress can also induce excitotoxicity due to persistent glutamate receptor overstimulation, which can lead to cell apoptosis (Sokka et al., 2007). It has also been shown that GRP78 is able to suppress ER stress and thereby can protect neurons against glutamate-induced excitotoxicity (Yu et al., 1999).

In addition to the pathogenesis of diabetes, ER stress is a major cause of neurodegeneration in aging and in different neurodegenerative diseases, such as in Alzheimer's disease, Parkinson's disease and Amyotrophic Lateral Sclerosis (Lee, 2005).

In conclusion, ER stress plays an important role in the development of the main symptoms of Wolfram syndrome: diabetes and neurodegeneration. Therefore, ER homeostasis could be a key target for prevention or therapy of Wolfram syndrome.

2.4 Neuroinflammation in neurodegeneration

Neuroinflammation is an inflammatory response within the brain and is mediated by the production of cytokines, chemokines, reactive oxygen species, and secondary messengers. These mediators are mainly produced by microglia and astroglia to maintain cellular homeostasis (DiSabato et al., 2016).

Microglia are myeloid-origin innate immune cells that express CX3CR1, CD11B, IBA1, and F4/80 (Ransohoff and Khoury, 2016). Microglia cells are constantly engaged because they are involved in three essential functions: (i) sensing their environment, (ii) conducting physiological housekeeping, and (iii) protecting against modified-self and non-self-injurious agents. For example, microglia failure to clean up debris and misfolded proteins can cause Aβ accumulation in Alzheimer's disease and α-synuclein accumulation in Parkinson's disease (Halliday and Stevens, 2011; Hickman et al., 2008). Dysregulation of any of these functions results in an imbalance that initiates or propagates neurodegeneration (Hickman et al., 2018).

Astroglia cells provide trophic, metabolic, and structural support for neurons and play an active role in complex neuronal-glial communication, synaptic signalling and regulation of blood flow (Seifert et al., 2006). Similarly to microglia cells, astroglia dysfunction can aggravate Aβ plague formation in Alzheimer's disease (Pihlaja et al., 2011) and pathophysiology in Parkinson's disease (Booth et al., 2017). Mild astrogliosis has also been detected in Wolfram syndrome patients (Genís et al., 1997; Shannon et al., 1999). However, neuroinflammation has not been studied in detail in connection with Wolfram syndrome.

Taken together, pathological chronic neuroinflammation implies that glial cell activation precedes and causes neuronal degeneration in chronic neurodegenerative diseases. Therefore, neuroinflammation could be the therapeutic target for neurodegenerative diseases. However experimental models of neurodegeneration fail to model neuroinflammation because glial cell activation occurs secondarily to neuronal damage (Streit et al., 2004). Hence, animal models in which neuroinflammation proceeds to neuronal damage are needed to model neuroinflammation.

2.5 Neurons and beta cells

WFS1 is highly expressed in the human adult pancreas and in the brain (Inoue et al., 1998), and therefore, pancreatic beta cells and neurons are both affected in Wolfram syndrome. Pancreatic beta cells and neurons are in constant demand for protein synthesis and secretion. Similarly to neurons, pancreatic beta cells have high hormone and enzyme secretory functions and have highly developed ER (Thakur et al., 2018). Also, the UPR is classically linked to the maintenance of cellular homeostasis in specialized secretory cells, such as pancreatic cells and neurons (Thakur et al., 2018). Neurons and pancreatic beta cells share similar characteristics, although they are not derived from a common tissue, and they are not developed from the same embryonic germ layer (Arntfield and van der Kooy, 2011). It has been shown that 15% of conserved beta cell markers are also expressed in neuronal tissue coding for proteins that are involved in neurotransmitter transport, synaptic vesicle formation and brain development (Martens et al., 2011). Additionally, the central nervous system major neurotransmitter, gamma amino butyric acid (GABA) (Kittler and Moss, 2003), is also produced by pancreatic beta cells (Adeghate and Ponery, 2002). GABA is a strong secretagogue of insulin in the pancreas, and the number of GABA-like immunoreactive cells is significantly reduced in diabetes (Adeghate and Ponery, 2002). Moreover, it has been shown that treatment with GABA has a protective and regenerative effect on pancreatic beta cells and thereby is able to reverse type 1 diabetes (Soltani et al., 2011). Thus, the study of common principles in neurons and pancreatic beta cells may provide a basis for prevention and treatment options for both Wolfram syndrome symptoms: diabetes mellitus and neurodegeneration.

2.6 Treatment strategies for Wolfram syndrome

It is essential to develop treatment strategies that are able to slow the progression of Wolfram syndrome and thereby extend life expectancy. Drug repurposing could be the best therapeutic option because of its fast translation into clinical practice, as the existing drugs have already been approved (Pallotta et al., 2019).

2.6.1 Diabetes drugs

2.6.1.1 Pioglitazone

Pioglitazone is used to treat type 2 diabetes in adults, particularly in those who are overweight. Pioglitazone is a selective agonist of peroxisome proliferator-activated receptor-gamma (PPARγ), which is expressed in adipose tissue, skeletal muscle, liver (Tyagi et al., 2011) and in the brain (Stump et al., 2016). PPARγ activation leads to an improved insulin sensitivity without an increase in insulin secretion (Janani and Ranjitha Kumari, 2015). Pioglitazone treatment has been performed in Wfs1-deficient mice who developed selective beta cell loss and severe insulin-deficient diabetes as early as 8 weeks. 20-week treatment with pioglitazone protected beta cells from apoptosis and almost completely prevented diabetes development. It was suggested that the therapeutic effect of pioglitazone was caused by reduced ER stress in pancreatic beta cells, although the precise mechanisms are not fully understood (Akiyama et al., 2009). Additionally, in a mice model of Alzheimer's disease, pioglitazone has been shown to reduce the numbers of activated microglia and Aβ deposition in the brain (Heneka et al., 2005). Moreover, a pilot study on patients with Alzheimer's disease demonstrated that pioglitazone resulted in cognitive and metabolic improvements (Hanyu et al., 2009). However, the neuroprotective effect of pioglitazone has not been studied in connection with Wolfram syndrome.

2.6.1.2 Glipizide

Glipizide is a sulphonylurea that acts on the sulfonylurea receptor (SUR1) which is expressed in the pancreatic beta cells and in the brain (Guiot et al., 2007). SUR1 activations cause closure of K-ATP channel which results in cell depolarization, opening of the voltage-gated calcium channels and promoting calcium ion influx. The increased flow of calcium is causing insulin secretion from the pancreatic beta cells and thereby is increasing the plasma concentrations of insulin (Sola et al., 2015). Hence, it is an effective glucose-lowering agent used to treat type 2 diabetes. Also, glipizide's neuroprotective effect has been shown in the mouse hippocampus, and it appears to be mediated by lowering the blood glucose level (Kim et al., 2014). However, acute treatment with glipizide was not anti-hyperglycaemic in Wfs1-deficient mice (Sedman et al., 2016).

2.6.1.3 GLP-1 receptor agonists

Glucagon-like peptide-1 (GLP-1) is an incretin that is released from the gut after a meal to increase glucose-dependent insulin secretion, slow gastric emptying and inhibit food intake. These antidiabetic effects make GLP-1 suitable for the treatment of type 2 diabetes mellitus. GLP-1 has a very short half-life (1.5–5 min), hence, its use in the clinical setting is limited (Müller et al., 2019). Therefore, GLP-1 analogues with a longer half-life have been created and can be used as an

anti-diabetic treatment. Currently, there are seven GLP-1 receptor agonists that are approved by the EMA (European Medicines Agency): short-acting exenatide and lixisenatide and long-acting liraglutide, exenatide, dulaglutide, and semaglutide. All previously mentioned GLP-1 analogues are administered subcutaneously; the first orally administered GLP-1 analogue is semaglutide tablet for once-daily oral use (Table 1) (Trujillo et al., 2021).

GLP-1 acts on the GLP-1 receptor that is expressed on the pancreatic beta cells and throughout the brain on neurons (Baggio and Drucker, 2014), astroglia cells (Reiner et al., 2016) and microglia cells (Spielman et al., 2017). GLP-1 receptor activation leads to an increase of intracellular cAMP, which then activates protein kinase A (PKA), and phosphoinositide 3-kinase (PI3K). After PI3K activation, different downstream signalling pathways are activated, which are involved in promoting cellular proliferation, inhibition of ER stress, oxidative stress, apoptosis, inflammation and protein aggregation (Athauda and Foltynie, 2016). Such cytoprotective properties could also be beneficial in the treatment of neurodegenerative diseases because diabetes mellitus and neurodegenerative diseases share common pathophysiological features, such as cellular stress, inflammation, insulin resistance and abnormal protein processing (Salcedo et al., 2012).

Of the previously listed GLP-1 receptor agonists, liraglutide has the highest homology (97% amino acid homology) to native GLP-1 and is also able to cross the blood-brain barrier (Hunter and Hölscher, 2012). For these reasons, the neuroprotective role of liraglutide has been studied in different neurodegenerative diseases, such as in animal models of stroke (Sato et al., 2013), Alzheimer's disease (Hansen et al., 2016) and Parkinson's disease (Liu et al., 2015).

From the above, it can be suggested that neuroprotective drugs used for diabetes mellitus could also possibly provide an effective treatment option for Wolfram syndrome. Exenatide's antihyperglycaemic effect has been shown in Wfs1-deficient mice (Sedman et al., 2016). However, the neuroprotective effect of GLP-1 receptor agonists has not been studied in connection with Wolfram syndrome.

Table 1. GLP-1 receptor agonists currently approved by the EMA (European Medicines Agency). Table is prepared according to (Trujillo et al., 2021).

	Drug	First approved in Europe	Dose	Half life
1	Exenatide (Byetta)	2006	5–10 μg twice daily	2.4 h
2	Lixisenatide (Adlyxin, Lyxumia)	2013	10–20 μg once daily	3 h
3	Liraglutide (Victoza)	2009	0.6–1.8 mg once daily	13 h
4	Exenatide (Bydureon)	2011	2 mg once weekly	not reported
5	Dulaglutide (Trulicity)	2014	0.75–1.5 mg once weekly	5 days
6	Semaglutide (Ozempic)	2018	0.25–1 mg once weekly	1 week
7	Oral Semaglutide (Rybelsus)	2020	3–14 mg once daily	1 week

2.6.2 BDNF mimetic 7,8-DHF

Brain-derived neurotrophic factor (BDNF) is a neurotrophin that binds to Tropomycin receptor kinase B (TRKB) receptor and regulates neuronal development, synaptic function and synaptic plasticity, and modulates neuronal survival (Huang and Reichardt, 2001). In addition to BDNF's neuronal roles, it is also important in regulating global metabolic function (Cai et al., 2012). BDNF conditional mutant mice developed obesity and had elevated serum levels of leptin, insulin, glucose, and cholesterol (Rios et al., 2001). In humans, mutation of *NTRK2*, which encodes TRKB, results in a unique human syndrome of hyperphagic obesity and global developmental delay with specific impairment of short-term memory, stereotyped behaviours, and impaired nociception (Yeo et al., 2004). BDNF levels significantly decrease with age, which is associated with increased risk for cardiovascular disease and metabolic syndrome (Golden et al., 2010).

BDNF use is limited in clinical practice mostly because of its inability to cross the blood-brain barrier (Poduslo and Curran, 1996). Therefore, small molecules acting as BDNF mimetics have been investigated, and the naturally occurring flavone 7,8-dihydroxyflavone (7,8-DHF) was found acting as a TRKB receptor agonist (Jang et al., 2010). *In vivo* 7,8-DHF is able to improve spatial learning and memory in cognitively impaired aged rats (Zeng et al., 2012) and prevent synaptic loss and memory deficits in a mouse model of Alzheimer's disease (Zhang et al., 2014). Additionally, *in vitro* 7,8-DHF reduces fat production and fat build-up (Choi et al., 2016). Currently, 7,8-DHF is available as a dietary supplement (https://nootropicsdepot.com/7-8-dihydroxyflavone-capsules/).

2.6.3 Ongoing clinical trials for Wolfram syndrome

2.6.3.1 Dantrolene

Dantrolene is a skeletal muscle relaxant and it is used for the treatment of malignant hyperthermia, which is a life threatening genetic sensitivity of skeletal muscles to volatile anaesthetics and to depolarizing neuromuscular blocking drugs occurring during or after anaesthesia (Krause et al., 2004; Mh, 1975). Dantrolene, an inhibitor of RYR1 and RYR2 (Oo et al., 2015), stabilizes ER calcium levels and thereby also provides neuroprotection in *in vivo* models of ischemia (Wei and Perry, 2002), epileptic seizures (Mikami et al., 2016) and spinal cord injury (Thorell et al., 2002). It has been demonstrated that dantrolene can prevent ER stress-mediated cell death in human and rodent Wolfram syndrome cell models. Moreover, 4-week dantrolene treatment suppressed calpain activation in brain lysates from Wfs1-deficient mice. Thus, it was concluded that dantrolene and other drugs that regulate ER calcium homeostasis could be used for the treatment of Wolfram syndrome and other diseases associated with ER dysfunction (Lu et al., 2014). Inspired by the previously mentioned results, a clinical trial of dantrolene in paediatric and adult patients with Wolfram syndrome was started in January 2017 in St. Louis, MO, USA, although its effectiveness and safety are still unknown (ClinicalTrials.gov: NCT02829268).

2.6.3.2 Valproate

Valproate is used as an antiepileptic drug, although its mechanism of action is still a matter of debate. Valproate can act via increasing the GABA concentration by reducing its degradation, blocking voltage-gated ion channels, and also by inhibiting histone deacetylase (Löscher, 2002; Rahman and Nguyen, 2020). Additionally, valproate inhibits ER stress-induced apoptosis and thereby has a neuroprotective effect (Kakiuchi et al., 2009). In Wfs1-deficient mice, it has been shown that acute treatment with valproate is effective in lowering blood glucose levels, possibly by potentiating insulin action (Terasmaa et al., 2011); however, chronic treatment with valproate for 3 months had no effect on glucose tolerance (Punapart et al., 2014). Nevertheless, a clinical trial of valproate in paediatric and adult patients with Wolfram syndrome was initiated in December 2018 in Birmingham, UK, and the efficacy, safety and tolerability of valproate are still unknown (ClinicalTrials.gov: NCT03717909).

2.7 Animal models for studying Wolfram syndrome

Well-characterized Wolfram syndrome animal models are essential to develop treatment strategies for Wolfram syndrome *in vivo*. Wfs1-deficient mouse models have mainly been used to study diabetes mellitus as the mice developed glucose intolerance (Ishihara, 2004; Riggs et al., 2005). Additionally, Wfs1-deficient mice have been used to describe WFS1 localization in the brain (Luuk et al., 2008) and to study the role of WFS1 in the development of mood disorders (Luuk et al., 2009). However, these animal models have not been studied systematically, and the main emphasis has been on diabetes. Relatively few studies have focused on neurodegeneration, and no systematic evaluation of all Wolfram syndrome symptoms has been done up to now. Thus, a more systematic approach is needed to better understand how far the Wolfram syndrome pathology develops in Wolfram syndrome animal models and how the phenotype correlates with Wolfram syndrome patients. To fill in the gap, our research group has created the Wfs1 KO rat. Rats have many advantages over mice for conducting physiological and neuroscience studies. The larger size of the rat offers experimental advantages, such as the possibility of repeated blood sampling, better anatomical resolution in MRI and more material for biochemical analysis (Iannaccone and Jacob, 2009).

3 AIMS OF THE STUDY

As there is no cure for Wolfram syndrome, animal models are needed to test the treatment options. WFS1 protein is expressed mostly in the brain and pancreas, which share many common features, and investigating the shared part might help in finding a treatment for Wolfram syndrome. GLP-1 receptor agonists and neurotrophic factors are potential cures for Wolfram syndrome. So far, all preclinical treatments have been done in mice, hence the aim of this thesis was to systematically characterize the Wolfram syndrome rat and use it for the evaluation of novel treatment strategies.

Specifically, the aims of this study are:

1. To evaluate the symptoms of Wolfram syndrome in Wfs1 KO rats.

2. To investigate if early intervention with liraglutide has a preventive effect on the progression of glucose intolerance in a rat model of Wolfram syndrome.

3. To investigate if late intervention with GLP-1 receptor agonist liraglutide has a neuroprotective effect and can thereby prevent the progression of inferior olive neurodegeneration in a rat model of Wolfram syndrome.

4. To investigate if liraglutide has a protective effect on the hippocampus as we have seen in the pancreas and in the brainstem and if 7,8-DHF alone or in combination with liraglutide has a neuroprotective effect on the hippocampus in a rat model of Wolfram syndrome.

4 MATERIALS AND METHODS

4.1 Experimental animals (Paper I, II, III, IV)

Generation of the Wfs1 KO rat line is described in Plaas et al. 2017. Briefly, exon 5 of Wfs1 gene was deleted using zinc-finger technology, resulting in a loss of 27 aa from the WFS1 protein sequence (aa 212–238) and a substitution of serine to alanine at position 239. Breeding and genotyping of Wfs1 exon 5 knock-out Sprague-Dawley rats (Wfs1 KO) were performed at the University of Tartu Laboratory Animal Centre. Rats were housed in cages in groups of 2 to 4 rats per cage under a 12-h light/dark cycle (lights on at 7 am). Only male rats were used. Rats had unlimited access to food and water except during testing. Sniff universal mouse and rat maintenance diet (Sniff cat# V1534) and reverse osmosis-purified water were used. Experiments were performed between 9 am and 5 pm. All experimental protocols were approved by the Estonian Project Authorisation Committee for Animal Experiments (No. 54, 23th of February 2015, Paper I), (No 103, 22nd of May 2017, Paper II and III), (No 155, 6th of January 2020, Paper IV), and all experiments were performed in accordance with the European Communities Directive of September 2010 (2010/63/EU) (Plaas et al., 2017; Seppa et al., 2019, 2021; Toots et al., 2018).

4.2 Animal experiments

4.2.1 Chronic liraglutide treatment (Paper II)

The rats were 2 months old at the beginning of the experiment. After the first IPGTT test, the rats were randomly allocated into the liraglutide or control groups (WT Sal, n = 15; WT Lira, n = 12; KO Sal, n=15; KO Lira, n=13). The liraglutide group animals received 0.4 mg/kg liraglutide (Novo Nordisk, Denmark), and the control group animals received a 0.9% saline solution subcutaneously. Injections of 1 ml/kg volume were made once a day between 8 and 11 am (or immediately after a glucose/insulin tolerance test). Rats were weighed once a week. Glucose tolerance and insulin tolerance tests were performed 24 hours after the previous liraglutide/saline injection. After 5 months of treatment, the rats were euthanized (Toots et al., 2018).

4.2.2 Chronic liraglutide treatment (Paper III)

The rats were 8 months old at the beginning of the experiment. Rats were randomly allocated into the liraglutide or control groups (WT Sal, n = 8; WT Lira, n = 10; KO Sal, n=6; KO Lira, n=8). The liraglutide group animals received 0.4 mg/kg liraglutide (Novo Nordisk, Denmark), and the control group animals received a 0.9% saline solution subcutaneously for 6 months. Injections of 1 ml/kg volume

were made once a day between 8 and 11 am. Rats were weighed once a week, and their base blood sugar level was measured once a month from the tail vein using a handheld glucometer (Accu-Check Go, Roche, Germany) (Seppa et al., 2019).

4.2.3 Chronic liraglutide and 7,8-DHF treatment (Paper IV)

The rats were 9 months old at the beginning of the experiment. Rats were randomly allocated into eight experimental groups: (WT Sal, n = 5; WT Lira, n = 5; WT Dhf, n= 5; WT Lira+Dhf, n=6; KO Sal, n=6; KO Lira, n=7; KO Dhf, n=7; KO Lira+Dhf, n= 8). Saline-treated animals served as control animals. Drugs were administered once a day between 8 and 11 am. Rats were weighed once a week, and their base blood sugar level was measured once a month from the tail vein using a handheld glucometer (Accu-Check Go, Roche, Germany). Liraglutide (Lira) from commercially available pens (NovaNordisk) was diluted with 0.9% saline and injected s.c. at a dose of 0.4 mg/kg. Saline was administered in a volume of 1ml/kg. BDNF mimetic 7,8-dihydroxyflavone (7,8-DHF, catalog #D1916, Tokyo Chemical Industry CO Ltd, Tokyo, Japan) was first dissolved in DMSO (at a concentration of 400 mg/ml) and was further diluted 1:20 with PEG-300/PBS mix (1:1). The final composition of the 7,8-DHF injection solution was 20 mg/ml 7,8-DHF in 5% DMSO, 47.5% PEG-300, 47.5%PBS. The drug or the saline solution was administered subcutaneously in a volume of 0.25 ml/kg, and the dose of 7,8-DHF was 5 mg/kg. Treatments lasted for 3.5 months. To avoid hyperglycaemia-induced symptoms, supportive insulin treatment (100IU/ml, Levemir, Novo Nordisk, Denmark) was initiated in hyperglycaemic Wfs1 KO rats. Animals with a blood glucose level of 10 mmol/L or more received 2 IU/kg insulin, and animals with a blood glucose level of 20 mmol/L or more received 6 IU/kg insulin twice per day injected subcutaneously (Seppa et al., 2021).

4.2.4 Intraperitoneal glucose tolerance tests (IPGTT) (Paper I, II)

Animals were deprived of food for 3 h before and during the experiment; water was available throughout the experiment. D-Glucose (Sigma-Aldrich) was dissolved in a 0.9% saline solution (20% w/vol) and administered intraperitoneally at a dose of 2 g/kg of body weight. Blood glucose levels were measured from the tail vein using a handheld glucometer (Accu-Check Go, Roche, Germany) before glucose administration and at the time points 30 min, 60 min, 120 min and 180 min after glucose administration. Blood samples were drawn and collected from the tail vein before and 30 min after glucose administration for further analyses (Plaas et al., 2017; Seppa et al., 2019; Toots et al., 2018).

4.2.5 *In vivo* magnetic resonance imaging (Paper I, III, IV)

Rats were anaesthetized using isoflurane (1.5–2.5% in 1.5 l/min medical oxygen) and placed on a heated animal bed throughout the MRI procedure. All scans were

performed using a 9.4T Bruker BioSpec 94/20 USR system connected to a 1 H circular polarized transceiver coil and running ParaVision 6.0.1® software (Bruker BioSpin Group, Bruker Corporations, Germany). Respiration and temperature were monitored using a respiration pillow and a rectal probe (SA Instruments Inc., Stony Brook, USA). Respiration rate was maintained at 35–50 breaths per minute. Two orientation pilot scans were performed to establish the position of the animal and identify anatomical landmarks relevant for planning the subsequent scan. The final T2-weighted Turbo RARE sequence was performed using the following parameters: repetition time (TR) 6803 ms, echo time (TE) 33 ms, flip angle 90 degrees, number of averages 5, imaging matrix $320 \times 320 \times 65$, spatial resolution $0.16 \times 0.16 \times 0.5$ mm. Volumes were segmented manually by an observer blinded to the genotype using ITK-SNAP (V3.6.0) software (Yushkevich et al., 2006). The Scalable Brain Atlas (Bakker et al., 2015) was used to determine the segmentation start.

In Paper I and III, for the medulla, segmentation began from the caudal end of the inferior colliculus and continued until reaching the most caudal level of the cerebellum (bregma −9.48 to −15.48 mm). In all animals, the medulla and EPS were measured on 12 consecutive slices (Plaas et al., 2017; Seppa et al., 2019).

In Paper IV, for the hippocampus, segmentation began from bregma –1.45 mm and continued to –5.82 mm until reaching the most caudal end of the thalamus. In all animals, the hippocampus was measured on 10 consecutive slices. From the same images, lateral ventricles were delineated based on the nearly saturated bright signal in T2-weighted images from bregma –3.32 mm to –4.57 mm (Seppa et al., 2021).

4.2.6 Morris water maze (Paper IV)

On experiment days, the rats were allowed to adapt to the experimental room for two hours. The Morris water maze consisted of a 180-cm-diameter plastic pool filled with room-temperature water (20–22 °C). The escape platform (diameter, 14 cm; height, 29 cm) was placed in a fixed position in the centre of one quadrant, 35 cm from the perimeter, and was hidden 1 cm beneath the water surface. Six black and white cues were fixed around the water maze. The water was tinted black using tempera paint to allow automatic video recording of albino rats with EthoVision software (Noldus Information Technology, Wageningen, Netherlands). The acquisition phase lasted four days, and four trials were performed per day. For each trial, an animal was placed into the pool at a pseudo-random location facing the wall of the pool. Rats were allowed to find the platform during a 60-sec session and were guided to the platform if they failed to find it. Rats had to remain on the platform for 30 sec before they were rescued and placed in a cage filled with paper towels. The next session started after a 60-sec rest period. Latency to find the platform and time in the target quadrant were recorded during the acquisition phase. The platform was removed on the probe day (fifth day of the experiment), rats were released at an unfamiliar location (same for all animals) and allowed to search for the platform for 60 sec. Time to find the platform and percentage of time in the target quadrant were recorded (Seppa et al., 2021).

4.3 Isolation of islets of Langerhans (Paper II)

Islets of Langerhans were isolated as described previously (Carter et al., 2009). 0.9 mg/ml collagenase (Sigma-Aldrich, #C7657) solution was injected into the common bile duct of euthanized animals; inflated pancreases were collected, and tissues were enzymatically dispersed. Most of the exocrine tissue was removed by gradient separation in Histopaque solution (Sigma-Aldrich). Islets of Langerhans were collected by hand from the remaining exocrine tissue under a stereo microscope (Toots et al., 2018).

4.4 RNA isolation, cDNA synthesis and gene expression analyses (Paper I, II, IV)

RNA was isolated using Direct-zol RNA MiniPrep (Zymo Research, R2052) according to the manufacturer's protocol. RNA concentration and quality were assessed with NanoDrop 2000c (Thermo Fisher Scientific). 500 ng RNA was used for cDNA synthesis. Random Hexamer Primers 120 µl 0.2 µg/ul (Thermo Fisher Scientific, Cat# SO14, dNTP Mix (10 mM) (Invitrogen, Cat# 18427013) and SuperScript III Reverse Transcriptase (200 units/µl) (Thermo Fisher Scientific, Cat# 18080044) were used to synthesize first-strand cDNA. Taqman Gene Expression Mastermix (Thermo Fisher Scientific, Cat# 4369016) and TaqMan Gene Expression Assays in reaction volume 10 ul were used for qRT-PCR. The following assays were used, as shown on table 2. *Hprt1* was used as an internal control, and the $2^{-\Delta Ct}$ method was used for relative quantification. *Xbp1* (X-box binding protein 1) splicing was analysed using rat *Xbp1*-specific PCR, as has been described previously (Yusta et al., 2006). Integrated density levels were measured using ImageJ software (Plaas et al., 2017; Seppa et al., 2021; Toots et al., 2018).

Table 2. TaqMan Gene Expression Assays

Gene	Assay ID	Paper
Chop	Rn00492098_g1	I, IV
Grp78	Rn00565250_m1	I, II, IV
FoxP2	Rn01456150_m1	I,
Wfs1	Rn00582735_m1	I,
Ip10	Rn01413889_g1	II, IV
Ki67	Rn01451446_m1	IV
Tlr2	Rn02133647_s1	IV
Tlr4	Rn00569848_m1	IV
Hprt1	Rn01527840_m1	I, II, IV

4.5 Insulin, C-peptide, and glucagon measurements (Paper II)

For serum separation, blood was allowed to clot at room temperature for 30 min and then was centrifuged for 15 min at 2000 × g at 4 °C. Blood serum samples were stored in −80 °C until further analysis. Serum insulin, c-peptide and glucagon levels were measured using ELISA kits: rat insulin ELISA kit (CrystalChem cat# 90060), rat C-peptide ELISA (CrystalChem cat# 90055), and rat glucagon ELISA (CrystalChem cat# 81519), according to the manufacturer's instructions (Toots et al., 2018).

4.6 Immunohistochemistry

4.6.1 Tissue preparation (Paper I, II, III)

Rats were anaesthetized with an intraperitoneal injection of ketamine (100 mg/kg) and dexmedetomidine (20 mg/kg) in a volume of 10 ml/kg. Thereafter, rats were perfused transcardially with 300 ml PBS and then with 300 ml 4% paraformaldehyde (PFA, Sigma-Aldrich) in a 0.1 M phosphate buffer (PB, pH 7.4). Tissues (pancreas or/and brain) were dissected and further fixed in the same fixative overnight at 4 °C. Tissues were placed in a 30% sucrose (AppliChem)/0.1 M PBS until they sank and then were frozen at –80 °C until further use.

4.6.2 Immunohistochemistry of the brainstem (Paper I)

40 µm thick sections of the brainstem were cut using a cryomicrotome (Microm HM-560) and collected on Superfrost Polysine Slides (Thermo Scientific). After washing with phosphate buffered saline (PBS) for 10 min, sections were permeabilized with 0.2% Triton X-100 (Naxo, Tartu, Estonia)/PBS solution for 40 min. Sections were further incubated in a blocking solution containing 5% donkey serum/1% bovine serum albumin (BSA, Sigma-Aldrich)/PBS for 2 h at room temperature. Primary and secondary antibodies were diluted in 0.1% Tween-20/1% BSA/PBS. Sections were incubated with primary antibodies for 12 h at 4 °C and were then washed with PBS for 1 h. Sections were incubated with the appropriate secondary antibody at room temperature for 2 h. After subsequent washes with PBS (1 h), cell nuclei were counterstained with DAPI (4′,6-diamidino-2-phenylindole, Sigma-Aldrich) at a 1:2000 dilution in 0.1% Tween-20/PBS for 15 min and further washed with PBS. Sections were mounted in Vectashield mounting medium (Vector Laboratories Inc.) and covered with a 0.17-mm coverslip (Deltalab). Images were taken with an Olympus FV-1000 (Olympus) confocal microscope or Olympus BX51 Fluorescence Microscope and annotated with Adobe Photoshop CC (Adobe Systems Incorporated).

Primary antibodies and their dilutions were as follows: goat anti-FOXP2 (1:400, Everest Biotech, Cat# EB05226, Lot# 160409) and rabbit anti-WFS1

(1:400), as previously described (Luuk et al., 2008). Secondary antibodies and their dilutions were as follows: FITC AffiniPure donkey anti-rabbit (1:1000, Jackson ImmunoResearch Lab., 711–095–152, RRID:AB_2315776) and Rhodamine Red-X-AffiniPure rabbit anti-goat (1:1000, Jackson ImmunoResearch Labs Cat# 305-297-003, RRID:AB_2339496) (Plaas et al., 2017).

4.6.3 Determination of Langerhans islet mass (Paper I, II)

Langerhans islet mass was estimated as has been previously described (Iglesias et al., 2012). Pancreases were weighed, and 40-µm-thick serial sections were cut at intervals of 400 µm. 20–30 slices per pancreas were obtained and analysed. Sections were washed with PBS for 3 × 5 min, permeabilized with 0.2% Triton X-100 (Naxo, Estonia)/PBS solution for 30 min, incubated in 0.5% H_2O_2/PBS for 1 h, and blocked in 5% donkey serum/1% bovine serum albumin (BSA, Sigma-Aldrich)/PBS for 1 h. Primary and secondary antibodies were diluted in 0.1% Tween-20/1% BSA/PBS. Sections were incubated with mouse anti-insulin antibody (1:800, Cell Signaling Technology Cat# 8138 S RRID: AB_10949314) for 1 h and washed with PBS for 3 × 10 min, followed by incubation with donkey anti-mouse peroxidase conjugated antibody (1:2000, Rockland Cat# 610-703-002 RRID: AB_219700) for 30 min and washed with PBS 3 × 5 min. Sections were incubated in 0.025% diaminobenzidine (Sigma Aldrich)/0.005% H_2O_2/0.05% $CoCl_2$ (Sigma Aldrich)/PBS for 15 min and washed with water. Dried sections were mounted using PeRtEx (HistoLab) and covered with a 0.17 mm coverslip (Deltalab). Images were taken using a Leica SCN 400 slide scanner at 20x magnification. The images obtained were analysed using ImageJ software. Langerhans islet mass was calculated using the following equation: Langerhans islet mass (mg) = pancreas weight (g) × relative Langerhans islet surface (total islet area mm^2 /total pancreas area mm^2) × 1000 (Plaas et al., 2017; Toots et al., 2018).

4.6.4 Immunohistochemistry of inferior olive (Paper III)

Brainstems were serially sectioned, 50 µm coronally from caudal to rostral, Bregma level −13.30 to −11.80 mm (Paxinos and Watson, 2014) on a Microm HM355 cryostat (Microm International GmbH, Walldorf, Germany). Systematic series of sections were saved in cryoprotectant solution. Sections were washed (3 × 5 min) in Tris buffered saline (TBS) containing 0.3% Triton X-100 (TBST buffer), and then endogenous peroxidases were deactivated by incubating in peroxidase block (hydrogen peroxide) for 10 min with gentle agitation. Next, sections were rinsed with TBS and incubated with target retrieval solution (Dako, Glostrup, Denmark) for 30 minutes at 80 °C and washed again with TBST (3 × 5 min). Sections were blocked with blocking solution containing 10% goat serum/1% bovine serum albumin (BSA, Sigma-Aldrich)/TBST or 1% bovine serum albumin (BSA, Sigma-Aldrich)/TBST for 1 h at room temperature. Primary

and secondary antibodies were diluted in 1% BSA/TBST. Sections were incubated with primary antibodies overnight at 4 °C with gentle agitation and were then washed with TBST (3 × 15 min). Sections were incubated with the appropriate secondary antibody at room temperature for 2 h. After subsequent washes with TBS (3 × 15 min), sections were placed in solution for DAB reaction (Sigma–Aldrich) (10 min). Sections were washed with TBS (3 × 10 min), mounted on SuperFrost glass slides (MenzelGlaser) using 0.5% Gelatine (Sigma–Aldrich) + 0.05% Chromalum (BDH Chemicals Ltd) dissolved in distilled water, dried at room temperature for 20 min, rehydrated in distilled water for 15 min, and dehydrated in a graded series of ethanol solutions (2 min in 96%, 5 min in 99%). Finally, sections were cleared for 3 × 5 min in xylene, and cover slips (No. 0, Hounisen) were mounted using Eukitt Quick-hardening mounting medium (Sigma–Aldrich) (Seppa et al., 2019).

Primary antibodies and their dilutions were as follows: rabbit anti-GRP78 antibody (Abcam ab31390; 1:2000), goat anti-IBA1 antibody (Abcam ab107159; 1:1000), and rabbit anti-GFAP antibody (Synaptic Systems ab887720; 1:1000). Secondary antibodies and their dilutions were as follows: goat anti-rabbit (DAKO, REF P0448; 1:400) and rabbit anti-goat (DAKO, REF PO449; 1:400) (Seppa et al., 2019).

For illustrative panels (Figure 13–15), a Leica DM750 light microscope, a Leica HI PLAN 40x lens (NA = 0.17) and a Leica ICC50 HD, controlled by Leica Application Suite v.4.6.0 software, were used (Leica Microsystems, Switzerland) (Seppa et al., 2019).

4.6.5 Stereological estimate of inferior olive neuron number (Paper III)

Sections were stained in 0.25% thionin (CAS 78338-22-4, Sigma–Aldrich, St. Louis, Missouri, USA) for 60 sec, rinsed in distilled water for 5 sec, and dehydrated in a graded series of ethanol solutions (1 min in 70%, 2 min in 96%, 5 min in 99%). After clearing in xylene for 3 × 5 min, cover slips (No. 0, Hounisen, Skander-borg, DK) were mounted using Eukitt Quick-hardening mounting medium (CAS 25608-33-7, Sigma–Aldrich, Steinheim, DE). Sections were analysed using an Olympus BX51 light microscope (Olympus) equipped with a Prior motorized stage, a Heidenhain microcator, an Olympus UPlanApo 4× lens (NA = 0.16), an Olympus UPlanSApo 60× oil lens (NA = 1.35) and an Olympus DP70 digital camera controlled by newCAST (Visiopharm, Hoersholm, Denmark) software. There are three major subnuclei in the inferior olive: the medial nucleus, dorsal nucleus and principal nucleus. Delineation of the region of interest (ROI) was performed using a 4× objective, and the analyses were performed with a 60× oil objective, with total magnification of 2791.36 (Figure 17). The total number of neurons, N(neu), in the inferior olive was estimated using the optical fractionator (Gundersen, 1977, 1986; Dorph-Petersen et al., 2001):

$$N(neu) = \left(\frac{1}{ssf}\right) \cdot \left(\frac{1}{asf}\right) \cdot \left(\frac{1}{hsf}\right) \cdot \sum Q^{-}(neu)$$

where ssf, asf and hsf are referred to as the section sampling fraction (1/4); the area sampling fraction (counting frame area/(dx×dy)), in which (dx×dy) indicates step length in the x- and y-direction; and height sampling fraction (h/t_{Q-}, respectively. The height is denoted h and Q^{-}weighted section thickness is denoted t_{Q-}, and $\sum Q^{-}$ (neu) is the total number of neurons counted per rat in all examined sections. The step lengths in the x- and y-direction were 123 µm, and the area of the unbiased counting frame was 2125 μm^2. The guard height was 5 µm, and the disector height, h, was 10 µm, determined following a z-axis analysis. Cell soma volume estimates of individual neurons were estimated using the spatial rotator (Rasmusson et al., 2013). A systematic set of sections was used for the determination of cell density using the optical disector for GRP78, IBA1 and GFAP positive cells. The numerical density of neurons N_v is given by (Gundersen, 1977):

$$N_v\,(\text{cell}) = \frac{\sum Q^{-}(cell)}{h \cdot (a/p) \cdot \sum P} = \frac{\sum Q^{-}(cell)}{h \cdot \left(\frac{counting\ frame\ area}{p}\right) \cdot \sum P}$$

where p denotes the number of test points per counting frame; P denotes total number of test points hitting the ROI, and $\sum Q^{-}$ (cell) marks the total number of cells counted per rat in all examined sections. The counting frame area was 2125 μm^2, and the height, h, was 10 µm (Seppa et al., 2019).

4.7 Data analysis (Paper I, II, III, IV)

GraphPad Prism version 5 software (GraphPad Software Inc., San Diego, CA, USA), STATISTICA 8 package (StatSoft Inc, Tulsa, OK, USA) or GBStat V 8 (Dynamic Microsystems Inc., Silverspring, MD, USA) were used for statistical analysis, and $p < 0.05$ was considered statistically significant. The data are presented as the mean ± SEM and were compared using factorial ANOVA followed by Fisher's LSD tests, one-way ANOVA followed by Tukey's HSD tests or repeated measures ANOVA followed by Bonferroni post hoc test (Plaas et al., 2017; Seppa et al., 2019, 2021; Toots et al., 2018).

5 RESULTS AND DISCUSSION

5.1 Paper I

5.1.1 Development of glucose intolerance

First symptom required for Wolfram syndrome diagnosis is diabetes mellitus, which manifests at the age of 6 years (Rigoli et al., 2018). Degeneration of WFS1-expressing pancreatic beta cells is the cause for inadequate secretion of insulin and developing diabetes mellitus (Cano et al., 2007). Therefore, our aim was to investigate the development of diabetes mellitus in the Wfs1 KO rat on the molecular and functional level.

ER stress response in the lysates of isolated islets of Langerhans was evaluated by performing real-time quantitative PCR (qRT-PCR) analysis of the ER stress markers *Grp78* and spliced *Xbp1*. At the age of 3 months, *Xbp1* expression was increased in Wfs1 KO animals compared to WT littermates (Figure 3c). At the age of 7 months, the difference had increased (Figure 3d). No significant differences were detected between genotypes in *Grp78* expression (Figure 3a, b). This was probably due to different expression dynamics of *Grp78* and spliced *Xbp1* in pancreatic islets (Plaas et al., 2017).

Next, the functionality of Langerhans islets was assessed through an intraperitoneal glucose tolerance test that was performed at the age of 2, 3 and 6 months. At the age of 2 and 3 months, Wfs1 KO rats showed a progressive decrease in glucose tolerance (Figure 4a, b), and at the age of 6 months, Wfs1 KO rats had developed glucose intolerance (Figure 4c), which was confirmed by an area-under-the-curve analysis (Figure 4d) (Plaas et al., 2017).

As cellular stress was increased in isolated Langerhans islets, and the functionality of the Langerhans islets decreases over time, our next purpose was to assess Langerhans islet mass in time. Therefore, quantitative histological analyses were performed, and similarly to glucose tolerance data, at the age of 3 months, Langerhans islet mass was unchanged between genotypes (Figure 5a). Langerhans islet mass started to decline from the age of 7 months (Figure 5b), and at the age of 14 months, the rate of decline increased (Figure 5c) (Plaas et al., 2017).

Reduced glucose tolerance was in accordance with progressive decline of Langerhans islets, and this confirms that developing glucose intolerance is due to the degeneration of pancreatic Langerhans islets. Therefore, our results indicate a similar course of the development of diabetes mellitus in Wolfram syndrome patients and Wfs1 KO rats.

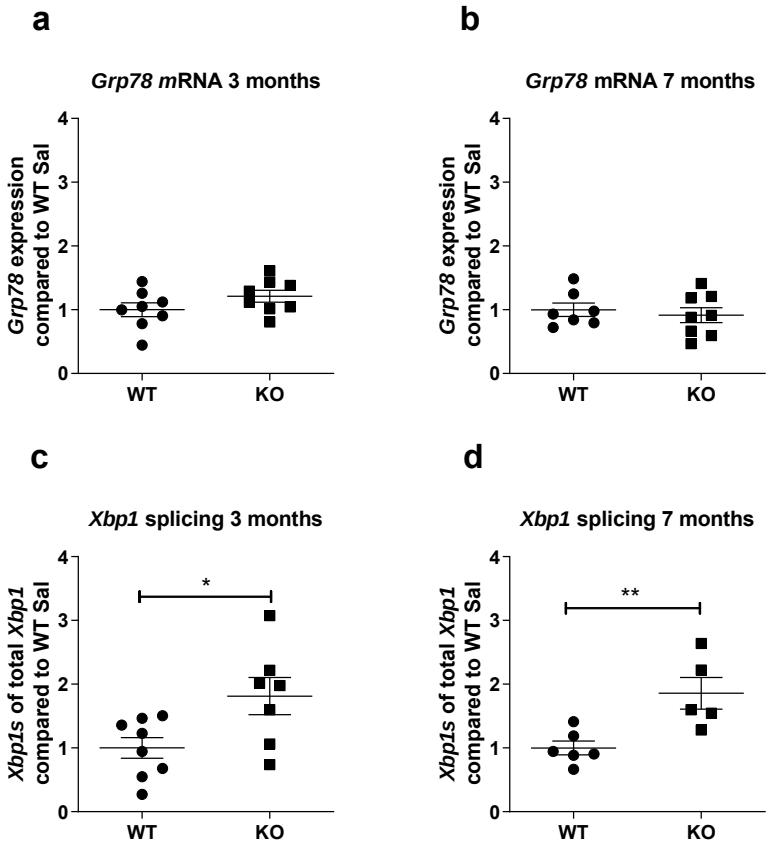

Figure 3. Wfs1 KO (KO) rats have elevated ER stress in Langerhans islets. qRT-PCR analysis of the ER stress markers (a, b) *Grp78* and (c, d) spliced *Xbp1* in lysates of isolated Langerhans islets at the age of 3 and 7 months. The data were compared using t-tests; *$p < 0.05$; **$p < 0.01$. The data are presented as the mean ± SEM, $n = 5$ to 8 (Plaas et al.,2017).

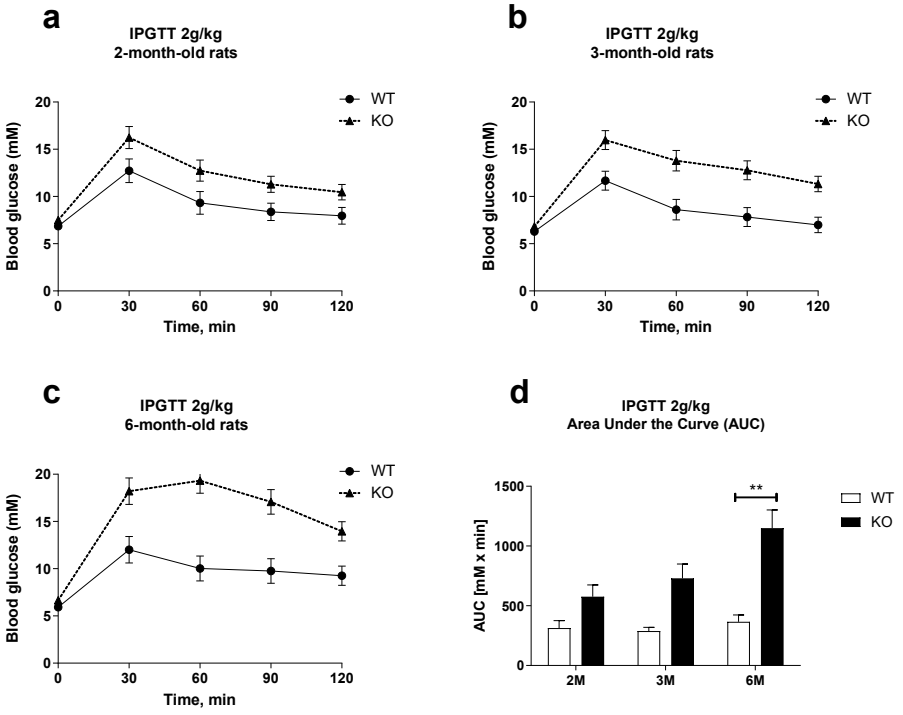

Figure 4. At the age of 6 months, Wfs1 KO (KO) rats have developed glucose intolerance. For intraperitoneal glucose tolerance tests (IPGTTs), blood glucose levels were measured after administration of glucose (2 g/kg i.p.), and the area under the curve was calculated. Glucose tolerance at the age of (a) 2 months, (b) 3 months and (c) 6 months. (d) Area-under-the-curve analyses from IPGTT results at different ages. The data were compared using two-way ANOVAs followed by Tukey's HSD tests; $^{**}p < 0.01$. The data are presented as the mean ± SEM, n = 6–8 (Plaas et al., 2017).

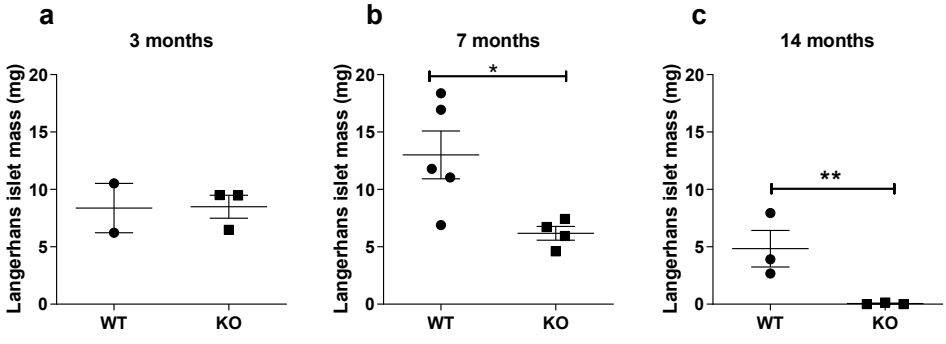

Figure 5. Wfs1 KO (KO) animals' Langerhans islet mass decreases in time. Quantitative histological analyses were performed to measure Langerhans islet mass. Langerhans islet mass at the age of (a) 3 months, (b) 7 months and (c) 14 months. The data were compared using two-way ANOVAs followed by Tukey's HSD tests; $^{*}p < 0.05$, $^{**}p < 0.01$. The data are presented as the mean ± SEM, n = 6–8 (Plaas et al., 2017).

5.1.2 Development of neurodegeneration

Quantitative neuroimaging studies have shown a loss of brainstem volume in Wolfram syndrome patients (Hershey et al., 2012; Lugar et al., 2016), and degeneration of the inferior olive is a recognized feature of Wolfram syndrome (Barrett and Bundey, 1997; Genís et al., 1997; Hilson et al., 2009; Khardori et al., 1983). Thus, we hypothesized that brainstem atrophy and inferior olive neurodegeneration are also present in Wfs1 KO rats. To test this hypothesis, we performed an immunohistochemistry analysis of the brainstem to find out if WFS1 is expressed in the olive nucleus. As FOXP2 (forkhead box P2) is visibly localized in all olive nucleus neurons throughout development, FOXP2 can be considered as a molecular marker of olive nucleus neurons (Fujita and Sugihara, 2012). Therefore, double immunofluorescence procedure was carried out and indeed, WFS1 is expressed in the brainstem, and WFS1 was localized mainly in the inferior olive (IO) (Figure 6a), exclusively in FOXP2-positive neurons (Figure 6c). FOXP2 neurons are excitatory neurons that terminate as climbing fibres in the cerebellum (Fujita and Sugihara, 2012). Climbing fibres play a central role in the execution and adaptation of motor behaviours (McKay et al., 2007) and thus, WFS1 might have a role in modulating motor behaviours.

Next, using gene expression analyses, ER stress levels were measured at the ventral brainstem at the level of the inferior olive. *Grp78* mRNA expression was unchanged at the age of 3 months, and at the age of 7 months, *Grp78* mRNA levels were elevated in Wfs1 KO animals compared to WT littermates (Figure 7b), which indicates ER stress at the level of the inferior olive. No significant differences were detected in *Chop* mRNA expression between Wfs1 KO and WT littermates (Figure 7c, d). This indicates that ATF6 pro-survival pathway of UPR response was activated and not the CHOP apoptosis pathway (Figure 2). Moreover, it has been shown that forced activation of the ATF6 UPR branch improved functional outcome and reduced infarct volume after stroke in conditional ATF6 knock-in mouse. Therefore, boosting UPR pro-survival pathways may be a promising therapeutic strategy for stroke and other ER associated diseases (Yu et al., 2017).

Quantitative *in vivo* MRI analysis revealed that, at the age of 15 months, brainstem volume per slice at the level of the inferior olive was reduced in Wfs1 KO rats compared to WT littermates (Figure 8d). Additionally, at the age of 15 months, the volume of the extraparenchymal space around the medulla was increased in Wfs1 KO rats compared to WT littermates, as seen in the total volume (Figure 8b) and in the volume per slice (Figure 8d).

Indeed, the reduced volume of medulla in Wfs1 KO rats shows similarities to the reduced volumes of medulla observed in Wolfram syndrome patients (Hershey et al., 2012). Additionally, the Wfs1 KO rat develops diabetes mellitus (Figure 4), as well as patients with Wolfram syndrome (Rohayem et al., 2011). Hence, the Wfs1 KO rat has the core symptoms of Wolfram syndrome. Therefore, the Wfs1 KO rat is a valuable Wolfram syndrome animal model and can be used to develop treatment strategies.

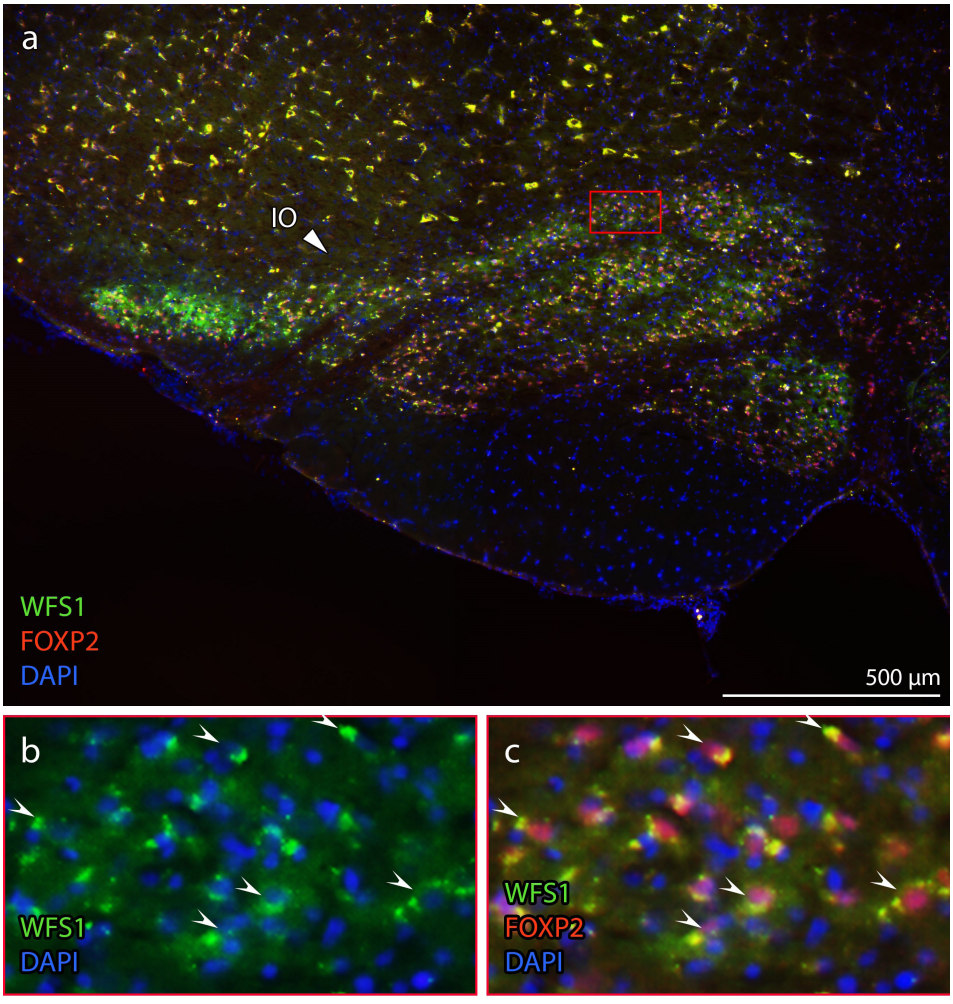

Figure 6. WFS1 protein is expressed in the inferior olive in the brainstem. (a–c) Immunohistochemical analysis revealed that WFS1 is localized in the inferior olive. (b) Higher magnification of the inferior olive from the red rectangle shows the cytoplasmic localization of WFS1 and that (c) WFS1 and FOXP2 were localized in the same set of cells in the IO (Plaas et al., 2017).

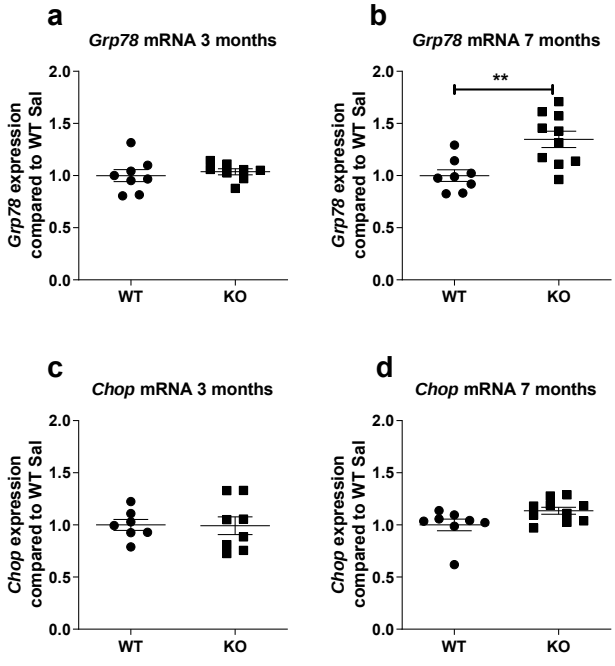

Figure 7. At the age of 7 months, Wfs1 KO (KO) rats have elevated ER stress in the brainstem at the level of the inferior olive. qRT-PCR analysis of the ER stress marker *Grp78* mRNA at the age of (a) 3 months and (b) 7 months and *Chop* mRNA at the age of (c) 3 and (d) 7 months. The data were compared using two-way ANOVAs followed by Tukey's HSD tests; $^{**}p < 0.01$. The data are presented as the mean ± SEM, n = 8 to 10 (Plaas et al., 2017).

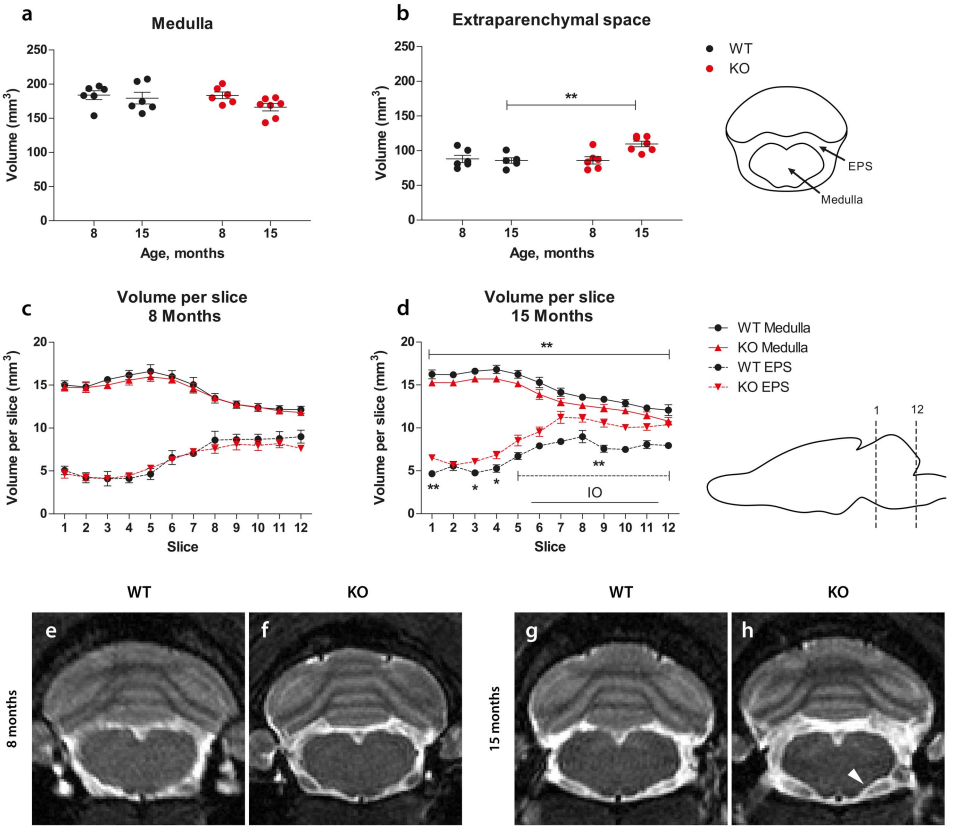

Figure 8. At the age of 15 months, Wfs1 KO (KO) rats have developed neurodegeneration in the brainstem at the level of the inferior olive. Results of quantitative MRI analysis of (a) the volume of medulla and (b) extraparechymal space (EPS). Volume per slice measurement data from (c) 8-month-old animals and from (d) 15-month-old animals. Representative MR images (e–h). At the age of 15 months, the ventral surface of the brainstem of Wfs1 KO rats appears to be more concave (arrowhead). The data were compared using two-way ANOVAs followed by Fisher's LSD tests; **$p < 0.01$ between genotypes. The data are presented as the mean ± SEM, n = 6–7 (Plaas et al., 2017).

5.1.3 Conclusion from Paper I

First, we showed that Wolfram syndrome rats develop ER stress in pancreatic Langerhans islets, degeneration of Langerhans islets and resultant glucose intolerance. Next, we described how WFS1 is expressed in the brainstem and that WFS1 was localized mainly in the inferior olive. In addition, in Wolfram syndrome rats' inferior olive there is elevated ER stress. Furthermore, at the level of the inferior olive, brainstem volume per slice was reduced, and the volume of the extraparenchymal space was increased. Together, these results demonstrate that ER stress occurs prior to cellular loss in the pancreas and decreases in brainstem volume in Wfs1 KO rats. Based on the information above, we conclude that the Wolfram syndrome rat develops glucose intolerance and neurodegeneration, and thus, the Wolfram syndrome rat model is suitable for investigating treatment options for Wolfram syndrome.

5.2 Paper II

The GLP-1 receptor agonist liraglutide was approved in Europe in 2009 for the treatment of diabetes mellitus and obesity, and since the approval, its neuroprotective effect has also been demonstrated in animal models of stroke (Sato et al., 2013), Alzheimer's disease (Hansen et al., 2016) and Parkinson's disease (Liu et al., 2015). As diabetes mellitus and neurodegeneration are also the core symptoms of Wolfram syndrome, our goal was to test the potential therapeutic effect of the GLP-1 receptor agonist liraglutide. We started with the liraglutide treatment before the development of diabetes to determine if liraglutide treatment can prevent the development of diabetes mellitus in the Wolfram syndrome rat model. At the beginning of the experiment, animals were 2 months old, and they were treated for 5 months with liraglutide (n=55, 12–15 per group) (Toots et al., 2018).

5.2.1 Liraglutide treatment protects against development of glucose intolerance

First, *in vivo* IPGTT was performed when the animals were 2 months old, and the results showed that there were no differences between the experimental groups at the beginning of the experiment (Figure 9a). Next, IPGTT's were performed after 2, 3.5, and 5 months of liraglutide treatment (Figure 9b–d). Figure 9 shows that saline-treated Wfs1 KO (KO Sal) animals develop glucose intolerance over time, while liraglutide-treated animals' glucose tolerance stayed at the same level as saline-treated wild-type (WT Sal) animals. This indicates that liraglutide treatment had a therapeutic effect and protected Wolfram syndrome rats from developing glucose intolerance (Toots et al., 2018).

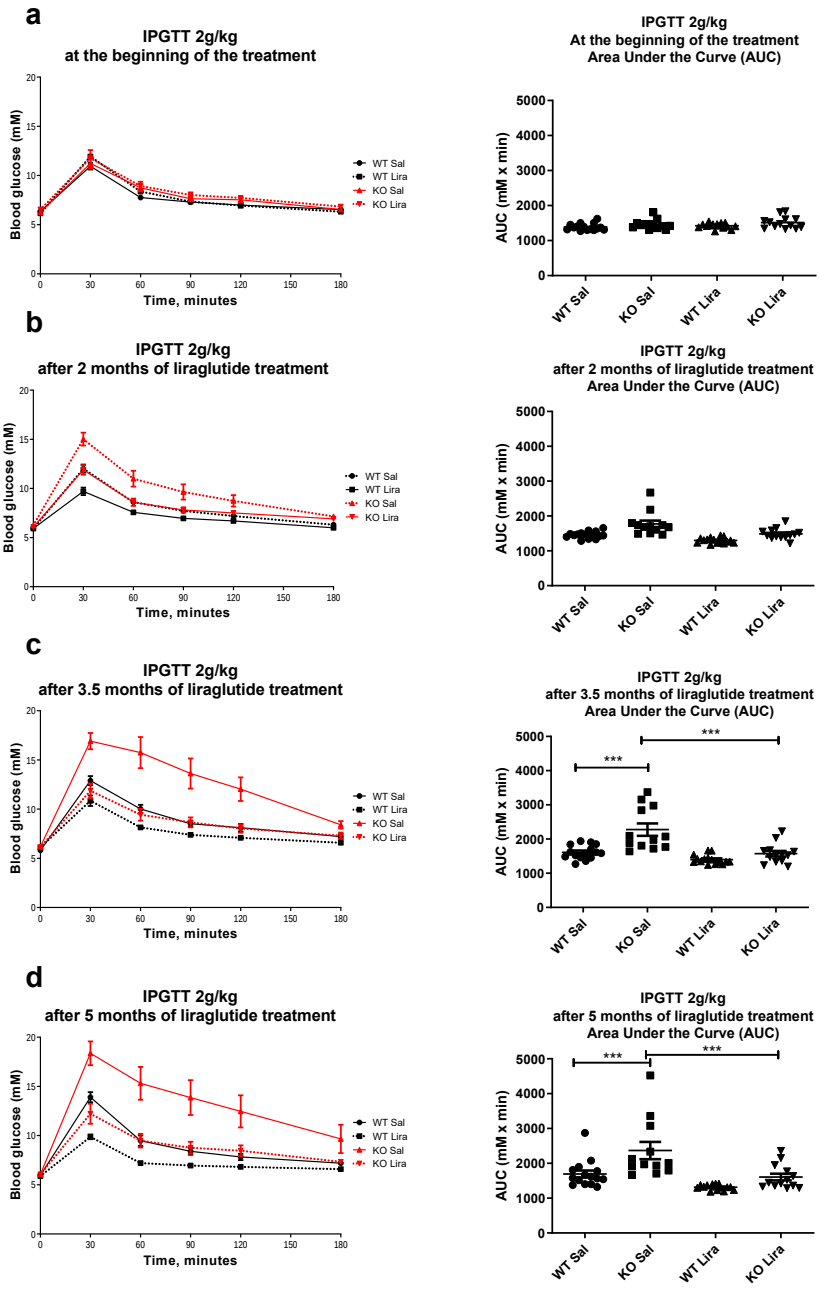

Figure 9. Liraglutide treatment protected Wfs1 KO (KO) rats from developing glucose intolerance. Intraperitoneal glucose tolerance tests (IPGTTs) were performed after administration of glucose (2 g/kg i.p.), and the area under the curve was calculated (a) at the beginning of the experiment, (b) after 2 months, (c) 3.5 months and (d) 5 months of liraglutide treatment. The data were compared using one-way ANOVA followed by Tukey's HSD tests; ***$p < 0.001$. The data are presented as the mean ± SEM, n=12–15 (Toots et al., 2018).

5.2.2 Liraglutide treatment protects Langerhans islets from ER stress

After 5 months of treatment, rats were euthanized, and gene expression analyses were performed to evaluate the effects of liraglutide treatment at the molecular level. First, ER stress marker *Grp78* mRNA levels were measured using qRT-PCR. In saline-treated Wfs1 KO animals, *Grp78* mRNA levels were elevated compared to WT Sal animals, which indicates ER stress in Wfs1 KO animals. Liraglutide treatment had a protective effect on Wfs1 KO rats' pancreatic islets, as liraglutide-treated Wfs1 KO rats' *Grp78* expression levels were indistinguishable from WT Sal animals (Figure 10a). Similarly to *Grp78* expression level, there was also a tendency to have elevated ER stress marker *Xbp1s* levels in Wfs1 KO animals, although the difference was not significant (Figure 10b). IP10 is an inflammatory chemokine that mediates immune responses through the activation and recruitment of leukocytes. IP10 is crucial for perpetuation of inflammation which leads to tissue damage (Vazirinejad et al., 2014). Here, inflammation marker *Ip10* mRNA levels were measured, and there was a tendency to have elevated inflammation in KO Sal animals, although the difference was not significant (Figure 10c). However, liraglutide treatment lowered the inflammation in Wfs1 KO animals compared to saline-treated Wfs1 KO animals, indicating an anti-inflammatory effect (Figure 10c). Cellular stress and inflammation lead to the development of diabetes mellitus (Oguntibeju, 2019) and by suppressing the inflammation and cellular stress, as we showed here and which has also been shown previously (Langlois et al., 2016), it could be possible to prevent the development of diabetes mellitus (Toots et al., 2018).

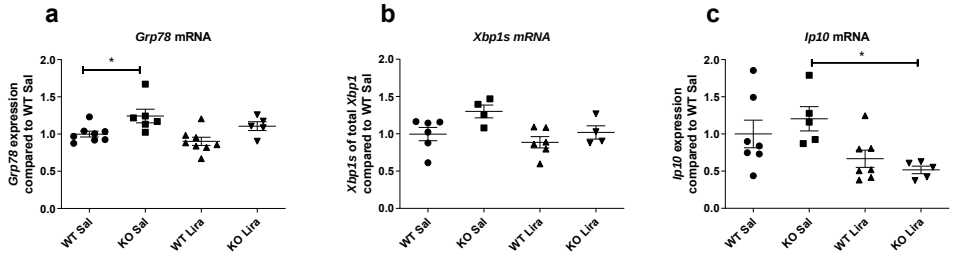

Figure 10. 5-month liraglutide treatment reduces cellular stress and inflammation in Wfs1 KO (KO) rats' pancreases. qRT-PCR analysis of isolated Langerhans islets, which were extracted from rats after 5 months of liraglutide treatment. ER stress markers (a) *Grp78* and (b) *Xbp1s*, inflammation marker (c) *Ip10*. The data were compared using factorial ANOVA followed by Tukey's HSD tests; *$p < 0.05$. The data are presented as the mean ± SEM, n = 4–8 (Toots et al., 2018).

5.2.3 Liraglutide treatment maintains Langerhans islet mass

We can suggest that in Wolfram syndrome rats, ER stress leads to inflammation and possibly to a decrease in insulin secretion, as seen in developed glucose intolerance in IPGTT. It is known that the human Langerhans islet consists mostly of insulin-secreting beta cells, which make up 60 percent of the total mass, along with 30% glucagon-producing α-cells and 10% somatostatin-producing δ-cells, pancreatic polypeptide-producing γ- or PP cells, and ghrelin-producing ε-cells (Da Silva Xavier, 2018). *WFS1* is mainly expressed in the islets' β-cells, and some expression is also found in δ-cells, but not in α-cells (Ueda et al., 2005). Hence, our next question was if glucose intolerance resulted from loss of insulin-secreting beta cell mass. To answer this question, our aim was to measure the Langerhans islet mass. Therefore, immunohistochemistry was performed. In agreement with previous results (Figure 5), Langerhans islet mass had declined in Wfs1 KO rats compared to WT saline-treated animals (Figure 11b), and liraglutide treatment was able to maintain Langerhans islets mass in Wfs1 KO animals. Surprisingly, Langerhans islet mass had also decreased in liraglutide-treated WT animals. Liraglutide is approved for chronic weight management in individuals with overweight or obesity (Garvey et al., 2020). Here we saw a strong body-weight-decreasing effect of liraglutide in both genotypes as well (Figure 11a). To take this into account, we divided Langerhans islet mass by body weight (Figure 11c), and consequently, the significance disappeared between WT animals' treatment groups (Figure 11c). Indeed, glucose intolerance might be caused by a decrease of the Langerhans islet mass, which in turn, is due to cellular stress and inflammation (Toots et al., 2018).

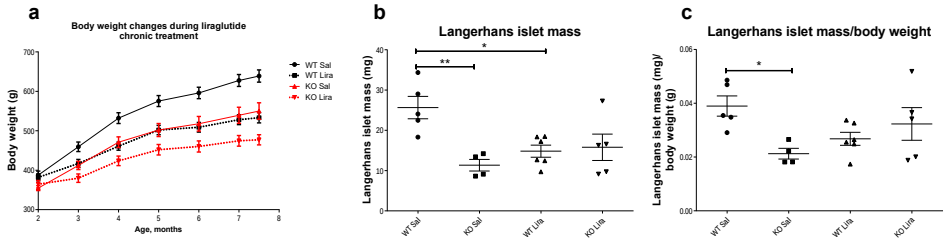

Figure 11. 5-month liraglutide treatment was able to maintain the mass of Langerhans islets in Wfs1 KO (KO) animals. To calculate the mass of Langerhans islets from the pancreas, immunohistochemistry was performed, and Langerhans islets were measured from anti-insulin antibody-stained pancreatic slices. (a) Body weight changes during liraglutide chronic treatment, (b) Langerhans islet mass, (c) Langerhans islet mass divided by body weight. The data were compared using one-way ANOVA followed by Tukey's HSD tests; *$p < 0.05$, **$p < 0.01$. The data are presented as the mean ± SEM, $n = 4–6$ (Toots et al., 2018).

5.2.4 Liraglutide treatment maintains Langerhans islet cells' cellular function

Liraglutide treatment had no statistically significant treatment effect on Langerhans islets' mass, although liraglutide treatment protected against the development of glucose intolerance *in vivo*. This may indicate that when the pancreatic beta cells are protected from cellular stress and inflammation, the cells retain their functionality and are able to secrete sufficient insulin. This hypothesis is confirmed by hormone measurements, which indicate that in liraglutide-treated Wfs1 KO animals, c-peptide and glucagon secretion was similar to WT Sal animals (Figure 12b, c). In addition, insulin secretion was slightly better in liraglutide-treated animals compared to Wfs1 KO saline-treated animals (Figure 12a).

Exenatide's acute antihyperglycaemic effect has been shown in a Wfs1-deficient mouse model (Sedman et al., 2016). Additionally, after publication of the current study, Kondo et al. showed in Wfs1-deficient mouse model that 4-week exenatide treatment resulted in restored glucose tolerance in IPGTT without affecting beta cell mass, similarly to our results (Kondo et al., 2018). They also described liraglutide's effect in a female Wolfram syndrome patient: 16 weeks of treatment with liraglutide modulated beta cell function and improved glycaemic control (Kondo et al., 2018). Furthermore, a recent study investigated a 15-year-old female patient with autosomal dominant WFS1-related disorder who had been on insulin-replacement therapy. Weekly subcutaneous administration of a GLP-1 agonist, dulaglutide, led to improved glycaemic control, and no additional insulin was needed thereafter (Scully and Wolfsdorf, 2020).

Our data and previous research indicate that liraglutide has a strong anti-inflammatory effect that maintains or restores cellular functionality. However, further research is required to clarify this phenomenon.

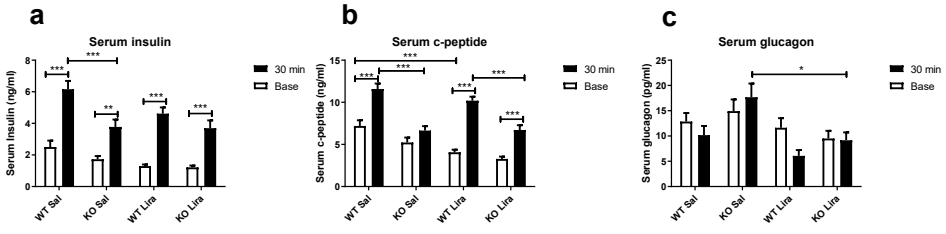

Figure 12. 5-month liraglutide treatment maintains Langerhans islet cells' cellular function in Wfs1 KO (KO) rats. Blood serum was collected before and 30 minutes after glucose administration during an intraperitoneal glucose tolerance test (IPGTT) and thereafter (a) insulin, (b) c-peptide and (c) glucagon levels were measured using ELISA kits. The data were compared using repeated measures ANOVA followed by Tukey's HSD tests; $*p < 0.05$, $**p < 0.01$, $***p < 0.001$. The data are presented as the mean ± SEM, n = 12–15 (Toots et al., 2018).

5.2.5 Conclusion from Paper II

5-month preventive liraglutide treatment protected Langerhans islets from ER stress, maintained Langerhans islets' cellular function and mass and thereby protected Wfs1 KO rats against development of glucose intolerance. Indeed, liraglutide had a protective effect against developing diabetes mellitus; however, it is still unknown whether liraglutide has a preventive or only delaying effect on diabetes in Wolfram syndrome rats. Additionally, liraglutide's effect on other Wolfram syndrome symptoms is still unknown (Toots et al., 2018).

5.3 Paper III

Wolfram syndrome rats develop brainstem atrophy at the level of the inferior olive (Figure 8d). Therefore, our next aim was to investigate whether liraglutide has a similar protective effect on the olive nucleus as it had on pancreatic beta cells. To mimic the relatively late diagnosis of Wolfram syndrome patients, we took 9-month-old animals who had already developed diabetes and treated them for 6 months with liraglutide (n = 32, 6–8 per group). Our goal was to determine the molecular changes in the olive nucleus after liraglutide treatment (Seppa et al., 2019).

5.3.1 Liraglutide treatment protects against ER stress in the inferior olive

First, stereological estimation of GRP78-positive cells (Figure 13a–d) was performed using the optical disector to estimate neuron densities. Since the volume of the different nuclei in the inferior olive was unchanged between groups (Figure 17), differences in neuron density can be regarded as changes in their total number. There were no differences in the medial nucleus (Figure 13e) nor in the dorsal nucleus (Figure 13f). However, there was an increased number of GRP78-positive cells in Wfs1 KO animals' principal nucleus (Figure 13g) and in all inferior olive nuclei together (Figure 13h). Liraglutide treatment decreased ER stress in Wfs1 KO animals' inferior olive (Figure 13g, h). This finding agrees with the previous results. Elevated ER stress levels are detected in Wfs1 KO rats' pancreases (Figure 3c, d) and in the ventral brainstem (Figure 7b). Additionally, liraglutide treatment reduced *Grp78* levels in Langerhans islets (Figure 10a). Thus, liraglutide treatment appears to have similar ER stress-lowering effects on both beta cells and on neurons in a rat model of Wolfram syndrome (Seppa et al., 2019). A similar ER stress response in beta cells and neurons suggests that the Wfs1 KO rat is a good animal model to study both diabetes and neurodegeneration (Seppa et al., 2019).

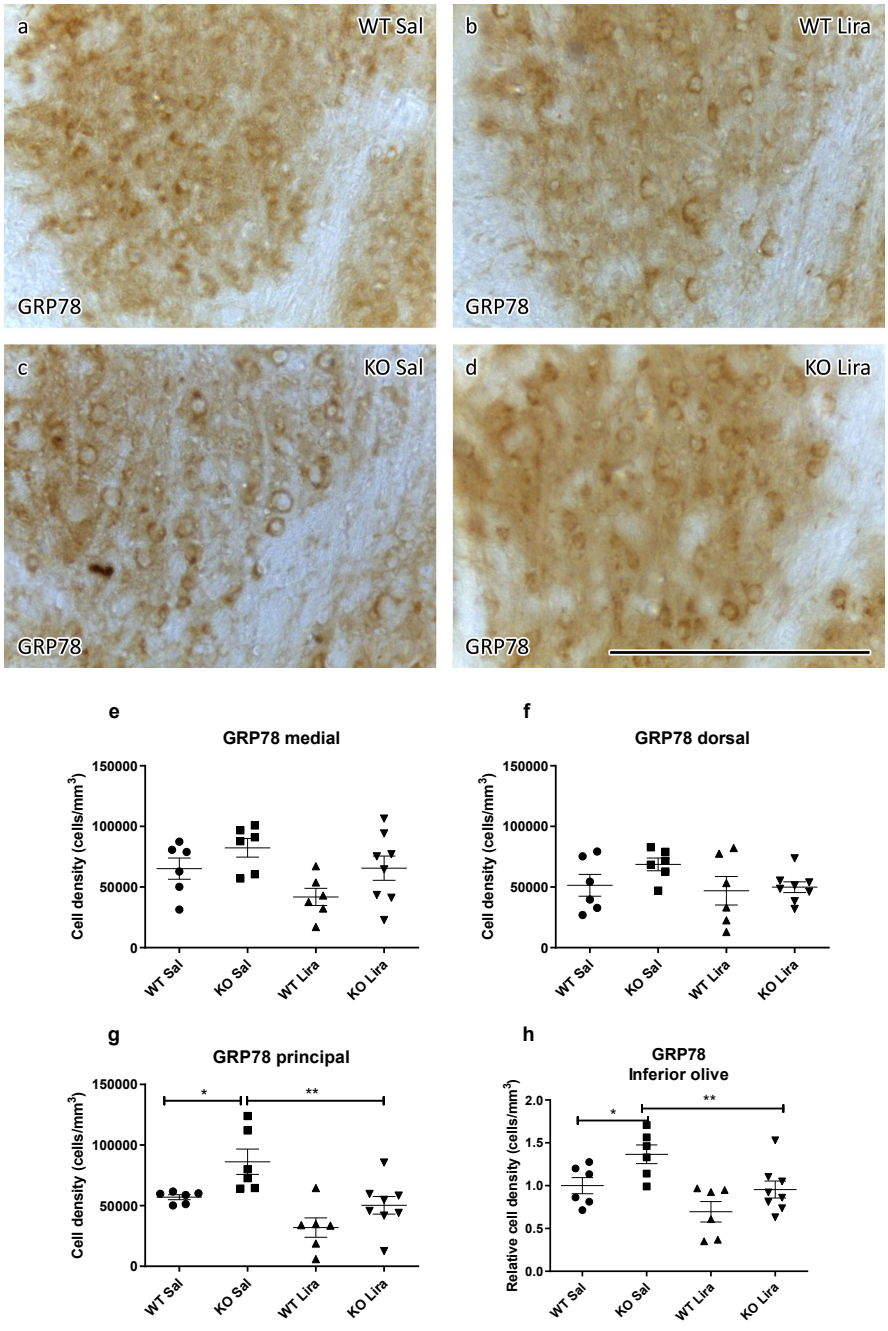

Figure 13. Liraglutide treatment protects Wfs1 KO (KO) rats against ER stress in the inferior olive. Representative histological images of GRP78-positive cells after 6 months of liraglutide/saline treatment in every treatment group and genotype (a) WT Sal, (b) WT Lira, (c) KO Sal, (d) KO Lira. Stereological quantification of cell density of GRP78-positive neurons was performed in the (a) medial nucleus; (b) dorsal nucleus; (c) principal nucleus; and (d) in all inferior olive nuclei together. The data were compared using factorial ANOVA followed by Fisher's LSD tests; *$p < 0.05$, **$p < 0.01$. The data are presented as the mean ± SEM, n = 6–8 per group. Scale bar 200 μm (Seppa et al., 2019).

5.3.2 Liraglutide treatment protects against neuroinflammation in the inferior olive

The neuroinflammation response, as measured by activated microglia (Hickman et al., 2018) and astroglia (Li et al., 2019) is a common feature of neurodegeneration. Hence, our next aim was to evaluate the neuroinflammatory response in the inferior olive. Therefore, the optical disector was used to estimate GFAP-positive astroglia cell densities in every treatment group (Figure 14 a–d), as GFAP is considered a marker protein for astrogliosis (Eng et al., 2000). The density of GFAP-positive astrocytes was increased in saline-treated Wfs1 KO animals compared to WT littermate animals, and liraglutide treatment protected Wfs1 KO animals from neuroinflammation (Figure 14e) (Seppa et al., 2019). Mild gliosis has also been reported in connection with Wolfram syndrome. A 37-year-old female Wolfram syndrome patient's post-mortem case study revealed mild gliosis in the spinal cord, hypothalamus, superior colliculi, inferior colliculi, vagus dorsal nuclei and ambiguus nuclei, in the anterior and dorsomedial nuclei of the thalamus, preoptic and paraventricular nuclei and in the substantia nigra (Genís et al., 1997). Also, a 38-year-old female Wolfram syndrome patient's case study showed widespread mild fibrillary gliosis in the superior and inferior colliculi, anterior and dorsomedial nucleus of the thalamus and, in addition, gliosis in the cochlear nuclei, mammillary bodies, mesencephalic, pontine and medullary tegmentum and the olfactory tracts and bulbs (Shannon et al., 1999). However, gliosis has not been described in the olive nucleus of Wolfram syndrome patients.

Ionized calcium-binding adapter molecule 1 (IBA1) is a microglial marker whose expression increases with microglial activation (Hopperton et al., 2018). Hence, to measure microglial activation, IBA1-poitive microglia cell densities in every treatment group were measured (Figure 15 a-d). IBA1-positive microglia cell density was increased in saline-treated Wfs1 KO animals compared to WT littermate animals, which indicates neuroinflammation in the inferior olive (Figure 15e). Treatment with liraglutide prevented such an increase in Wfs1 KO animals, indicating a neuroprotective effect (Seppa et al., 2019).

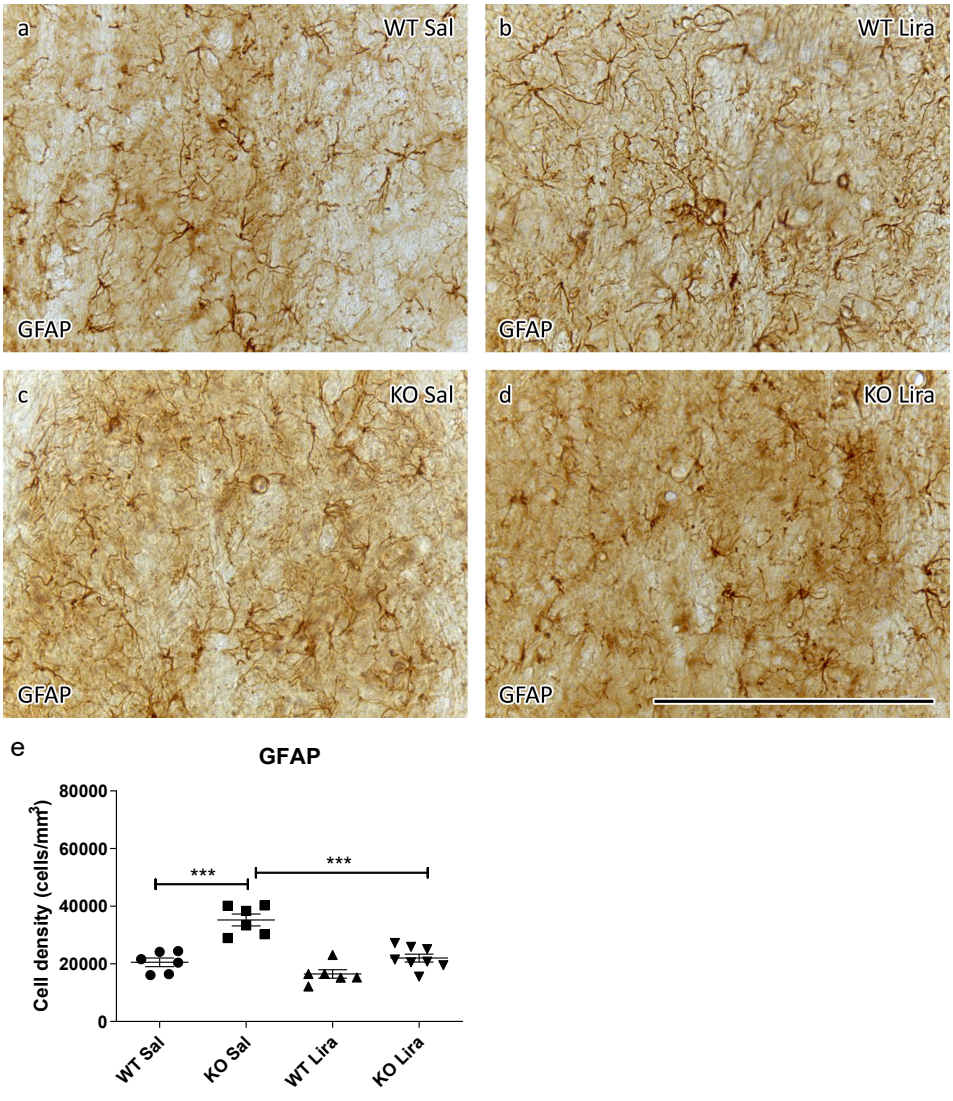

Figure 14. Liraglutide treatment protects against neuroinflammation in the inferior olive of Wfs1 KO (KO) rats. Representative histological images of GFAP positive astroglia cells after 6 months of liraglutide/saline treatment in every treatment group and genotype (a) WT Sal, (b) WT Lira, (c) KO Sal, (d) KO Lira. (e) Stereological quantification of GFAP-positive cells in the inferior olive after 6 months of liraglutide treatment. The data were compared using factorial ANOVA followed by Fisher's LSD tests, ***$p < 0.001$. The data are presented as the mean ± SEM, n = 6–8 per group. Scale bar 200 μm (Seppa et al., 2019).

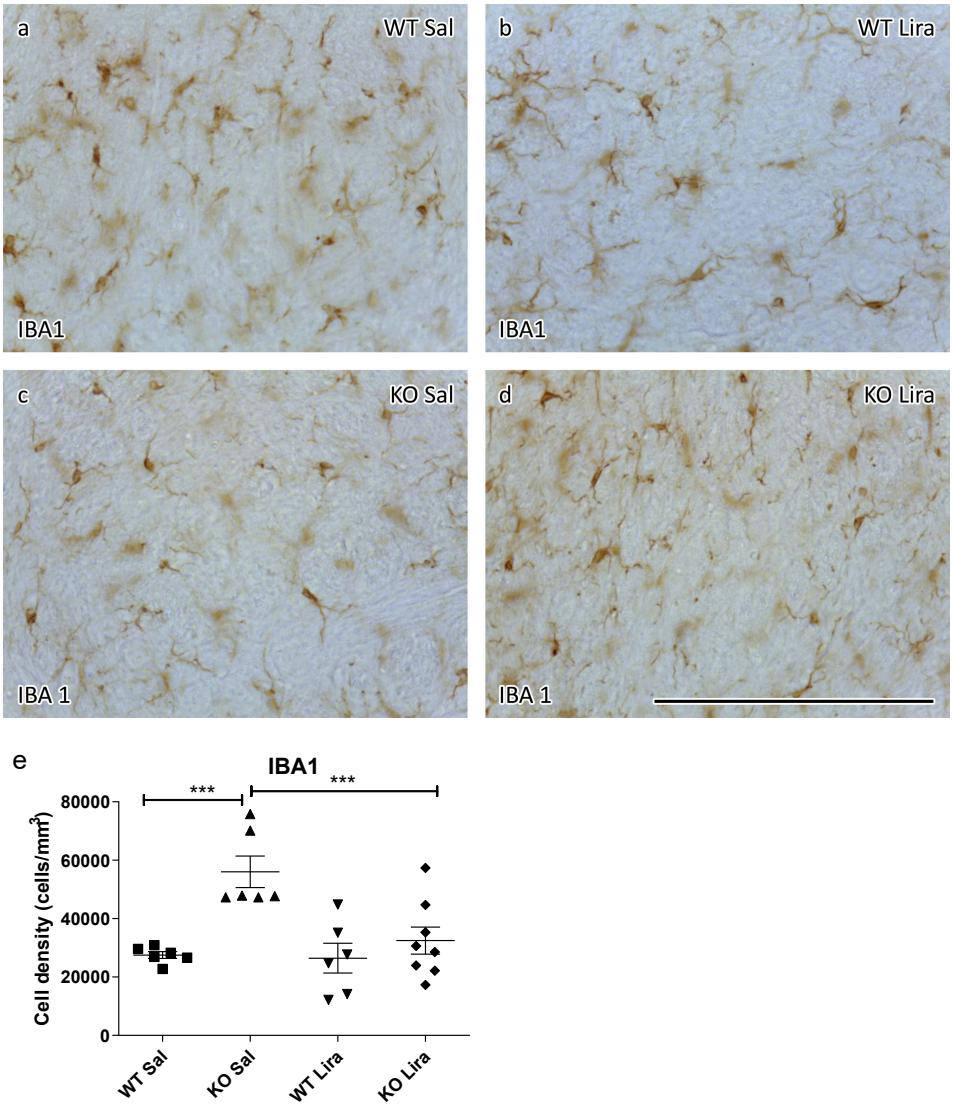

Figure 15. Liraglutide treatment protects against neuroinflammation in Wfs1 KO (KO) rats' inferior olive. Representative histological images of IBA1 positive microglia cells after 6 months of liraglutide/saline treatment in every treatment group and genotype (a) WT Sal, (b) WT Lira, (c) KO Sal, (d) KO Lira. (e) Stereological quantification of IBA1-positive cells in the inferior olive after 6 months of liraglutide treatment. The data were compared using factorial ANOVA followed by Fisher's LSD tests, ***$p < 0.001$. The data are presented as the mean ± SEM, n = 6–8 per group. Scale bar 200 µm (Seppa et al., 2019).

A connection between microglia and *Wfs1* has been reported previously, namely, hemin-treated microglia induced increased levels of *Wfs1*, along with increased levels of iNOS, TNF-α, HMOX1, NRF2, *Xbp-1* and spliced *Xbp-1* in mouse microglial cell line (Sayeed et al., 2017). Hemin is a toxic, endogenous break-down product of hemoglobin and partly causes stroke secondary injury, which involves microglia-induced inflammatory response (Robinson et al., 2009). This suggests that Wfs1 has a role in the activated microglia-induced inflammatory response. Moreover, knockdown of *Wfs1* in neurons and glial cells resulted in premature death and significantly exacerbated behavioural deficits in flies, suggesting that *Wfs1* has also an important function in glia cells (Sakakibara et al., 2018), and therefore, the role of Wfs1 in microglia activation is an important issue for future research.

The ability of liraglutide to enhance cytoprotective phenotypes has been demonstrated across different experimental neurodegeneration models, such as in animal models of stroke (Sato et al., 2013), Alzheimer's disease (Hansen et al., 2016) and Parkinson's disease (Liu et al., 2015). However, this is the first time that neuroinflammation has been described in a Wolfram syndrome animal model (Seppa et al., 2019).

5.3.3 Wfs1 KO rats have increased neuronal swelling

Next, the soma volume of individual neurons was measured using the spatial rotator. Neuronal volume was increased in all inferior olive subnuclei of Wfs1 KO rats compared to WT littermates (Figure 16a–d). Neuronal volume increase indicates possible neuronal swelling in Wfs1 KO animals. Neuronal swelling is a cytopathological response in which extracellular Na+ and other cations enter neurons and accumulate intracellularly. This results in an influx of anions and water, which in turn results in osmotic expansion of the cell. Additionally, neuronal swelling may include glutamate receptor activation and inhibition of Na+/K+–ATPase (Liang et al., 2007). Axonal swelling has also been shown in Wolfram syndrome patients. One Wolfram syndrome patient's post-mortem study showed occasional axonal swelling in the inferior olivary nuclear complex, in the dorsal motor nucleus of the vagus, in the medullary and pontine reticular formation and in the raphe nuclei (Shannon et al., 1999). In another post-mortem study, Purkinje cells showed axonal ballooning (Genís et al., 1997). It has previously been shown that there is an increased vulnerability to excitotoxicity-induced neurodegeneration in Wfs1 deficient flies (Sakakibara et al., 2018). Therefore, neuronal swelling might be induced due to Wolfram syndrome-related neuropathology caused by excitotoxicity. Liraglutide treatment decreased neuronal swelling in the medial nucleus in Wfs1 KO animals (Figure 16a), and hence, liraglutide treatment might have an anti-excitotoxicity effect. Liraglutide's ability to rescue neuronal cells from oxidative stress and glutamate excitotoxicity-induced cell death has also been previously shown (Li et al., 2015) and thus it can be suggested that liraglutide provides neuroprotection through this mechanism (Seppa et al., 2019).

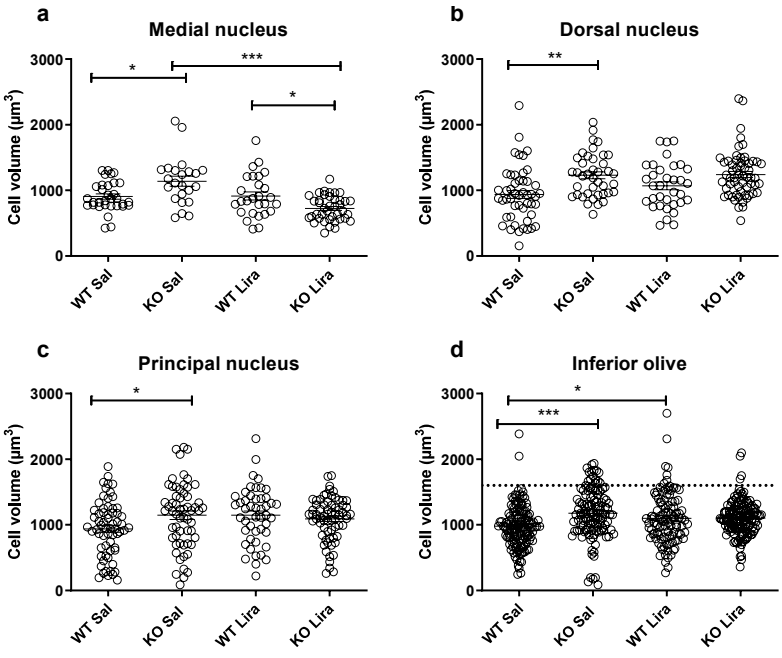

Figure 16. Neuronal volume was increased in Wfs1 KO (KO) animals. Neuronal cell volume in (a) medial nucleus, (b) dorsal nucleus, (c) principal nucleus and (d) in all inferior olive (IO) nuclei together. (d) In Wfs1 KO (KO Sal) animals, there is an increased number of large neurons (1600 µm^3 and above, dotted line), as compared to liraglutide-treated Wfs1 KO animals, indicating that liraglutide treatment prevented neurons from swelling. The data were compared using one-way ANOVA followed by Tukey's HSD tests; *$p < 0.05$, **$p < 0.01$, ***$p < 0.001$. The data are presented as the mean ± SEM, n = 4–7 per group (Seppa et al., 2019).

5.3.4 The total number of neurons in the inferior olive

Post-mortem neuropathological examinations have revealed neuronal loss in Wolfram syndrome patients' brainstems (Genís et al., 1997; Hilson et al., 2009; Shannon et al., 1999), although it is not known when the neuronal loss starts and if Wolfram syndrome rats have similar neuronal loss compared to Wolfram syndrome patients (Seppa et al., 2019).

Therefore, to determine if 14-month-old Wfs1 KO animals have inferior olive degeneration, stereological quantification of the total number of neurons in the inferior olive was performed. Stereology was done under the assumption that the volume of the three nuclei of the inferior olive was unchanged between the groups (Figure 17 a–d). Thionin staining effectively stained neurons (Figure 17, illustrative panel above). The total number of neurons in the inferior olive was estimated in three major subnuclei in the inferior olive – in the medial nucleus, dorsal nucleus, and principal nucleus – using the optical fractionator (Figure 17). Our results indicate that in the dorsal nucleus, there was an increased number of neurons in liraglutide-treated KO animals compared to saline-treated Wfs1 KO animals (Figure 18b) (Seppa et al., 2019).

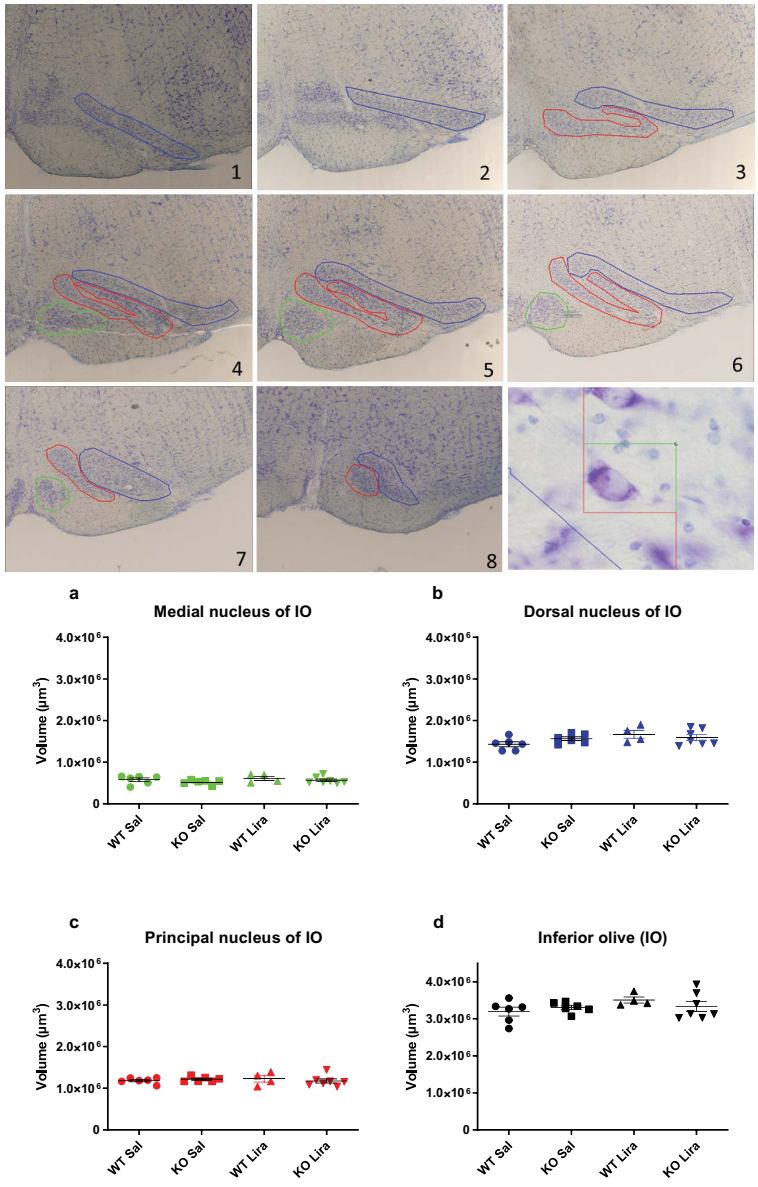

Figure 17. The total number of neurons in the inferior olive was estimated using the optical fractionator. Above, in the illustrative panel, three major subnuclei in the inferior olive are visible: the medial nucleus (green line), dorsal nucleus (blue line) and principal nucleus (red line). A systematic set of sections, 8 slides per animal, were Thionin stained from bregma level –12 until –14.76, delineation of the region of interest (ROI) was performed using a 4× objective (images 1– 8), and the counting was performed with a 60× oil objective (lower right image) using newCAST (Visiopharm, Hoersholm, Denmark) software. Volume of the inferior olive (a) medial nucleus; (b) dorsal nucleus; (c) principal nucleus; and (d) in all inferior olive (IO) nuclei together. Stereology was performed under the assumption that the volume of the three nuclei of the inferior olive was unchanged between the groups. Delineation of the region of interest (ROI) was performed using a 4× objective, and the ROI volume was calculated using newCAST (Visiopharm, Hoersholm, Denmark) software (Seppa et al., 2019).

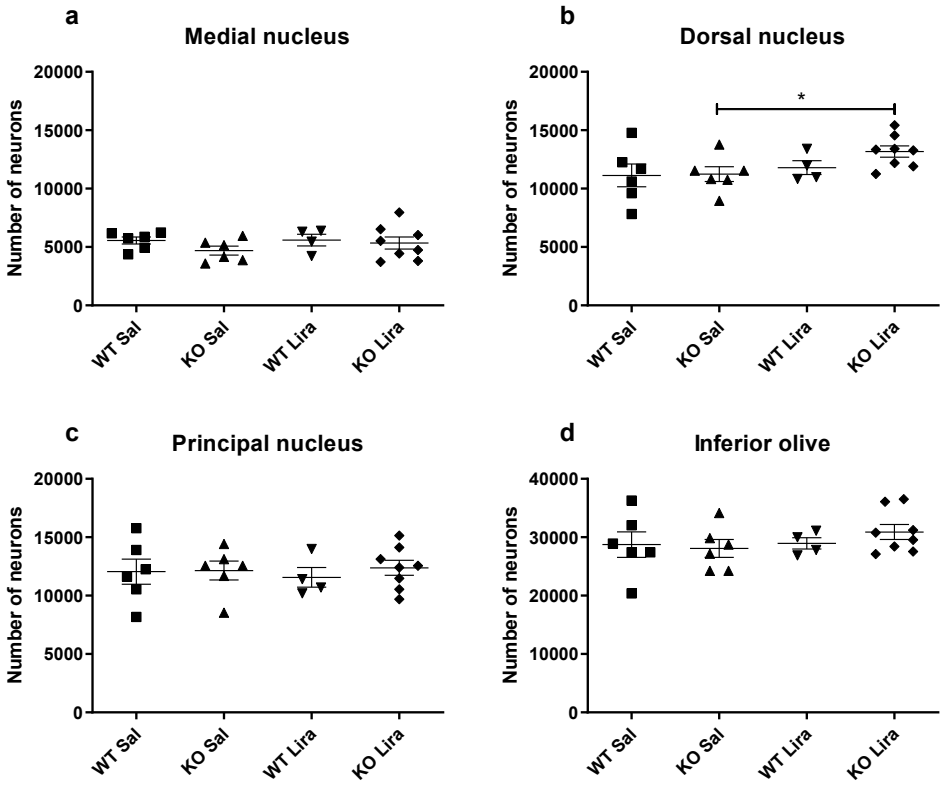

Figure 18. After liraglutide treatment, there was an increased number of neurons in Wfs1 KO (KO) animals' dorsal nucleus. Stereological quantification of the total number of neurons in the inferior olive after 6 months of liraglutide treatment. Total number of neurons in the (a) medial nucleus, (b) dorsal nucleus, (c) principal nucleus, and (d) in all inferior olive (IO) nuclei together. The data were compared using factorial ANOVA followed by Fisher's LSD tests; *$p < 0.05$. The data are presented as the mean ± SEM, n = 4–8 per group (Seppa et al., 2019).

We found no reduction in the number of neurons in the Wfs1 KO animals compared to WT littermates. Probably, the experiment was completed before neurodegeneration could occur. The liraglutide treatment protected the inferior olive from inflammation and ER stress as it did in the pancreas. However, the question remains whether cellular loss follows inflammation and ER-stress in the inferior olive as it does in the pancreatic Langerhans islets.

5.3.5 Brainstem volume increased with age

Wolfram syndrome rats have reduced brainstem volume, although it is not known when the volume decrease starts (Figure 8a, d). Therefore, magnetic resonance imaging (MRI) analyses were performed to measure the brainstem's anatomical

changes during liraglutide treatment (Figure 19a). T2-weighted *in vivo* MRI analysis revealed that brainstem volume increased with age in all experimental groups, although in Wfs1 KO animals, the increase was smaller (Figure 19b). At the age of 14 months, after 6 months of liraglutide treatment, there was no decrease in the brainstem volume as we have seen in 15-month-old Wfs1 KO animals (Figure 8a, d). Additionally, there was no increase in the EPS volume as we have seen in 15-month-old Wfs1 KO animals (Figure 8b, d). The experiment probably ended before the changes could occur. However, similarly to our previous results (Figure 8h), the ventral surface of the brainstem of Wfs1 KO animals appears to be more concave than in WT littermates (Figure 19a). Possibly, the concaved brainstem ventral surface may occur prior to volume depletion and subsequent degeneration (Seppa et al., 2019).

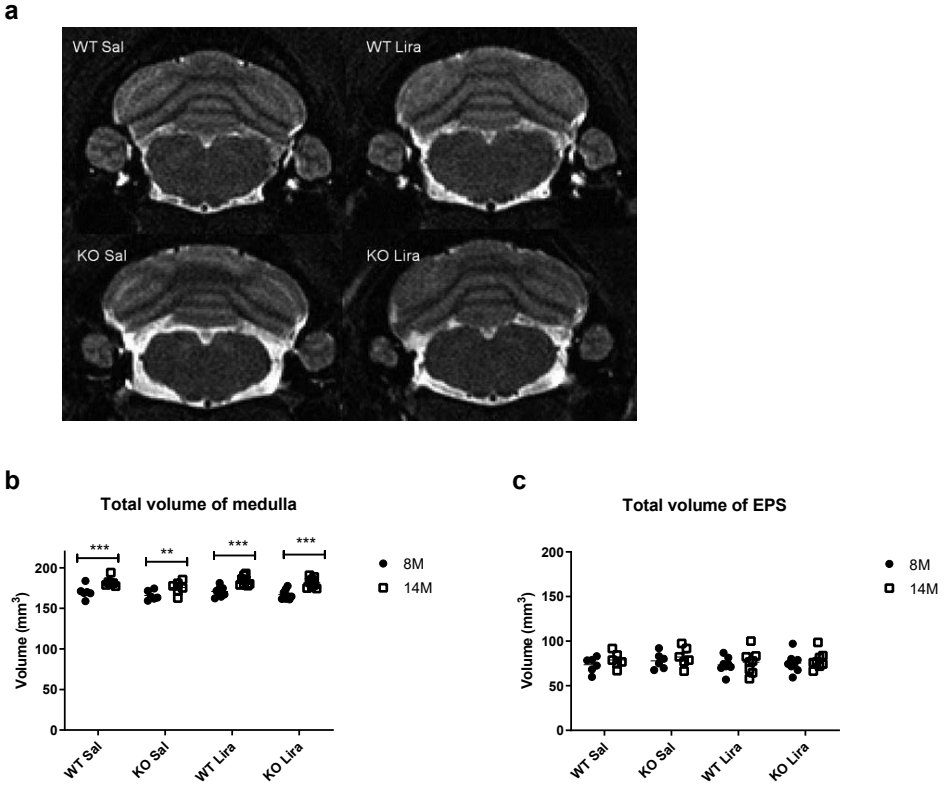

Figure 19. Brainstem volume increased with age in all experimental groups. (a) Representative T2-weighted MR images of the medulla of saline-treated WT and Wfs1 KO (KO), liraglutide-treated WT and Wfs1 KO rats were taken from the level of the inferior olive (bregma approx. −12.63 mm). Quantitative MRI analysis of (b) medullary volume and (c) extraparenchymal space (EPS) were manually traced by an observer blinded to the genotypes of the rats from T2 images using ITK-SNAP software. The volumes of the segmented structures were calculated as volume per slice from bregma level −9.48 to −15.48 mm. The data were compared using repeated measures ANOVA followed by Bonferroni post hoc tests; $^{**}p < 0.01$, $^{***}p < 0.001$. The data are presented as the mean ± SEM, n = 6–10 per group (Seppa et al., 2019).

5.3.6 Conclusion from Paper III

Late intervention with liraglutide was able to protect against ER stress in the inferior olive. Moreover, it was the first time that microglia and astroglia activation, also defined as neuroinflammation, was described in a Wolfram syndrome animal model, and liraglutide treatment protected the inferior olive against neuroinflammation. Additionally, liraglutide treatment protected Wolfram syndrome rats from neuronal swelling. Altogether, liraglutide had a neuroprotective effect on an aged Wolfram syndrome rats.

5.4 Paper IV

Wolfram syndrome is associated with cognitive decline and mood disorders. Therefore, our aim was to investigate (i) if liraglutide has a protective effect on the hippocampus as we have seen in the pancreas and in the brainstem and (ii) if 7,8-DHF alone or in combination with liraglutide has a neuroprotective effect on the hippocampus. Thus, we took 9-month-old Wolfram syndrome rats and their WT littermates and treated them daily with liraglutide, 7,8-DHF or with a combination of liraglutide and 7,8-DHF up to the age of 12.5 months (n=47, 5–8 per group).

5.4.1 Cellular stress response in the hippocampus

Since we have detected ER-stress and inflammation in the pancreas (Figure 3, 10), medulla (Figure 7) and in the inferior olive (Figure 13), our next aim was to investigate the cellular stress response in the hippocampus.

Indeed, there is also some dysregulation in the cellular stress response in Wfs1 KO animals' hippocampus compared to WT control animals. The absence of CHOP is associated with apoptosis and impaired memory performance (Chen et al., 2012). Here, *Chop* mRNA levels were downregulated in Wfs1 KO rats compared to WT controls (Figure 20a) (Seppa et al., 2021).

GRP78 is the key mediator of the UPR pathway (Lee, 2005), and interestingly, *Grp78* mRNA expression in treatment groups was different between genotypes (Figure 20b). In WT animals, 7,8-DHF treatment decreased *Grp78* expression, while in Wfs1 KO rats, 7,8-DHF had no effect on *Grp78* mRNA expression. In Wfs1 KO animals treated with liraglutide and co-treated with liraglutide and 7,8-DHF, *Grp78* levels were decreased compared to saline-treated WT and Wfs1 KO animals.

Hmox1 is upregulated in response to oxidative stress to provide protection (Ryter and Tyrrell, 2000). *Hmox1* was elevated in WT animals treated with the combination of 7,8-DHF and liraglutide (Figure 20c). Moreover, there was a tendency to find decreased *Hmox1* levels in liraglutide treatment groups in both genotypes (Seppa et al., 2021).

It has been shown that TLR2 and TLR4 have opposing functions. TLR2 deficiency in mice resulted in impaired hippocampal neurogenesis, whereas the absence of TLR4 is associated with enhanced proliferation and neuronal differentiation (Rolls et al., 2007). Here, hippocampal *Tlr2* levels were downregulated in Wfs1 KO rats compared to WT control rats (Figure 20d), and in *Tlr4* expression, there was no difference between genotypes. In liraglutide-treated Wfs1 KO animals, *Tlr4* was upregulated (Figure 20e). KI67 is used as a marker for cell proliferation (Gerdes et al., 1983). *Ki67* expression was not increased in liraglutide-treated Wfs1 KO animals (Figure 21f). Therefore, we cannot confirm the association between *Tlr4* expression decrease and enhanced proliferation (Seppa et al., 2021).

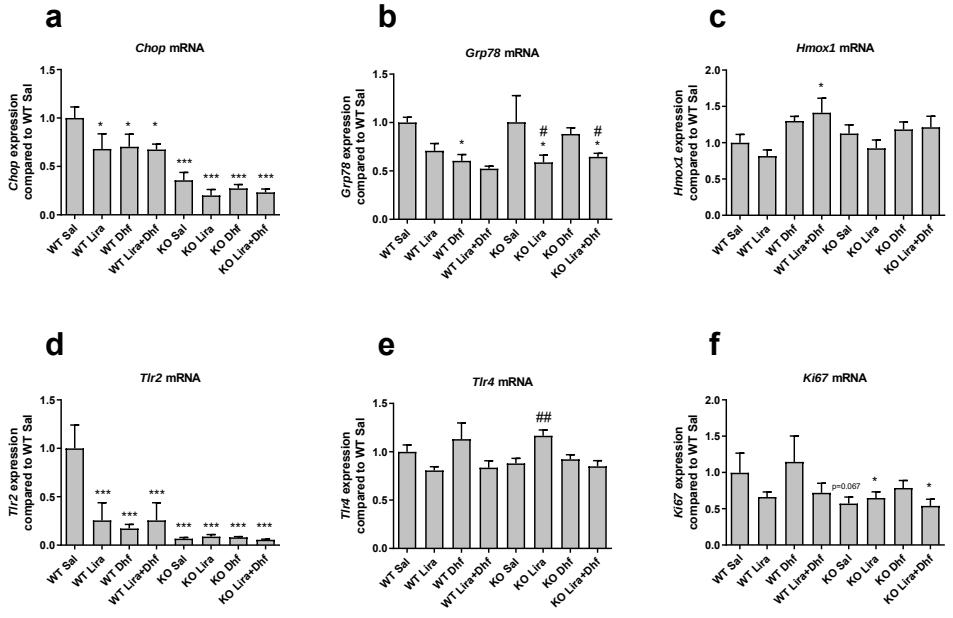

Figure 20. Gene expression analyses from 12.5-month-old animals' hippocampus after 3.5 months of treatment. (a) *Chop*, (b) *Grp78*, (c) *Hmox1*, (d) *Tlr2*, (e) *Tlr4*, (f) *Ki67*. Gene expression data were compared using factorial ANOVA followed by Fisher's LSD tests; * $p<0.05$; ** $p<0.01$; *** $p<0.001$ compared to WT Sal animals and # $p<0.05$; ## $p<0.01$ compared to KO Sal animals. The data are presented as the mean ± SEM, n = 5–8 per group (Seppa et al., 2021).

5.4.2 Liraglutide treatment protects against inflammation and lateral ventricle enlargement

Lateral ventricle enlargement is associated with neurodegeneration in Alzheimer's disease (Nestor et al., 2008). In addition, ventricular enlargement has been reported in TRL2-deficient mice (Park et al., 2015). Since we saw that TLR2 is downregulated in Wfs1 KO rats, our goal was to determine whether ventricular

enlargement is also present in Wfs1 KO rats. Therefore, we performed *in vivo* magnetic resonance imaging (MRI) analyses at the beginning of the experiment, at the age of 9 months and after 3.5 months of treatment when the animals were 12 months old (Figure 21a). Lateral ventricle volume was increased over time in saline-treated Wfs1 KO animals, which indicates a new symptom of neurodegeneration in the Wolfram syndrome rat.

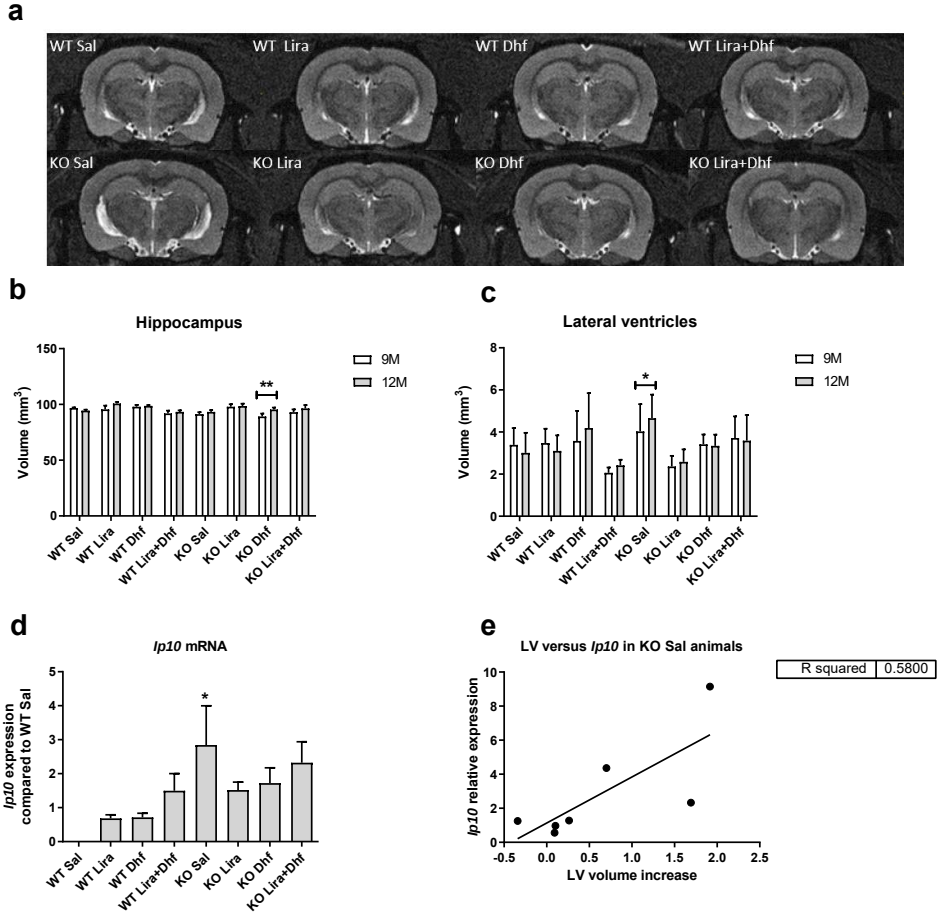

Figure 21. Wfs1 KO animals have increased volume of lateral ventricles. (a) Representative MR images of the hippocampus and lateral ventricles of WT and Wfs1 KO (KO) animals from every treatment group. Results of quantitative MRI analyses of (b) hippocampus and (c) lateral ventricles. Gene expression analyses of the hippocampus were performed to measure (d) *Ip10* mRNA levels. (e) Positive correlation between lateral ventricle volume and *Ip10* mRNA expression. Data are analysed with repeated measures ANOVA followed by Fisher LSD post hoc test, *$p < 0.05$ and **$p < 0.01$ compared to WT Sal animals, ##$p < 0.01$, ### $p < 0.001$ compared to KO Sal animals. Data are presented as mean ± SEM, n = 5–8 (Seppa et al., 2021).

Mildly dilated lateral ventricles has been also reported in one female Wolfram syndrome patient's post-mortem study (Shannon et al., 1999). Liraglutide, 7,8-DHF or their combination prevented Wfs1 KO rats from lateral ventricle enlargement, and thus all treatment combinations had a neuroprotective effect (Figure 21c). No hippocampal atrophy was accompanied by enlargement of the lateral ventricles (Figure 21b). This coincides with patient data, as hippocampal atrophy is not detected in Wolfram syndrome patients (Hershey et al., 2012; Hilson et al., 2009; Lugar et al., 2016). Only in a couple of Wolfram syndrome patients there was a tendency for hippocampal volume decrease, but it was not significant (Zmyslowska et al., 2014), and therefore, hippocampal atrophy is presumably not part of Wolfram syndrome pathology (Seppa et al., 2021).

Inflammatory marker *Ip10* levels were elevated in saline-treated Wfs1 KO animals compared to saline-treated WT animals (Figure 21d), and treatment with liraglutide, 7,8-DHF or with the combination of liraglutide and 7,8-DHF prevented such an increase of inflammation marker *Ip10* in the hippocampus. Thus, liraglutide and 7,8-DHF showed strong neuroprotective effects alone and in combination in the hippocampus. Additionally, in saline-treated Wfs1 KO animals, *Ip10* levels and lateral ventricle volume were increased, linear regression analyses was performed and a positive correlation was observed between *Ip10* levels and lateral ventricle volume increase (R^2 =0.580) (Figure 21e) (Seppa et al., 2021). This indicates that lateral ventricle increase can be associated with increased inflammation in the hippocampus.

The protective effect of liraglutide was also seen in the Paper II, in which 5-month treatment with liraglutide protected Wfs1 KO animals' pancreatic islets from an increase in *Ip10* gene expression. Hence, liraglutide anti-inflammatory properties are similar in the pancreatic islets and in the hippocampus (Seppa et al., 2021).

5.4.3 Liraglutide treatment maintained cognitive function

As cognitive decline correlates with increased volume of the lateral ventricles (Carmichael et al., 2007), we performed the Morris water maze experiment to evaluate the cognitive abilities of 12-month old Wfs1 KO rats. During probe day, Wfs1 KO rats needed significantly more time to reach the platform, and they spent less time in the target quadrant compared to saline-treated control animals (Figure 22a, b), which indicates cognitive decline in Wfs1 KO animals. Cognitive decline is also a described Wolfram syndrome symptom (Chaussenot et al., 2011), which additionally shows that the Wfs1 KO rat is a valuable Wolfram syndrome model. Treatment with liraglutide, 7,8-DHF or their combination kept the Wfs1 KO animals' cognitive capacity similar to the control animals, which reveals an impressive neuroprotective effect of these treatments (Seppa et al., 2021).

12-month-old Wolfram syndrome rats had developed cognitive decline, ventricular enlargement, and inflammation in the hippocampus. These symptoms

are also the symptoms of Alzheimer's Disease (Chou et al., 2009; Dubois et al., 2014; Nestor et al., 2008; Pini et al., 2016; Xia et al., 2000), which suggests a similar course of neurodegeneration in both diseases. Therefore, Wolfram syndrome studies may also lead to the development of novel treatments options for other neurodegenerative diseases (Seppa et al., 2021).

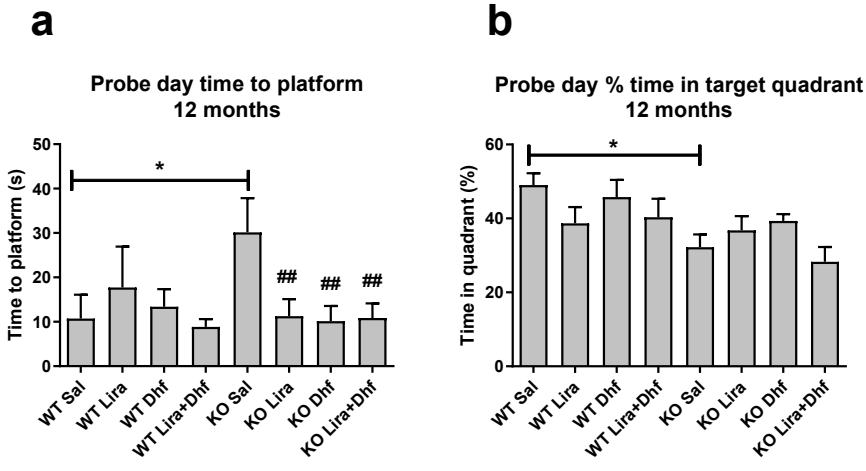

Figure 22. Morris water maze experiment results. Morris water maze was performed to evaluate Wfs1 KO (KO) rats' cognition. (a) Time to reach the platform on the probe day, (b) time spent in target quadrant on the probe day. Data are analysed with repeated measures ANOVA followed by Fisher LSD post hoc test, *$p<0.05$ compared to WT Sal animals, ##$p<0.01$ compared to KO Sal animals. Data are presented as mean ± SEM, n=5–8 (Seppa et al., 2021).

5.4.4 Conclusion from Paper IV

Liraglutide had a protective effect on the hippocampus, as we have seen previously in the pancreas and in the inferior olive. Liraglutide treatment protected against inflammation in hippocampus and against lateral ventricle enlargement; moreover, liraglutide treatment maintained cognitive function. Similarly to liraglutide, BDNF mimetic 7,8-DHF also had a neuroprotective effect.

Concluding remarks

Wolfram syndrome is a rare hereditary disorder that is caused by dysfunctional WFS1 protein (Inoue et al., 1998; Strom et al., 1998). Wolfram syndrome starts with diabetes mellitus followed by optic nerve atrophy and neurodegeneration (Barrett et al., 1995). Wolfram syndrome's first symptom, diabetes mellitus, can effectively be controlled with insulin replacement therapy; however, currently there is no treatment to stop neurodegeneration. In order to investigate Wolfram syndrome caused by WFS1 deficiency, our research group has created the Wfs1 KO rat (Plaas et al., 2017). The aim of this thesis is to characterize the Wolfram syndrome rat model to be able to use it for the evaluation of new treatment strategies, with a particular focus on neurodegeneration associated with Wolfram syndrome, which has been little studied compared to diabetes mellitus.

The first paper focused on characterizing the Wfs1 KO rats' phenotype. As a result of the non-functional WFS1 protein, all of the main symptoms of Wolfram syndrome were present, such as diabetes mellitus and neurodegeneration, including ER stress in the brainstem, increased extraparenchymal area around the brainstem, and decreased volume per slice of the brainstem on the level of the olive nucleus. Consequently, the symptoms in the Wfs1 KO rat appear to be similar to those of Wolfram syndrome patients, and hence, it can be defined as the Wolfram syndrome rat and can be used to evaluate new treatment strategies (Plaas et al., 2017).

Drug reproposing involves the use of de-risked compounds, and it is used increasingly to treat both common and rare diseases (Pushpakom et al., 2019). In recent years, diabetes drugs have been investigated for neuroprotective properties because neurodegenerative diseases and diabetes mellitus share common pathophysiological features, such as cellular stress, inflammation, insulin resistance and abnormal protein processing (Salcedo et al., 2012). Thus, in the following papers, our aim was to investigate the effect of the antidiabetic drug liraglutide on Wolfram syndrome symptoms.

The second paper focused on the diabetic phenotype. GLP-1 receptor agonists are used for the treatment of type 2 diabetes because they increase glucose-dependent insulin release from beta cells and thereby reduce postprandial glucose levels. To investigate if liraglutide has a preventive effect on Wolfram syndrome rats' diabetic phenotype, we started chronic treatment before the onset of disease symptoms, at the age of 2 months, and the treatment lasted for 5 months. Indeed, the results indicate that early treatment with liraglutide prevented the development of diabetes mellitus in Wfs1 KO animals (Toots et al., 2018).

Next, in the third paper, our aim was to investigate whether liraglutide could also have a therapeutic effect on brainstem neurodegeneration. It is known that GLP-1 receptors are also expressed in neurons, astrocytes and in microglia cells; hence, we hypothesized that liraglutide could also have a neuroprotective effect in Wolfram syndrome. In order to mimic human patients who are diagnosed with Wolfram syndrome after the development of diabetes, we started treatment in 9-month-old animals who had already developed glucose intolerance, and the

treatment lasted for 6 months. Our results suggest that, in Wolfram syndrome rats, neuroinflammation proceeds to neuronal damage, and additionally, Wolfram syndrome rats develop ER stress and neuronal swelling in the inferior olive. 6-month liraglutide treatment reduced neuroinflammation, neuronal swelling and ER stress in the inferior olive of Wolfram syndrome rats. Hence, this paper investigated for the first time liraglutide's neuroprotective effect in connection with Wolfram syndrome.

The fourth paper studied the neuronal phenotype further and evaluated for the first time the effect of BDNF mimetic 7,8-DHF on an aged Wolfram syndrome rat hippocampus. 9-month-old Wolfram syndrome rats and wild-type (WT) control animals were treated for 3.5 months with liraglutide, 7,8-DHF or with a combination of liraglutide and 7,8-DHF. We found that liraglutide, 7,8-DHF and their co-treatment all prevented lateral ventricle enlargement, improved learning in the Morris water maze and reduced inflammation in the hippocampus. Thus, liraglutide, 7,8-DHF and their co-treatment could potentially be used as a therapeutic intervention to induce neuroprotection (Seppa et al., 2021).

Altogether, chronic treatment with liraglutide protected Wfs1 KO rats against development of glucose intolerance and was neuroprotective in the brainstem and in the hippocampus. Additionally, BDNF mimetic 7,8-DHF had a similar neuroprotective effect compared to liraglutide.

This thesis systematically characterized the Wolfram syndrome rat, for which the phenotype correlates with Wolfram syndrome patients. The fastest way to get a new treatment in practice is drug repurposing, as the side effects and safety are already known. The current thesis demonstrates a significant therapeutic effect of the GLP-1 receptor agonist liraglutide to prevent or slow the onset of symptoms of Wolfram syndrome in the Wolfram syndrome rat model. Therefore, early diagnosis and treatment with GLP-1 receptor agonists may also prove to be a promising treatment option for Wolfram syndrome patients by significantly improving their quality of life. Thus, such a systematic approach could also be used to study other rare diseases.

Further investigations will continue in humans. Inspired by preclinical studies with liraglutide, researchers from St. Louis, MO, USA have initiated a liraglutide clinical trial (https://thesnowfoundation.org/clinical-trials/). This clinical trial will clarify if liraglutide has a similar preventive effect on the development of diabetes and on neurodegeneration in Wolfram syndrome patients.

CONCLUSIONS

I Wfs1 KO rats developed both diabetes mellitus and neurodegeneration. The results demonstrate that ER stress occurs prior to cellular loss in the pancreas and to decreases in the brainstem volume of Wfs1 KO rats.

II Liraglutide treatment protected the Langerhans islets from ER stress and thus maintained Langerhans islets' cellular function and mass and protected Wfs1 KO rats against developing glucose intolerance.

III Liraglutide treatment protected Wfs1 KO rats' inferior olive against ER stress, neuronal swelling and neuroinflammation, as measured by an increased number of IBA positive microglia cells and GFAP positive astroglia cells. Thereby, it had a neuroprotective effect.

IV Liraglutide treatment protected Wfs1 KO rats' hippocampus against inflammation, prevented ventricular enlargement and maintained cognitive function. Similarly to liraglutide, 7,8-DHF alone and in combination with liraglutide protected the hippocampus against inflammation and maintained cognitive function in Wfs1 KO rats. Therefore, both treatments had relatively similar neuroprotective effects.

SUMMARY IN ESTONIAN

Wolframi sündroom on haruldane autosomaalse retsessiivse pärandumismustriga haigus, mida põhjustab *WFS1* geeni poolt kodeeritud Wolframiini valgu düsfunktsioon. Wolframi sündroomi esimene sümptom on insuliinist sõltuv diabeet ning sellele järgnevad nägemisnärvi atroofia, magediabeet ja neuroloogilised komplikatsioonid. Insuliinist sõltuv diabeet on kontrollitav insuliini asendusraviga, seega on Wolframi sündroomiga patsientidele enim muret valmistav neurodegeneratsioon, millele puudub ravi. Seepärast on oluline välja töötada neuroprotektiivseid ravimeetodeid, mis oleksid võimelised aeglustama haiguse kulgu ja seeläbi pikendama Wolframi sündroomiga patsientide eluiga.

Wolframiini valgu düsfunktsioonist põhjustatud Wolframi sündroomi uurimiseks on meie uurimisrühm loonud Wfs1 KO roti, kelle *Wfs1* geeni viies kodeeriv ekson on deleteeritud. Antud doktoritöö eesmärgiks oli iseloomustada Wfs1 KO roti fenotüüpi, eesmärgiga kasutada seda uute ravistrateegiate väljatöötamisel. Antud töös pöörati erilist tähelepanu Wolframi sündroomiga seotud neurodegeneratsioonile, mida on insuliinist sõltuva diabeediga võrreldes vähe uuritud.

Esimene uuring keskendus Wfs1 KO rottide fenotüübi iseloomustamisele. Mittefunktsionaalse Wolframiini valgu tagajärjel kujunesid Wfs1 KO rotil kõik Wolframi sündroomi peamised sümptomid nagu insuliinist sõltuv diabeet ja neurodegeneratsioon, sealhulgas ajutüves esinev endoplasmaatilise retiikulumi (ER)-stress, ajutüve ümbritseva ekstraparenhümaalse ala pindala suurenemine ja ajutüve ruumala vähenemine oliivtuumade tasandil. Seega näib, et Wfs1 KO roti sümptomid on sarnased Wolframi sündroomiga patsientide omadega ja seetõttu saab Wfs1 KO rotti pidada Wolframi sündroomi loommudeliks ja seda saab kasutada uute ravistrateegiate hindamiseks.

Kiireim viis uue praktikas kasutatava ravi saamiseks on olemasolevatele ravimitele uue näidustuse leidmine, kuna kõrvalmõjud ja ohutus on juba teada. Antud lähenemist kasutatakse üha sagedamini nii erinevate haiguste kui ka harvikhaiguste raviks. Viimastel aastatel on uuritud diabeediravimite neuroprotektiivseid omadusi, kuna neurodegeneratiivsetel haigustel ja diabeedil on ühised patofüsioloogilised tunnused nagu rakustress, põletik, insuliiniresistentsus ja valkude voltumise häired. Sellest tulenevalt oli meie eesmärk uurida diabeediravimi liraglutiidi mõju Wolframi sündroomi põhisümptomitele: insuliinist sõltuvale diabeedile ja neurodegeneratsioonile.

Teine uuring keskendus liraglutiidi mõju uurimisele insuliinist sõltuva diabeedi fenotüübile Wolframi sündroomi rottidel. GLP-1 retseptori agoniste kasutatakse teist tüüpi diabeedi raviks, kuna need suurendavad glükoosist sõltuvat insuliini vabanemist beeta-rakkudest ja vähendavad seeläbi söögijärgset glükoositaset. Et uurida, kas liraglutiidil on ennetav toime Wolframi sündroomi rottidel esineva insuliinist sõltuva diabeedi väljakujunemisele, alustasime kroonilist ravi enne haigusnähtude ilmnemist kui loomad olid 2 kuu vanused ning ravi kestis 5 kuud. Tulemused näitasid, et varajane ravi liraglutiidiga hoidis tõepoolest ära diabeedi tekke Wolframi sündroomi rottidel.

Kolmanda uuringu eesmärk oli uurida, kas liraglutiidil võib olla terapeutiline toime ka ajutüve neurodegeneratsioonile. On teada, et GLP-1 retseptoreid ekspresseeritakse neuronites, astrotsüütides ja mikrogliia rakkudes, mistõttu oli meie hüpoteesiks, et liraglutiidil võib olla Wolframi sündroomi korral ka neuroprotektiivne toime. Wolframi sündroomiga patsientide jäljendamiseks, kellel diagnoositakse Wolframi sündroom üldjuhul pärast diabeedi tekkimist, alustasime liraglutiidi ravi 9-kuustel loomadel, kellel oli juba tekkinud glükoositalumatus ja ravi kestis 6 kuud. Meie tulemused näitavad, et Wolframi sündroomi rottidel eelneb neuropõletik neurodegeneratsioonile ja lisaks tekivad Wolframi sündroomiga rottidel oliivtuumades ER stress ja neuronite ruumala suurenemine. 6-kuu pikkune liraglutiidi ravi vähendas Wolframi sündroomi rottide oliivtuumades neuropõletikku, neuronite ruumala suurenemist ja ER-stressi. Seega näidati selles uurimistöös esmakordselt liraglutiidi neuroprotektiivset toimet Wolframi sündroomi loommudelis.

Neljas uuring keskendus neurodegeneratsioonile ning esmakordselt hinnati BDNF-i mimeetiku 7,8-dihüdroksüflavooni (7,8-DHF) toimet vananenud Wolframi sündroomi rottide hipokampusele. 9 kuu vanuseid Wolframi sündroomi rotte ja nende metsiktüüpi (WT) kontroll-loomi raviti 3,5 kuud liraglutiidi, 7,8-DHF või liraglutiidi ja 7,8-DHF kombinatsiooniga. Leidsime, et nii liraglutiid, 7,8-DHF kui ka nende samaaegne ravi hoidis ära Wolframi sündroomi rottide külgvatsakeste ruumala suurenemise, parandas õppimist Morrise veelabürindis ja vähendas põletikku hipokampuses. Seega võiks liraglutiidi, 7,8-DHF ja nende koos kasutamist potentsiaalselt tarvitada neuroprotektiivse ravina.

Kokkuvõttes kaitses krooniline ravi liraglutiidiga Wfs1 KO rotte glükoositalumatuse tekke eest ning oli neuroprotektiivne ajutüves ja hipokampuses. Lisaks oli BDNF-i mimeetikul 7,8-DHF-l liraglutiidiga sarnane neuroprotektiivne toime.

Antud doktoritöös kirjeldati süstemaatiliselt Wolframi sündroomi rotte, kelle fenotüüp korreleerub Wolframi sündroomiga patsientidega. Sellisel loommudelil saadud tulemustel on head eeldused olla reprodutseeritavad inimkatsetes ning samuti on hea tõenäosus sellisel loommudelil tõestatud ravi edukaks siirdamiseks kliinilisse meditsiini. Käesolev doktoritöö näitas GLP-1 retseptori agonisti liraglutiidi olulist terapeutilist toimet Wolframi sündroomi loommudelis Wolframi sündroomi sümptomite tekke ärahoidmisel või aeglustamisel. Seetõttu võib varajane diagnoosimine ja ravi GLP-1 retseptori agonistidega osutuda paljutõotavaks ravivõimaluseks ka Wolframi sündroomiga patsientidele, parandades oluliselt nende elukvaliteeti. Lisaks saaks sellist süstemaatilist lähenemist kasutada ka teiste harvikhaiguste uurimiseks.

Lähtudes liraglutiidi prekliinilisetst uuringutest on algatatud liraglutiidi kliiniline uuring (https://thesnowfoundation.org/clinical-trials/). See kliiniline uuring annab selgust, kas liraglutiidil on sarnane ennetav toime diabeedi arengule ja neurodegeneratsioonile nagu on kirjeldatud Wolframi sündroomi rottidel. Kokkuvõtvalt võib järeldada, et meie uuringud on Wolframi sündroomi uurimisel olnud olulised.

REFERENCES

Adeghate, E., and Ponery, A.S. (2002). GABA in the endocrine pancreas: cellular localization and function in normal and diabetic rats. Tissue Cell *34*, 1–6.

Akiyama, M., Hatanaka, M., Ohta, Y., Ueda, K., Yanai, A., Uehara, Y., Tanabe, K., Tsuru, M., Miyazaki, M., Saeki, S., et al. (2009). Increased insulin demand promotes while pioglitazone prevents pancreatic beta cell apoptosis in Wfs1 knockout mice. Diabetologia *52*, 653–663.

Apostolova, L.G., Green, A.E., Babakchanian, S., Hwang, K.S., Chou, Y.-Y., Toga, A.W., and Thompson, P.M. (2012). Hippocampal Atrophy and Ventricular Enlargement in Normal Aging, Mild Cognitive Impairment (MCI), and Alzheimer Disease: Alzheimer Dis. Assoc. Disord. *26*, 17–27.

Arntfield, M.E., and van der Kooy, D. (2011). β-Cell evolution: How the pancreas borrowed from the brain: The shared toolbox of genes expressed by neural and pancreatic endocrine cells may reflect their evolutionary relationship. BioEssays *33*, 582–587.

Athauda, D., and Foltynie, T. (2016). The glucagon-like peptide 1 (GLP) receptor as a therapeutic target in Parkinson's disease: mechanisms of action. Drug Discov. Today *21*, 802–818.

Baggio, L.L., and Drucker, D.J. (2014). Glucagon-like peptide-1 receptors in the brain: controlling food intake and body weight. J. Clin. Invest. *124*, 4223–4226.

Bakker, R., Tiesinga, P., and Kötter, R. (2015). The Scalable Brain Atlas: Instant Web-Based Access to Public Brain Atlases and Related Content. Neuroinformatics *13*, 353–366.

Barrett, T.G., and Bundey, S.E. (1997). Wolfram (DIDMOAD) syndrome. J. Med. Genet. *34*, 838–841.

Barrett, T.G., Bundey, S.E., and Macleod, A.F. (1995). Neurodegeneration and diabetes: UK nationwide study of Wolfram (DIDMOAD) syndrome. The Lancet *346*, 1458–1463.

Bischoff, A.N., Reiersen, A.M., Buttlaire, A., Al-lozi, A., Doty, T., Marshall, B.A., and Hershey, T. (2015). Selective cognitive and psychiatric manifestations in Wolfram Syndrome. Orphanet J. Rare Dis. *10*, 66.

Booth, H.D.E., Hirst, W.D., and Wade-Martins, R. (2017). The Role of Astrocyte Dysfunction in Parkinson's Disease Pathogenesis. Trends Neurosci. *40*, 358–370.

Cai, H., Cong, W., Ji, S., Rothman, S., Maudsley, S., and Martin, B. (2012). Metabolic Dysfunction in Alzheimer's Disease and Related Neurodegenerative Disorders. Curr. Alzheimer Res. *9*, 5–17.

Cano, A., Molines, L., Valéro, R., Simonin, G., Paquis-Flucklinger, V., Vialettes, B., and French Group of Wolfram Syndrome (2007). Microvascular diabetes complications in Wolfram syndrome (diabetes insipidus, diabetes mellitus, optic atrophy, and deafness [DIDMOAD]): an age- and duration-matched comparison with common type 1 diabetes. Diabetes Care *30*, 2327–2330.

Carmichael, O.T., Kuller, L.H., Lopez, O.L., Thompson, P.M., Dutton, R.A., Lu, A., Lee, S.E., Lee, J.Y., Aizenstein, H.J., Meltzer, C.C., et al. (2007). Cerebral Ventricular Changes Associated With Transitions Between Normal Cognitive Function, Mild Cognitive Impairment, and Dementia: Alzheimer Dis. Assoc. Disord. *21*, 14–24.

Carter, J.D., Dula, S.B., Corbin, K.L., Wu, R., and Nunemaker, C.S. (2009). A Practical Guide to Rodent Islet Isolation and Assessment. Biol. Proced. Online *11*, 3–31.

Chaussenot, A., Bannwarth, S., Rouzier, C., Vialettes, B., Mkadem, S.A.E., Chabrol, B., Cano, A., Labauge, P., and Paquis-Flucklinger, V. (2011). Neurologic features and genotype-phenotype correlation in Wolfram syndrome. Ann. Neurol. *69*, 501–508.

Chen, C.-M., Wu, C.-T., Chiang, C.-K., Liao, B.-W., and Liu, S.-H. (2012). C/EBP Homologous Protein (CHOP) Deficiency Aggravates Hippocampal Cell Apoptosis and Impairs Memory Performance. PLoS ONE *7*, e40801.

Choi, J.W., Lee, C.W., Lee, J., Choi, D.J., Sohng, J.K., and Park, Y.I. (2016). 7,8-Dihydroxyflavone inhibits adipocyte differentiation via antioxidant activity and induces apoptosis in 3T3-L1 preadipocyte cells. Life Sci. *144*, 103–112.

Chou, Y.-Y., Leporé, N., Avedissian, C., Madsen, S.K., Parikshak, N., Hua, X., Shaw, L.M., Trojanowski, J.Q., Weiner, M.W., Toga, A.W., et al. (2009). Mapping correlations between ventricular expansion and CSF amyloid and tau biomarkers in 240 subjects with Alzheimer's disease, mild cognitive impairment and elderly controls. NeuroImage *46*, 394–410.

Da Silva Xavier, G. (2018). The Cells of the Islets of Langerhans. J. Clin. Med. *7*, 54.

DiSabato, D.J., Quan, N., and Godbout, J.P. (2016). Neuroinflammation: the devil is in the details. J. Neurochem. *139*, 136–153.

Dorph-Petersen, K.A., Nyengaard, J.R., and Gundersen, H.J. (2001). Tissue shrinkage and unbiased stereological estimation of particle number and size. J. Microsc. *204*, 232–246.

Dubois, B., Feldman, H.H., Jacova, C., Hampel, H., Molinuevo, J.L., Blennow, K., DeKosky, S.T., Gauthier, S., Selkoe, D., Bateman, R., et al. (2014). Advancing research diagnostic criteria for Alzheimer's disease: the IWG-2 criteria. Lancet Neurol. *13*, 614–629.

Eng, L.F., Ghirnikar, R.S., and Lee, Y.L. (2000). Glial Fibrillary Acidic Protein: GFAP Thirty-One Years (1969–2000). Neurochem. Res. *25*, 1439–1451.

Fonseca, S.G., Fukuma, M., Lipson, K.L., Nguyen, L.X., Allen, J.R., Oka, Y., and Urano, F. (2005). WFS1 Is a Novel Component of the Unfolded Protein Response and Maintains Homeostasis of the Endoplasmic Reticulum in Pancreatic β-Cells. J. Biol. Chem. *280*, 39609–39615.

Fonseca, S.G., Ishigaki, S., Oslowski, C.M., Lu, S., Lipson, K.L., Ghosh, R., Hayashi, E., Ishihara, H., Oka, Y., Permutt, M.A., et al. (2010). Wolfram syndrome 1 gene negatively regulates ER stress signaling in rodent and human cells. J. Clin. Invest. *120*, 744–755.

Fujita, H., and Sugihara, I. (2012). FoxP2 expression in the cerebellum and inferior olive: Development of the transverse stripe-shaped expression pattern in the mouse cerebellar cortex. J. Comp. Neurol. *520*, 656–677.

Garvey, W.T., Birkenfeld, A.L., Dicker, D., Mingrone, G., Pedersen, S.D., Satylganova, A., Skovgaard, D., Sugimoto, D., Jensen, C., and Mosenzon, O. (2020). Efficacy and Safety of Liraglutide 3.0 mg in Individuals With Overweight or Obesity and Type 2 Diabetes Treated With Basal Insulin: The SCALE Insulin Randomized Controlled Trial. Diabetes Care *43*, 1085–1093.

Genís, D., Dávalos, A., Molins, A., and Ferrer, I. (1997). Wolfram syndrome: a neuropathological study. Acta Neuropathol. (Berl.) *93*, 426–429.

Gerdes, J., Schwab, U., Lemke, H., and Stein, H. (1983). Production of a mouse monoclonal antibody reactive with a human nuclear antigen associated with cell proliferation. Int. J. Cancer *31*, 13–20.

Golden, E., Emiliano, A., Maudsley, S., Windham, B.G., Carlson, O.D., Egan, J.M., Driscoll, I., Ferrucci, L., Martin, B., and Mattson, M.P. (2010). Circulating Brain-

Derived Neurotrophic Factor and Indices of Metabolic and Cardiovascular Health: Data from the Baltimore Longitudinal Study of Aging. PLoS ONE *5*, e10099.

Guiot, Y., Stevens, M., Marhfour, I., Stiernet, P., Mikhailov, M., Ashcroft, S.J.H., Rahier, J., Henquin, J.-C., and Sempoux, C. (2007). Morphological localisation of sulfonylurea receptor 1 in endocrine cells of human, mouse and rat pancreas. Diabetologia *50*, 1889–1899.

Gundersen, H.J. (1986). Stereology of arbitrary particles. A review of unbiased number and size estimators and the presentation of some new ones, in memory of William R. Thompson. J. Microsc. *143*, 3–45.

Gundersen, H.J.G. (1977). Notes on the estimation of the numerical density of arbitrary profiles: the edge effect. J. Microsc. *111*, 219–223.

Halliday, G.M., and Stevens, C.H. (2011). Glia: Initiators and progressors of pathology in Parkinson's disease: Glia in Parkinson's Disease. Mov. Disord. *26*, 6–17.

Hamezah, H.S., Durani, L.W., Ibrahim, N.F., Yanagisawa, D., Kato, T., Shiino, A., Tanaka, S., Damanhuri, H.A., Ngah, W.Z.W., and Tooyama, I. (2017). Volumetric changes in the aging rat brain and its impact on cognitive and locomotor functions. Exp. Gerontol. *99*, 69–79.

Hansen, H.H., Barkholt, P., Fabricius, K., Jelsing, J., Terwel, D., Pyke, C., Knudsen, L.B., and Vrang, N. (2016). The GLP-1 receptor agonist liraglutide reduces pathology-specific tau phosphorylation and improves motor function in a transgenic hTauP301L mouse model of tauopathy. Brain Res. *1634*, 158–170.

Hanyu, H., Sato, T., Kiuchi, A., Sakurai, H., and Iwamoto, T. (2009). Pioglitazone improved cognition in a pilot study on patients with alzheimer's disease and mild cognitive impairment with diabetes mellitus: Letters to the editor. J. Am. Geriatr. Soc. *57*, 177–179.

Heneka, M.T., Sastre, M., Dumitrescu-Ozimek, L., Hanke, A., Dewachter, I., Kuiperi, C., O'Banion, K., Klockgether, T., Van Leuven, F., and Landreth, G.E. (2005). Acute treatment with the PPARγ agonist pioglitazone and ibuprofen reduces glial inflammation and Aβ1–42 levels in APPV717I transgenic mice. Brain *128*, 1442–1453.

Hershey, T., Lugar, H.M., Shimony, J.S., Rutlin, J., Koller, J.M., Perantie, D.C., Paciorkowski, A.R., Eisenstein, S.A., Permutt, M.A., and the Washington University Wolfram Study Group (2012). Early Brain Vulnerability in Wolfram Syndrome. PLoS ONE *7*, e40604.

Hickman, S., Izzy, S., Sen, P., Morsett, L., and El Khoury, J. (2018). Microglia in neurodegeneration. Nat. Neurosci. *21*, 1359–1369.

Hickman, S.E., Allison, E.K., and El Khoury, J. (2008). Microglial Dysfunction and Defective – Amyloid Clearance Pathways in Aging Alzheimer's Disease Mice. J. Neurosci. *28*, 8354–8360.

Hilson, J.B., Merchant, S.N., Adams, J.C., and Joseph, J.T. (2009). Wolfram syndrome: a clinicopathologic correlation. Acta Neuropathol. (Berl.) *118*, 415–428.

Hofmann, S. (2003). Wolfram syndrome: structural and functional analyses of mutant and wild-type wolframin, the WFS1 gene product. Hum. Mol. Genet. *12*, 2003–2012.

Hopperton, K.E., Mohammad, D., Trépanier, M.O., Giuliano, V., and Bazinet, R.P. (2018). Markers of microglia in post-mortem brain samples from patients with Alzheimer's disease: a systematic review. Mol. Psychiatry *23*, 177–198.

Huang, E.J., and Reichardt, L.F. (2001). Neurotrophins: Roles in Neuronal Development and Function. Annu. Rev. Neurosci. *24*, 677–736.

Hunter, K., and Hölscher, C. (2012). Drugs developed to treat diabetes, liraglutide and lixisenatide, cross the blood brain barrier and enhance neurogenesis. BMC Neurosci. *13*, 33.

Iannaccone, P.M., and Jacob, H.J. (2009). Rats! Dis. Model. Mech. *2*, 206–210.

Iglesias, J., Barg, S., Vallois, D., Lahiri, S., Roger, C., Yessoufou, A., Pradevand, S., McDonald, A., Bonal, C., Reimann, F., et al. (2012). PPARβ/δ affects pancreatic β cell mass and insulin secretion in mice. J. Clin. Invest. *122*, 4105–4117.

Inoue, H., Tanizawa, Y., Wasson, J., Behn, P., Kalidas, K., Bernal-Mizrachi, E., Mueckler, M., Marshall, H., Donis-Keller, H., Crock, P., et al. (1998). A gene encoding a transmembrane protein is mutated in patients with diabetes mellitus and optic atrophy (Wolfram syndrome). Nat. Genet. *20*, 143–148.

Ishihara, H. (2004). Disruption of the WFS1 gene in mice causes progressive-cell loss and impaired stimulus-secretion coupling in insulin secretion. Hum. Mol. Genet. *13*, 1159–1170.

Jakobsen, C.H., Størvold, G.L., Bremseth, H., Follestad, T., Sand, K., Mack, M., Olsen, K.S., Lundemo, A.G., Iversen, J.G., Krokan, H.E., et al. (2008). DHA induces ER stress and growth arrest in human colon cancer cells: associations with cholesterol and calcium homeostasis. J. Lipid Res. *49*, 2089–2100.

Janani, C., and Ranjitha Kumari, B.D. (2015). PPAR gamma gene – A review. Diabetes Metab. Syndr. Clin. Res. Rev. *9*, 46–50.

Jang, S.-W., Liu, X., Yepes, M., Shepherd, K.R., Miller, G.W., Liu, Y., Wilson, W.D., Xiao, G., Blanchi, B., Sun, Y.E., et al. (2010). A selective TrkB agonist with potent neurotrophic activities by 7,8-dihydroxyflavone. Proc. Natl. Acad. Sci. *107*, 2687–2692.

Kakiuchi, C., Ishigaki, S., Oslowski, C.M., Fonseca, S.G., Kato, T., and Urano, F. (2009). Valproate, a Mood Stabilizer, Induces WFS1 Expression and Modulates Its Interaction with ER Stress Protein GRP94. PLoS ONE *4*, e4134.

Khardori, R., Stephens, J.W., Page, O.C., and Dow, R.S. (1983). Diabetes Mellitus and Optic Atrophy in Two Siblings: A Report on a New Association and a Review of the Literature. Diabetes Care *6*, 67–70.

Kim, C.-H., Park, S.-H., Sim, Y.-B., Kim, S.-S., Kim, S.-J., Lim, S.-M., Jung, J.-S., and Suh, H.-W. (2014). Effect of tolbutamide, glyburide and glipizide administered supraspinally on CA3 hippocampal neuronal cell death and hyperglycemia induced by kainic acid in mice. Brain Res. *1564*, 33–40.

Kittler, J.T., and Moss, S.J. (2003). Modulation of GABAA receptor activity by phosphorylation and receptor trafficking: implications for the efficacy of synaptic inhibition. Curr. Opin. Neurobiol. *13*, 341–347.

Kondo, M., Tanabe, K., Amo-Shiinoki, K., Hatanaka, M., Morii, T., Takahashi, H., Seino, S., Yamada, Y., and Tanizawa, Y. (2018). Activation of GLP-1 receptor signalling alleviates cellular stresses and improves beta cell function in a mouse model of Wolfram syndrome. Diabetologia.

Krause, T., Gerbershagen, M.U., Fiege, M., Weißhorn, R., and Wappler, F. (2004). Dantrolene ? A review of its pharmacology, therapeutic use and new developments. Anaesthesia *59*, 364–373.

Kumar, S. (2010). Wolfram syndrome: important implications for pediatricians and pediatric endocrinologists. Pediatr. Diabetes *11*, 28–37.

La Morgia, C., Maresca, A., Amore, G., Gramegna, L.L., Carbonelli, M., Scimonelli, E., Danese, A., Patergnani, S., Caporali, L., Tagliavini, F., et al. (2020). Calcium

mishandling in absence of primary mitochondrial dysfunction drives cellular pathology in Wolfram Syndrome. Sci. Rep. *10*, 4785.

Langlois, A., Dal, S., Vivot, K., Mura, C., Seyfritz, E., Bietiger, W., Dollinger, C., Peronet, C., Maillard, E., Pinget, M., et al. (2016). Improvement of islet graft function using liraglutide is correlated with its anti-inflammatory properties. Br. J. Pharmacol. *173*, 3443–3453.

Lee, A.S. (2005). The ER chaperone and signaling regulator GRP78/BiP as a monitor of endoplasmic reticulum stress. Methods *35*, 373–381.

Leiva-Santana, C., Carro-Martinez, A., Monge-Argiles, A., and Palao-Sanchez, A. (1993). [Neurologic manifestations in Wolfram's syndrome]. Rev. Neurol. (Paris) *149*, 26–29.

Li, K., Li, J., Zheng, J., and Qin, S. (2019). Reactive Astrocytes in Neurodegenerative Diseases. Aging Dis. *10*, 664.

Li, Y., Bader, M., Tamargo, I., Rubovitch, V., Tweedie, D., Pick, C.G., and Greig, N.H. (2015). Liraglutide is neurotrophic and neuroprotective in neuronal cultures and mitigates mild traumatic brain injury in mice. J. Neurochem. *135*, 1203–1217.

Liang, D., Bhatta, S., Gerzanich, V., and Simard, J.M. (2007). Cytotoxic edema: mechanisms of pathological cell swelling. Neurosurg. Focus 1–9.

Liu, W., Jalewa, J., Sharma, M., Li, G., Li, L., and Hölscher, C. (2015). Neuroprotective effects of lixisenatide and liraglutide in the 1-methyl-4-phenyl-1,2,3,6-tetrahydropyridine mouse model of Parkinson's disease. Neuroscience *303*, 42–50.

Löscher, W. (2002). Basic Pharmacology of Valproate: A Review After 35 Years of Clinical Use for the Treatment of Epilepsy. CNS Drugs *16*, 669–694.

Lu, S., Kanekura, K., Hara, T., Mahadevan, J., Spears, L.D., Oslowski, C.M., Martinez, R., Yamazaki-Inoue, M., Toyoda, M., Neilson, A., et al. (2014). A calcium-dependent protease as a potential therapeutic target for Wolfram syndrome. Proc. Natl. Acad. Sci. *111*, E5292–E5301.

Lugar, H.M., Koller, J.M., Rutlin, J., Marshall, B.A., Kanekura, K., Urano, F., Bischoff, A.N., Shimony, J.S., and Hershey, T. (2016). Neuroimaging evidence of deficient axon myelination in Wolfram syndrome. Sci. Rep. *6*, 21167.

Lugar, H.M., Koller, J.M., Rutlin, J., Eisenstein, S.A., Neyman, O., Narayanan, A., Chen, L., Shimony, J.S., and Hershey, T. (2019). Evidence for altered neurodevelopment and neurodegeneration in Wolfram syndrome using longitudinal morphometry. Sci. Rep. *9*, 6010.

Luuk, H., Koks, S., Plaas, M., Hannibal, J., Rehfeld, J.F., and Vasar, E. (2008). Distribution of Wfs1 protein in the central nervous system of the mouse and its relation to clinical symptoms of the Wolfram syndrome. J. Comp. Neurol. *509*, 642–660.

Luuk, H., Plaas, M., Raud, S., Innos, J., Sütt, S., Lasner, H., Abramov, U., Kurrikoff, K., Kõks, S., and Vasar, E. (2009). Wfs1-deficient mice display impaired behavioural adaptation in stressful environment. Behav. Brain Res. *198*, 334–345.

Martens, G.A., Jiang, L., Hellemans, K.H., Stangé, G., Heimberg, H., Nielsen, F.C., Sand, O., Van Helden, J., Gorus, F.K., and Pipeleers, D.G. (2011). Clusters of Conserved Beta Cell Marker Genes for Assessment of Beta Cell Phenotype. PLoS ONE *6*, e24134.

McKay, B.E., Engbers, J.D.T., Mehaffey, W.H., Gordon, G.R.J., Molineux, M.L., Bains, J.S., and Turner, R.W. (2007). Climbing Fiber Discharge Regulates Cerebellar Functions by Controlling the Intrinsic Characteristics of Purkinje Cell Output. J. Neurophysiol. *97*, 2590–2604.

Mh, D. (1975). Evaluation of a muscle relaxant: dantrolene sodium (Dantrium) (JAMA).

Mikami, Y., Kanemaru, K., Okubo, Y., Nakaune, T., Suzuki, J., Shibata, K., Sugiyama, H., Koyama, R., Murayama, T., Ito, A., et al. (2016). Nitric Oxide-induced Activation of the Type 1 Ryanodine Receptor Is Critical for Epileptic Seizure-induced Neuronal Cell Death. EBioMedicine *11*, 253–261.

Müller, T.D., Finan, B., Bloom, S.R., D'Alessio, D., Drucker, D.J., Flatt, P.R., Fritsche, A., Gribble, F., Grill, H.J., Habener, J.F., et al. (2019). Glucagon-like peptide 1 (GLP-1). Mol. Metab. *30*, 72–130.

Nestor, S.M., Rupsingh, R., Borrie, M., Smith, M., Accomazzi, V., Wells, J.L., Fogarty, J., and Bartha, R. (2008). Ventricular enlargement as a possible measure of Alzheimer's disease progression validated using the Alzheimer's disease neuroimaging initiative database. Brain *131*, 2443–2454.

Oguntibeju, O.O. (2019). Type 2 diabetes mellitus, oxidative stress and inflammation: examining the links. Int. J. Physiol. Pathophysiol. Pharmacol. *11*, 45–63.

Oo, Y.W., Gomez-Hurtado, N., Walweel, K., van Helden, D.F., Imtiaz, M.S., Knollmann, B.C., and Laver, D.R. (2015). Essential Role of Calmodulin in RyR Inhibition by Dantrolene. Mol. Pharmacol. *88*, 57–63.

Pallotta, M.T., Tascini, G., Crispoldi, R., Orabona, C., Mondanelli, G., Grohmann, U., and Esposito, S. (2019). Wolfram syndrome, a rare neurodegenerative disease: from pathogenesis to future treatment perspectives. J. Transl. Med. *17*, 238.

Park, S.J., Lee, J.Y., Kim, S.J., Choi, S.-Y., Yune, T.Y., and Ryu, J.H. (2015). Toll-like receptor-2 deficiency induces schizophrenia-like behaviors in mice. Sci. Rep. *5*, 8502.

Paul, M.S., and M Das, J. (2019). Neuroanatomy, Superior and Inferior Olivary Nucleus (Superior and Inferior Olivary Complex). In StatPearls, (Treasure Island (FL): StatPearls Publishing), p.

Pihlaja, R., Koistinaho, J., Kauppinen, R., Sandholm, J., Tanila, H., and Koistinaho, M. (2011). Multiple cellular and molecular mechanisms Are involved in human Aβ clearance by transplanted adult astrocytes. Glia *59*, 1643–1657.

Pini, L., Pievani, M., Bocchetta, M., Altomare, D., Bosco, P., Cavedo, E., Galluzzi, S., Marizzoni, M., and Frisoni, G.B. (2016). Brain atrophy in Alzheimer's Disease and aging. Ageing Res. Rev. *30*, 25–48.

Plaas, M., Seppa, K., Reimets, R., Jagomäe, T., Toots, M., Koppel, T., Vallisoo, T., Nigul, M., Heinla, I., Meier, R., et al. (2017). Wfs1-deficient rats develop primary symptoms of Wolfram syndrome: insulin-dependent diabetes, optic nerve atrophy and medullary degeneration. Sci. Rep. *7*, 10220.

Poduslo, J.F., and Curran, G.L. (1996). Permeability at the blood-brain and blood-nerve barriers of the neurotrophic factors: NGF, CNTF, NT-3, BDNF. Mol. Brain Res. *36*, 280–286.

Punapart, M., Eltermaa, M., Oflijan, J., Sütt, S., Must, A., Kõks, S., Schalkwyk, L.C., Fernandes, C., Vasar, E., Soomets, U., et al. (2014). Effect of Chronic Valproic Acid Treatment on Hepatic Gene Expression Profile in *Wfs1* Knockout Mouse. PPAR Res. *2014*, 1–11.

Pushpakom, S., Iorio, F., Eyers, P.A., Escott, K.J., Hopper, S., Wells, A., Doig, A., Guilliams, T., Latimer, J., McNamee, C., et al. (2019). Drug repurposing: progress, challenges and recommendations. Nat. Rev. Drug Discov. *18*, 41–58.

Rahman, M., and Nguyen, H. (2020). Valproic Acid. In StatPearls, (Treasure Island (FL): StatPearls Publishing), p.

Ransohoff, R.M., and Khoury, J.E. (2016). Microglia in Health and Disease. Cold Spring Harb. Perspect. Biol. *8*, a020560.

Rasmusson, A., Hahn, U., Larsen, J.O., Gundersen, H.J.G., Jensen, E.B.V., and Nyengaard, J.R. (2013). The spatial rotator: THE SPATIAL ROTATOR. J. Microsc. *250*, 88–100.

Reiner, D.J., Mietlicki-Baase, E.G., McGrath, L.E., Zimmer, D.J., Bence, K.K., Sousa, G.L., Konanur, V.R., Krawczyk, J., Burk, D.H., Kanoski, S.E., et al. (2016). Astrocytes Regulate GLP-1 Receptor-Mediated Effects on Energy Balance. J. Neurosci. *36*, 3531–3540.

Riggs, A.C., Bernal-Mizrachi, E., Ohsugi, M., Wasson, J., Fatrai, S., Welling, C., Murray, J., Schmidt, R.E., Herrera, P.L., and Permutt, M.A. (2005). Mice conditionally lacking the Wolfram gene in pancreatic islet beta cells exhibit diabetes as a result of enhanced endoplasmic reticulum stress and apoptosis. Diabetologia *48*, 2313–2321.

Rigoli, L., Bramanti, P., Di Bella, C., and De Luca, F. (2018). Genetic and clinical aspects of Wolfram syndrome 1, a severe neurodegenerative disease. Pediatr. Res. *83*, 921–929.

Rios, M., Fan, G., Fekete, C., Kelly, J., Bates, B., Kuehn, R., Lechan, R.M., and Jaenisch, R. (2001). Conditional Deletion Of Brain-Derived Neurotrophic Factor in the Postnatal Brain Leads to Obesity and Hyperactivity. Mol. Endocrinol. *15*, 1748–1757.

Robinson, S.R., Dang, T.N., Dringen, R., and Bishop, G.M. (2009). Hemin toxicity: a preventable source of brain damage following hemorrhagic stroke. Redox Rep. *14*, 228–235.

Rohayem, J., Ehlers, C., Wiedemann, B., Holl, R., Oexle, K., Kordonouri, O., Salzano, G., Meissner, T., Burger, W., Schober, E., et al. (2011). Diabetes and Neurodegeneration in Wolfram Syndrome: A multicenter study of phenotype and genotype. Diabetes Care *34*, 1503–1510.

Rolls, A., Shechter, R., London, A., Ziv, Y., Ronen, A., Levy, R., and Schwartz, M. (2007). Toll-like receptors modulate adult hippocampal neurogenesis. Nat. Cell Biol. *9*, 1081–1088.

Ryter, S.W., and Tyrrell, R.M. (2000). The heme synthesis and degradation pathways: role in oxidant sensitivity. Free Radic. Biol. Med. *28*, 289–309.

Sakakibara, Y., Sekiya, M., Fujisaki, N., Quan, X., and Iijima, K.M. (2018). Knockdown of wfs1, a fly homolog of Wolfram syndrome 1, in the nervous system increases susceptibility to age- and stress-induced neuronal dysfunction and degeneration in Drosophila. PLOS Genet. *14*, e1007196.

Salcedo, I., Tweedie, D., Li, Y., and Greig, N.H. (2012). Neuroprotective and neurotrophic actions of glucagon-like peptide-1: an emerging opportunity to treat neurodegenerative and cerebrovascular disorders: Neurological benefits of GLP-1 receptor activation. Br. J. Pharmacol. *166*, 1586–1599.

Samara, A., Rahn, R., Neyman, O., Park, K.Y., Samara, A., Marshall, B., Dougherty, J., and Hershey, T. (2019). Developmental hypomyelination in Wolfram syndrome: new insights from neuroimaging and gene expression analyses. Orphanet J. Rare Dis. *14*, 279.

Sato, K., Kameda, M., Yasuhara, T., Agari, T., Baba, T., Wang, F., Shinko, A., Wakamori, T., Toyoshima, A., Takeuchi, H., et al. (2013). Neuroprotective Effects of Liraglutide for Stroke Model of Rats. Int. J. Mol. Sci. *14*, 21513–21524.

Sayeed, M.S.B., Alhadidi, Q., and Shah, Z.A. (2017). Cofilin signaling in hemin-induced microglial activation and inflammation. J. Neuroimmunol. *313*, 46–55.

Scully, K.J., and Wolfsdorf, J.I. (2020). Efficacy of GLP-1 Agonist Therapy in Autosomal Dominant WFS1-Related Disorder: A Case Report. Horm. Res. Paediatr. 1–6.

Sedman, T., Rünkorg, K., Krass, M., Luuk, H., Plaas, M., Vasar, E., and Volke, V. (2016). Exenatide Is an Effective Antihyperglycaemic Agent in a Mouse Model of Wolfram Syndrome 1. J. Diabetes Res. *2016*, 1–7.

Seifert, G., Schilling, K., and Steinhäuser, C. (2006). Astrocyte dysfunction in neurological disorders: a molecular perspective. Nat. Rev. Neurosci. *7*, 194–206.

Seppa, K., Toots, M., Reimets, R., Jagomäe, T., Koppel, T., Pallase, M., Hasselholt, S., Mikkelsen, M., Nyengaard, J.R., Vasar, E., et al. (2019). GLP-1 receptor agonist liraglutide has a neuroprotective effect on an aged rat model of Wolfram syndrome. Scientific Reports.

Seppa, K., Jagomäe, T., Kukker, K.G., Reimets, R., Pastak, M., Vasar, E., Terasmaa, A., and Plaas, M. (2021). Liraglutide, 7,8-DHF and their co-treatment prevents loss of vision and cognitive decline in a Wolfram syndrome rat model. Sci. Rep. *11*, 2275.

Shannon, P., Becker, L., and Deck, J. (1999). Evidence of widespread axonal pathology in Wolfram syndrome. Acta Neuropathol. (Berl.) *98*, 304–308.

Sokka, A.-L., Putkonen, N., Mudo, G., Pryazhnikov, E., Reijonen, S., Khiroug, L., Belluardo, N., Lindholm, D., and Korhonen, L. (2007). Endoplasmic Reticulum Stress Inhibition Protects against Excitotoxic Neuronal Injury in the Rat Brain. J. Neurosci. *27*, 901–908.

Sola, D., Rossi, L., Schianca, G.P.C., Maffioli, P., Bigliocca, M., Mella, R., Corlianò, F., Fra, G.P., Bartoli, E., and Derosa, G. (2015). State of the art paper Sulfonylureas and their use in clinical practice. Arch. Med. Sci. *4*, 840–848.

Soltani, N., Qiu, H., Aleksic, M., Glinka, Y., Zhao, F., Liu, R., Li, Y., Zhang, N., Chakrabarti, R., Ng, T., et al. (2011). GABA exerts protective and regenerative effects on islet beta cells and reverses diabetes. Proc. Natl. Acad. Sci. *108*, 11692–11697.

Spielman, L.J., Gibson, D.L., and Klegeris, A. (2017). Incretin hormones regulate microglia oxidative stress, survival and expression of trophic factors. Eur. J. Cell Biol. *96*, 240–253.

Streit, W.J., Mrak, R.E., and Griffin, W.S.T. (2004). Microglia and neuroinflammation: a pathological perspective. J. Neuroinflammation *1*, 14.

Strom, T. (1998). Diabetes insipidus, diabetes mellitus, optic atrophy and deafness (DIDMOAD) caused by mutations in a novel gene (wolframin) coding for a predicted transmembrane protein. Hum. Mol. Genet. *7*, 2021–2028.

Strom, T.M., Hörtnagel, K., Hofmann, S., Gekeler, F., Scharfe, C., Rabl, W., Gerbitz, K.D., and Meitinger, T. (1998). Diabetes insipidus, diabetes mellitus, optic atrophy and deafness (DIDMOAD) caused by mutations in a novel gene (wolframin) coding for a predicted transmembrane protein. Hum. Mol. Genet. *7*, 2021–2028.

Stump, M., Guo, D.-F., Lu, K.-T., Mukohda, M., Cassell, M.D., Norris, A.W., Rahmouni, K., and Sigmund, C.D. (2016). Nervous System Expression of PPARγ and Mutant PPARγ Has Profound Effects on Metabolic Regulation and Brain Development. Endocrinology *157*, 4266–4275.

Takeda, K. (2001). WFS1 (Wolfram syndrome 1) gene product: predominant subcellular localization to endoplasmic reticulum in cultured cells and neuronal expression in rat brain. Hum. Mol. Genet. *10*, 477–484.

Takei, D., Ishihara, H., Yamaguchi, S., Yamada, T., Tamura, A., Katagiri, H., Maruyama, Y., and Oka, Y. (2006). WFS1 protein modulates the free Ca^{2+} concentration in the endoplasmic reticulum. FEBS Lett. *580*, 5635–5640.

Terasmaa, A., Soomets, U., Oflijan, J., Punapart, M., Hansen, M., Matto, V., Ehrlich, K., Must, A., Kõks, S., and Vasar, E. (2011). Wfs1 mutation makes mice sensitive to insulin-like effect of acute valproic acid and resistant to streptozocin. J. Physiol. Biochem. *67*, 381–390.

Thakur, P.C., Miller-Ocuin, J.L., Nguyen, K., Matsuda, R., Singhi, A.D., Zeh, H.J., and Bahary, N. (2018). Inhibition of endoplasmic-reticulum-stress-mediated autophagy enhances the effectiveness of chemotherapeutics on pancreatic cancer. J. Transl. Med. *16*, 190.

Thorell, W.E., Leibrock, L.G., and Agrawal, S.K. (2002). Role of RyRs and IP3 Receptors after Traumatic Injury to Spinal Cord White Matter. J. Neurotrauma *19*, 335–342.

Timberlake, M., and Dwivedi, Y. (2019). Linking unfolded protein response to inflammation and depression: potential pathologic and therapeutic implications. Mol. Psychiatry *24*, 987–994.

Toots, M., Seppa, K., Jagomäe, T., Koppel, T., Pallase, M., Heinla, I., Terasmaa, A., Plaas, M., and Vasar, E. (2018). Preventive treatment with liraglutide protects against development of glucose intolerance in a rat model of Wolfram syndrome. Sci. Rep. *8*, 10183.

Trujillo, J.M., Nuffer, W., and Smith, B.A. (2021). GLP-1 receptor agonists: an updated review of head-to-head clinical studies. Ther. Adv. Endocrinol. Metab. *12*, 204201882199732.

Tyagi, S., Sharma, S., Gupta, P., Saini, A., and Kaushal, C. (2011). The peroxisome proliferator-activated receptor: A family of nuclear receptors role in various diseases. J. Adv. Pharm. Technol. Res. *2*, 236.

Ueda, K., Kawano, J., Takeda, K., Yujiri, T., Tanabe, K., Anno, T., Akiyama, M., Nozaki, J., Yoshinaga, T., Koizumi, A., et al. (2005). Endoplasmic reticulum stress induces Wfs1 gene expression in pancreatic β-cells via transcriptional activation. Eur. J. Endocrinol. *153*, 167–176.

Uno, T., and Shibata, M. (2001). Role of inferior olive and thoracic IML neurons in non-shivering thermogenesis in rats. Am. J. Physiol.-Regul. Integr. Comp. Physiol. *280*, R536–R546.

Urano, F. (2016). Wolfram Syndrome: Diagnosis, Management, and Treatment. Curr. Diab. Rep. *16*.

Vazirinejad, R., Ahmadi, Z., Kazemi Arababadi, M., Hassanshahi, G., and Kennedy, D. (2014). The Biological Functions, Structure and Sources of CXCL10 and Its Outstanding Part in the Pathophysiology of Multiple Sclerosis. Neuroimmunomodulation *21*, 322–330.

Wang, M., Wey, S., Zhang, Y., Ye, R., and Lee, A.S. (2009). Role of the Unfolded Protein Response Regulator GRP78/BiP in Development, Cancer, and Neurological Disorders. Antioxid. Redox Signal. *11*, 2307–2316.

Wei, H., and Perry, D.C. (2002). Dantrolene Is Cytoprotective in Two Models of Neuronal Cell Death. J. Neurochem. *67*, 2390–2398.

Xia, M.Q., Bacskai, B.J., Knowles, R.B., Qin, S.X., and Hyman, B.T. (2000). Expression of the chemokine receptor CXCR3 on neurons and the elevated expression of its ligand IP-10 in reactive astrocytes: in vitro ERK1/2 activation and role in Alzheimer's disease. J. Neuroimmunol. *108*, 227–235.

Yeo, G.S.H., Connie Hung, C.-C., Rochford, J., Keogh, J., Gray, J., Sivaramakrishnan, S., O'Rahilly, S., and Farooqi, I.S. (2004). A de novo mutation affecting human TrkB associated with severe obesity and developmental delay. Nat. Neurosci. *7*, 1187–1189.

Yu, Z., Luo, H., Fu, W., and Mattson, M.P. (1999). The Endoplasmic Reticulum Stress-Responsive Protein GRP78 Protects Neurons Against Excitotoxicity and Apoptosis: Suppression of Oxidative Stress and Stabilization of Calcium Homeostasis. Exp. Neurol. *155*, 302–314.

Yu, Z., Sheng, H., Liu, S., Zhao, S., Glembotski, C.C., Warner, D.S., Paschen, W., and Yang, W. (2017). Activation of the ATF6 branch of the unfolded protein response in neurons improves stroke outcome. J. Cereb. Blood Flow Metab. *37*, 1069–1079.

Yushkevich, P.A., Piven, J., Hazlett, H.C., Smith, R.G., Ho, S., Gee, J.C., and Gerig, G. (2006). User-guided 3D active contour segmentation of anatomical structures: Significantly improved efficiency and reliability. NeuroImage *31*, 1116–1128.

Yusta, B., Baggio, L.L., Estall, J.L., Koehler, J.A., Holland, D.P., Li, H., Pipeleers, D., Ling, Z., and Drucker, D.J. (2006). GLP-1 receptor activation improves β cell function and survival following induction of endoplasmic reticulum stress. Cell Metab. *4*, 391–406.

Zeng, Y., Lv, F., Li, L., Yu, H., Dong, M., and Fu, Q. (2012). 7,8-dihydroxyflavone rescues spatial memory and synaptic plasticity in cognitively impaired aged rats: Spatial memory and synaptic plasticity in rats. J. Neurochem. *122*, 800–811.

Zhang, Z., Liu, X., Schroeder, J.P., Chan, C.-B., Song, M., Yu, S.P., Weinshenker, D., and Ye, K. (2014). 7,8-Dihydroxyflavone Prevents Synaptic Loss and Memory Deficits in a Mouse Model of Alzheimer's Disease. Neuropsychopharmacology *39*, 638–650.

Zinszner, H., Kuroda, M., Wang, X., Batchvarova, N., Lightfoot, R.T., Remotti, H., Stevens, J.L., and Ron, D. (1998). CHOP is implicated in programmed cell death in response to impaired function of the endoplasmic reticulum. Genes Dev. *12*, 982–995.

Zmyslowska, A., Malkowski, B., Fendler, W., Borowiec, M., Antosik, K., Gnys, P., Baranska, D., and Mlynarski, W. (2014). Central Nervous System PET-CT Imaging Reveals Regional Impairments in Pediatric Patients with Wolfram Syndrome. PLoS ONE *9*, e115605.

ACKNOWLEDGEMENTS

Most of all, I want to thank my supervisor, Mario Plaas and my co-supervisors Anton Terasmaa and Eero Vasar, who made it possible to conduct research on such an interesting topic. I appreciate all the co-authors, as the studies presented in this thesis are the result of teamwork and would not have been possible alone. I want to thank Jens Randel Nyengaard for the opportunity to work in his lab during 2018. I am very thankful to the reviewers, Tambet Tõnissoo and Kalle Kilk, for their time. My gratitude goes to my family, Jörg, and my friends for supporting me during my studies.

***

This research was conducted at the Institute of Biomedicine and Translational Medicine at the University of Tartu. This research was supported by the European Union through the European Regional Development Fund (Project No. 2014-2020.4.01.15-0012) and by grants IUT20–64, PSG471, IUT20-41, PUT784 from the Estonian Research Council and by Eye Hope Foundation iVZW, Damme, Belgium (www.eyehopefoundation.org). The Centre for Stochastic Geometry and Advanced Bioimaging was supported by the Villum Foundation.

ORIGINAL PUBLICATIONS

CURRICULUM VITAE

Name	Kadri Seppa
Date of birth	April 8, 1993
Address	Ravila 14b, 50412, Tartu, Estonia
E-mail	kadri.seppa@ut.ee

Education

04.09.2017–...	University of Tartu, Faculty of Medicine, PhD (Neuroscience)
01.08.2018–29.12.2018	Visiting doctoral student, Aarhus University (Aarhus Universitet), Department of Clinical Medicine – Core Centre for Molecular Morphology, Section for Stereology and Microscopy, Denmark
04.04.2016–31.07.2016	Bielefeld University (Universität Bielefeld), Germany, MSc, Molecular Cell Biology, Erasmus Exchange Program
31.08.2015–21.06.2017	University of Tartu, Faculty of Science and Technology, MSc (Gene technology)
01.04.2014–30.09.2014	Brandenburg University of Technology (Brandenburgische Technische Universität), Germany, BSc, Biotechnology, Erasmus Exchange Program
03.09.2012–17.06.2015	University of Tartu, Faculty of Science and Technology, BSc (Biology)
01.09.2009–16.06.2012	Hugo Treffner Gymnasium, Tartu, Estonia

Professional employment

01.07.2017–...	University of Tartu, Faculty of Medicine, Institute of Biomedicine and Translational Medicine, Specialist
01.10.2016–31.03.2017	Estonian Veterinary and Food Laboratory, Department of molecular analysis, Chief specialist

Professional training

2017 Competence course in laboratory animal science, according to directive 2010/63/EU, Estonian University of Life Sciences

Honors & awards

2020 Valda and Bernard Õun Memorial scholarship
2019 Nadia Walter Scholarship

International scientific meetings

2021 1st ESN virtual conference "Future perspectives for european neuroschemistry – a young scientist's conference" (European Society for Neurochemistry).

2019 Neuroscience 2019 (Chicago, IL, Society for Neuroscience).
2019 23rd ESN Biennial Meeting (Milan, European Society for Neurochemistry).

Dissertations supervised

2020 Kaia Grete Kukker, Bachelor of Science, Volumetric changes in the hippocampus and lateral ventricles after chronic liraglutide treatment in a rat model of Wolfram syndrome

Professional Memberships

2019−... Member of European Society for Neurochemistry (ESN) young scientist steering committee

Publications

Seppa, K., Jagomäe, T., Kukker, K.G., Reimets, R., Pastak, M., Vasar, E., Terasmaa, A., Plaas, M., 2021. Liraglutide, 7,8-DHF and their co-treatment prevents loss of vision and cognitive decline in a Wolfram syndrome rat model. Sci. Rep. 11, 2275. https://doi.org/10.1038/s41598-021-81768-6

Seppa, K., Toots, M., Reimets, R., Jagomäe, T., Koppel, T., Pallase, M., Hasselholt, S., Krogsbæk Mikkelsen, M., Randel Nyengaard, J., Vasar, E., Terasmaa, A., Plaas, M., 2019. GLP-1 receptor agonist liraglutide has a neuroprotective effect on an aged rat model of Wolfram syndrome. Sci. Rep. 9, 15742. https://doi.org/10.1038/s41598-019-52295-2

Toots, M., Seppa, K., Jagomäe, T., Koppel, T., Pallase, M., Heinla, I., Terasmaa, A., Plaas, M., Vasar, E., 2018. Preventive treatment with liraglutide protects against development of glucose intolerance in a rat model of Wolfram syndrome. Sci. Rep. 8, 10183. https://doi.org/10.1038/s41598-018-28314-z

Plaas, M., Seppa, K., Reimets, R., Jagomäe, T., Toots, M., Koppel, T., Vallisoo, T., Nigul, M., Heinla, I., Meier, R., Kaasik, A., Piirsoo, A., Hickey, M.A., Terasmaa, A., Vasar, E., 2017. Wfs1-deficient rats develop primary symptoms of Wolfram syndrome: insulin-dependent diabetes, optic nerve atrophy and medullary degeneration. Sci. Rep. 7, 10220. https://doi.org/10.1038/s41598-017-09392-x

ELULOOKIRJELDUS

Nimi	Kadri Seppa
Sünniaeg	8. aprill, 1993
Aadress	Ravila 14b, 50412, Tartu, Eesti
E-mail	kadri.seppa@ut.ee

Hariduskäik

04.09.2017–...	Tartu Ülikool, Meditsiiniteaduste valdkond, PhD (Neuroteadused)
01.08.2018–29.12.2018	Külalisdoktorant, Aarhusi Ülikool (Aarhus Universitet), Stereoloogia ja mikroskoopia osakond
04.04.2016–31.07.2016	Bielefeldi Ülikool (Universität Bielefeld), Saksamaa, MSc, Molekulaarne rakubioloogia, Erasmuse üliõpilasvahetus
31.08.2015–21.06.2017	Tartu Ülikool, Loodus ja täppisteaduste valdkond, MSc (Geenitehnoloogia)
01.04.2014–30.09.2014	Brandenburgi Tehnikaülikool (Brandenburgische Technische Universität), Saksamaa, BSc, Biotehnoloogia, Erasmuse üliõpilasvahetus
03.09.2012–17.06.2015	Tartu Ülikool, Loodus- ja tehnoloogiateaduskond, BSc (Bioloogia)
01.09.2009–16.06.2012	Hugo Treffneri Gümnaasium

Teenistuskäik

01.07.2017–...	Tartu Ülikool, Meditsiiniteaduste valdkond, bio- ja siirdemeditsiini instituut, siirdemeditsiini laborispetsialist
01.10.2016–31.03.2017	Veterinaar- ja toidulaboratoorium, molekulaaranalüüsi osakonna peaspetsialist

Erialane enesetäiendus

2017 Läbitud katseloomateaduse kursus vastavalt direktiivile 2010/63/EU, Eesti maaülikool

Tunnustused

2020 Valda ja Bernard Õuna mälestusfondi stipendium
2019 Nadia Walteri stipendium

Rahvusvahelised teaduskonverentsid

2021 1st ESN virtual conference “Future perspectives for european neurochemistry – a young scientist’s conference” (European Society for Neurochemistry).
2019 Neuroscience 2019 (Chicago, IL, Society for Neuroscience).
2019 23rd ESN Biennial Meeting (Milan, European Society for Neurochemistry).

Juhendamised

2020 Kaia Grete Kukker, Bakalaureusetöö, Hipokampuse ja külgvatsakeste ruumala muutuse uurimine liraglutiidi kroonilise manustamise järel Wolframi sündroomi rotimudelis

Teadusorganisatsiooniline tegevus

2019−... Euroopa neurokeemia seltsi noorteadlaste juhtkomitee liige, European Society for Neurochemistry (ESN)

Publikatsioonid

Seppa, K., Jagomäe, T., Kukker, K.G., Reimets, R., Pastak, M., Vasar, E., Terasmaa, A., Plaas, M., 2021. Liraglutide, 7,8-DHF and their co-treatment prevents loss of vision and cognitive decline in a Wolfram syndrome rat model. Sci. Rep. 11, 2275. https://doi.org/10.1038/s41598-021-81768-6

Seppa, K., Toots, M., Reimets, R., Jagomäe, T., Koppel, T., Pallase, M., Hasselholt, S., Krogsbæk Mikkelsen, M., Randel Nyengaard, J., Vasar, E., Terasmaa, A., Plaas, M., 2019. GLP-1 receptor agonist liraglutide has a neuroprotective effect on an aged rat model of Wolfram syndrome. Sci. Rep. 9, 15742. https://doi.org/10.1038/s41598-019-52295-2

Toots, M., Seppa, K., Jagomäe, T., Koppel, T., Pallase, M., Heinla, I., Terasmaa, A., Plaas, M., Vasar, E., 2018. Preventive treatment with liraglutide protects against development of glucose intolerance in a rat model of Wolfram syndrome. Sci. Rep. 8, 10183. https://doi.org/10.1038/s41598-018-28314-z

Plaas, M., Seppa, K., Reimets, R., Jagomäe, T., Toots, M., Koppel, T., Vallisoo, T., Nigul, M., Heinla, I., Meier, R., Kaasik, A., Piirsoo, A., Hickey, M.A., Terasmaa, A., Vasar, E., 2017. Wfs1-deficient rats develop primary symptoms of Wolfram syndrome: insulin-dependent diabetes, optic nerve atrophy and medullary degeneration. Sci. Rep. 7, 10220. https://doi.org/10.1038/s41598-017-09392-x

DISSERTATIONES NEUROSCIENTIAE UNIVERSITATIS TARTUENSIS

1. **Sirli Raud.** Cholecystokinin$_2$ receptor deficient mice: changes in function of GABA-ergic system. Tartu, 2005.
2. **Kati Koido.** Single-nucleotide polymorphism profiling of 22 candidate genes in mood and anxiety disorders. Tartu, 2005.
3. **Dzhamilja Safiulina.** The studies of mitochondria in cultured cerebellar granule neurons: characterization of mitochondrial function, volume homeostasis and interaction with neurosteroids. Tartu, 2006.
4. **Tarmo Areda.** Behavioural and neurogenetic study of mechanisms related to cat odour induced anxiety in rodents. Tartu, 2006.
5. **Aleksei Nelovkov.** Behavioural and neurogenetic study of molecular mechanisms involved in regulation of exploratory behaviour in rodents. Tartu, 2006.
6. **Annika Vaarmann**. The studies on cystatin B deficient mice: neurochemical and behavioural alterations in animal model of progressive myoclonus epilepsy of Unverricht-Lundborg type. Tartu, 2007.
7. **Urho Abramov.** Sex and environmental factors determine the behavioural phenotype of mice lacking CCK_2 receptors: implications for the behavioural studies in transgenic lines. Tartu, 2008.
8. **Hendrik Luuk.** Distribution and behavioral effects of WFS1 protein in the central nervous system. Tartu, 2009.
9. **Anne Must.** Studies on molecular genetics of male completed suicide in Estonian population. Tartu, 2009.
10. **Kaido Kurrikoff**. Involvement of cholecystokinin in chronic pain mechanisms and endogenous antinociception. Tartu, 2009.
11. **Anu Aonurm-Helm.** Depression-like phenotype and altered intracellular signalling in neural cell adhesion molecule (NCAM)-deficient mice. Tartu, 2010.
12. **Silva Sütt.** Role of endocannabinoid system and *Wfs1* in regulation of emotional behaviour: behavioural, pharmacological and genetic studies. Tartu, 2010.
13. **Mari-Anne Philips.** Characterization of *Myg1* gene and protein: expression patterns, subcellular localization, gene deficient mouse and functional polymorphisms in human. Tartu, 2010.
14. **Ranno Rätsep.** Genetics of psoriasis and vitiligo, focus on IL10 family cytokines. Tartu, 2010.
15. **Kairit Joost.** Selective screening of metabolic diseases in Estonia: the application of new diagnostic methods. Tartu, 2012, 143 p.
16. **Monika Jürgenson.** A complex phenotype in mice with partial or complete deficiency of the NCAM protein. Tartu, 2012, 117 p.

17. **Ene Reimann.** Description of the cytokines and cutaneous neuroendocrine system in the development of vitiligo. Tartu, 2012, 117 p.
18. **Jürgen Innos.** Behavioural, pharmacological and neurochemical characterisation of limbic system-associated membrane protein (LSAMP) deficient mice. Tartu, 2013, 113 p.
19. **Kaili Anier.** The role of DNA methylation in the development of cocaine-induced behavioural sensitisation. Tartu, 2013, 147 p.
20. **Maarika Liik.** Cognitive functioning, perceived cognition, subjective complaints and symptoms of depression in patients with epilepsy: neuropsychological assessment and spet brain imaging study. Tartu, 2014, 124 p.
21. **Sten Ilmjärv.** Estimating differential expression from multiple indicators. Tartu, 2015, 125 p.
22. **Paula Reemann.** The effects of microenvironment on skin cells. Tartu, 2015, 146 p.
23. **Tanel Visnapuu.** Pharmacological and behavioral characterization of the monoaminergic and GABA-ergic systems of Wfs1-deficient mice. Tartu, 2015, 107 p.
24. **Indrek Heinla.** Behavioural and genetic comparison of B6 and 129Sv mouse lines focusing on the anxiety profile and the expression of *Lsamp* gene. Tartu, 2016, 115 p.
25. **Liina Haring.** Cognitive functioning after first psychotic episode. Tartu, 2017, 146 p.
26. **Triin Tekko.** Neurodevelopmental Approach in the Study of the Function of *Wfs1* and *Lsamp*, Potential Targets in the Regulation of Emotional Behaviour. Tartu, 2018, 194 p.
27. **Alina Altpere.** Targeting of mechanisms of elevated anxiety in female Wfs1-deficient mice. Tartu, 2018, 98 p.
28. **Maarja Toots.** Pharmacological challenge in rodent models of Wolfram syndrome with emphasis on diabetic phenotype. Tartu, 2018, 114 p.
29. **Katyayani Singh.** Neuropsychiatric endophenotypes – focusing on IgLON adhesion molecules in the mouse brain. Tartu, 2019, 148 p.
30. **Kattri-Liis Eskla.** Therapeutic strategies for ischemia reperfusion injury. Tartu, 2019, 138 p.
31. **Hardo Lilleväli**. Hyperphenylalaninaemias and neurophysiological disorders associated with the condition. Tartu, 2020, 134 p.
32. **Roman Balõtšev**. Interaction between the immune and metabolic systems in different stages of schizophrenia spectrum disorders. Tartu, 2020, 164 p.
33. **Mari Urb**. DNA methylation in the predisposition, expression and abstinence of cocaine addiction. Tartu, 2020, 147 p.
34. **Liisa Leppik.** Alterations in metabolomic profile of lipids, amino acids and biogenic amines in the early course of schizophrenia spectrum disorders. Tartu, 2021, 173 p.